CHANGE DETECTION WITH REMOTE SENSING

RELATING NOAA-AVHRR TO ENVIRONMENTAL IMPACT OF AGRICULTURE IN EUROPE

Promotoren
Prof.dr.ir. M. Molenaar, hoogleraar Spatial Data Acquisition and Geoinformatics, ITC Enschede
Prof.dr. S.M. de Jong, hoogleraar Geo-informatiekunde met bijzondere aandacht voor Remote Sensing, Wageningen Universiteit
Co-promotor
Dr.ir. J.G.P.W. Clevers, universitair hoofddocent bij het Laboratorium voor Geo-informatiekunde en Remote Sensing, Wageningen Universiteit

Promotiecommissie
Prof.dr. R. Leemans, RIVM en Wageningen Universiteit
Prof.dr. F.D. van der Meer, Technische Universiteit Delft en ITC
Prof.dr. G. Menz, University of Bonn
Prof.dr.ir. A. Stein, Wageningen Universiteit en ITC

CHANGE DETECTION WITH REMOTE SENSING

RELATING NOAA-AVHRR
TO ENVIRONMENTAL IMPACT OF AGRICULTURE IN EUROPE

ELISABETH ADDINK

STELLINGEN

Waarnemingseenheden gebaseerd op biofysisch factoren komen beter overeen met patronen in NOAA-AVHRR beelden dan eenheden afgeleid van socio-economische factoren.

NOAA-AVHRR beelden lijken ongeschikt voor het opsporen van veranderingen in landbedekking in Europa.

Geostatistische methoden bieden de beste oplossing voor het vervangen van kleine wolken in NOAA-AVHRR beelden door reflectiewaarden van het onderliggende landschap.

Onnauwkeurigheden in plaatsbepaling en classificatie, gecombineerd met spectrale variatie maken satellietbeelden ongeschikt voor het opsporen van veranderingen op (sub)pixel niveau.

Voor het betrouwbaar opsporen van veranderingen met remote sensing is het van het grootste belang dat sensoren over langere tijd operationeel blijven.

Negatieve conclusies zijn moeilijker te trekken dan positieve. Bovendien zijn positieve conclusies leuker om te trekken dan negatieve, ondanks het vaak gehoorde en troostend bedoelde 'negatieve resultaten zijn ook resultaten'.

Na een vergelijkende studie van ruim zes jaar is de conclusie dat van alle transportmogelijkheden die een forens ter beschikking staan, carpoolen kan worden aanbevolen als een gezellige, goedkope en flexibele optie.

Tijdens het uitvoeren van promotieonderzoek is de uitdrukking 'dat is makkelijker gezegd dan gedaan' vaak van toepassing, maar tijdens het schrijven van het proefschrift kan hij beter worden vervangen door 'dat is makkelijker bedacht dan beschreven'.

Gezien de grote waarschijnlijkheid van korte tijdelijke aanstellingen na een promotie, vormt het vierjarig promotieonderzoek een uitgelezen gelegenheid om naast een proefschrift ook van een kind te bevallen.

Hoe eenvoudiger de oplossing, hoe groter het ongeloof dat hij nog niet bestond.

Stellingen behorende bij het proefschrift van Elisabeth Addink,
'Change detection with remote sensing.
Relating NOAA-AVHRR to environmental impact of agriculture in Europe'
Wageningen, vrijdag 9 november 2001.

TABLE OF CONTENTS

DANKWOORD

Toen ik als kleuter een paar keer in een vliegtuig had gezeten, had ik zo mijn eigen ideeën over hoe de wereld in elkaar zat. Bij het vliegen is het opstijgen immers een veel duidelijker beweging dan het landen; het opstijgen gaat heel snel, het landen gaat heel langzaam. Ik merkte daardoor wel dat we naar boven gingen maar niet dat we ook weer naar beneden kwamen. En aangezien je met een vliegtuig altijd naar een ander land vliegt, lag de conclusie voor de hand: landen liggen op elkaar gestapeld, gescheiden door de lucht.

Het leven in deze gestapelde wereld zou veel praktische problemen kennen waar we in onze bolle wereld nooit mee te maken hebben. Met de auto op vakantie zou een flinke klus worden, en de terugreis met het vliegtuig overigens ook. Tegelijkertijd zouden er veel minder grensconflicten voorkomen en trekvogels zouden veel sneller van Siberië naar Afrika en terug kunnen vliegen (voor een 'non-birding spouse' een aantrekkelijk idee). Voor remote sensing zou deze gestapelde wereld veel problemen hebben opgeleverd, maar met alle hulp en steun die ik tijdens mijn promotieonderzoek heb gekregen zou het zelfs dan wel zijn gelukt om uiteindelijk een proefschrift bij elkaar te schrijven.

Het driemanschap dat waakte over het ontstaan van dit proefschrift vulde elkaar perfect aan. Martien Molenaar was de bewaker van de grote lijnen. Hoewel ik het pragmatische geografische denken uit Utrecht soms wel miste, heb jij me laten zien hoe belangrijk het is om heldere concepten als uitgangspunt te nemen. En hoewel ik formules maar niets vond ("die zijn voor saaie mensen"), staan er uiteindelijk zelfs nieuwe formules in dit proefschrift. Jan Clevers was de bewaker 'binnen de grote lijnen'. Als enige van de drie was jij van begin tot eind in Wageningen en had je altijd tijd om mee te denken en mijn verhalen aan te horen als ik het niet zag zitten. Dankzij jou staan alle puntjes op de i's waar ik ze was vergeten. En Steven de Jong waakte over de praktische kanten van de grote lijnen. Als ideeën niet bleken te werken kwam jij met een serie suggesties en zonder jouw aanhoudende "begin nou eindelijk eens met schrijven" had ik nu waarschijnlijk nog steeds niet meer dan een opzet voor de inhoudsopgave. Onze eerste samenwerking dateert al van de zomer van 1991 in de Ardèche. Ik ben blij dat je ook nog een paar jaar naar Wageningen bent gekomen en actief betrokken was bij mijn promotie. Ik moet jullie alle drie bedanken voor de snelheid waarmee ik dit proefschrift uiteindelijk af kon ronden. De volgende keer dat ik zo'n boekwerk moet produceren zal ik niet meer proberen om in twee maanden vijf hoofdstukken te schrijven.

Het RIVM wil ik bedanken voor de financiering van het grootste deel, ruim vijf jaar, van dit onderzoek. Binnen het RIVM waren Reinier van den Berg en de eerste jaren ook Rob van de Velde de drijvende kracht achter de begeleidingscommissie, waarin ook Kees Meinardi, Hans Veldkamp, Peter Burrough, Pauline van Gaans (beide van Universiteit Utrecht) en het Wagenings driemanschap zaten. Allen bedankt. Officieel zat ook Rik Leemans in de

commissie, maar zoals ik het me herinner vielen de bijeenkomsten meestal samen met jouw reizen naar uithoeken van de wereld. Ik verbaasde me telkens weer over de afspraken die ik met je had als je wel in Nederland was. Ondanks je overvolle agenda nam je altijd ruim de tijd om alles door te spreken en de snelheid waarmee je mijn stukken en ideeën in je opnam en vervolgens van commentaar voorzag was duizelingwekkend. Als ik vanuit Bilthoven weer naar Utrecht reed tolde mijn hoofd van alle nieuwe plannen.

Marcel de Wit was mijn collega-AIO binnen dit project. Hoewel de ontwerpers een route hadden geschetst, waarin de twee promotieonderzoeken samen één groot model zouden opleveren, kwamen wij al snel tot de conclusie dat dat niet zou gaan lukken. Maar dat mocht de pret niet drukken en we bleven goed en regelmatig contact houden. Het waren altijd leuke ochtenden daar beneden in de Zonneveldvleugel.

Alfred Stein was degene die me op het spoor van geostatistiek zette voor het oplossen van mijn wolkenprobleem. Edzer Pebesma heeft op afstand Gstat in Wageningen geïnstalleerd en zonder Gstat had mijn promotieleven er volkomen anders uitgezien. Kees van Diepen heeft me ingewijd in de wereld van oogstschattingen en WOFOST, en Hendrik Boogaard heeft alle oogstgegevens voor het studiegebied tevoorschijn getoverd. Kees Bol zorgde dat de workstations altijd bleven draaien, dat mijn tapes met honderden satellietbeelden in no time in mijn directory kwamen, en als ik de computer 's nachts door wilde laten rekenen, dat de processen niet halverwege werden afgebroken.

Collega's binnen de vakgroep en later binnen het Centrum voor Geo-informatie boden technische ondersteuning en een fijne werkomgeving. Henk Schok heeft meegedacht over menig Imagine-raadsel. John Stuiver heeft me de wondere wereld van ArcInfo getoond. De eerste paar jaar aan de andere kant van de stad en later op dezelfde gang, waren Gerard Nieuwenhuis, Sander Mücher, Henk Kramer en Allard de Wit altijd bereid om hun ervaring met NOAA-AVHRR, Imagine en werken op Europese schaal te delen. Monica Wachowicz heeft me vaak met engels geholpen in ruil voor 'Nederlandse les'. De pannenkoekenmaaltijden en strooptochten bij Unitas, en later de lunches in Alterra-Oost, het bommen, het bouwen van bananen, en de (variaties op) taart geserveerd op de hangplek waren een leuke aanvulling op het werk. Alle voormalige en huidige GIRS-ers en CGI-ers, bedankt!

Met mijn kamergenoten Sytze de Bruin, John van Smaalen en Marlies Sanders heb ik heel wat afgediscussieerd en –gefantaseerd, en koffie of liever thee gedronken op de AIO-zaal op Landmeetkunde. Zonder jullie had ik veel minder koekjes gegeten, niet als een AI-wagentje door de zaal gereden en vooral een veel minder gezellige tijd gehad. Sytze wil ik ook nog bedanken voor alle computerhulp en de goede tijd in Alterra.

Toen mijn AIO-aanstelling was afgelopen, maar mijn proefschrift nog niet was afgerond, heb ik een jaar lang gewerkt aan een BCRS-project. Hoewel het oorspronkelijk niet de opzet was, is uiteindelijk al het werk dat ik binnen dat project

heb gedaan ook in dit proefschrift opgenomen. MERILanders Freek van der Meer, Andrew Skidmore, Wim Bakker, Gerrit Epema, Steven de Jong en Jan Clevers bedankt voor het meedenken en –schrijven.

All satellite images that I used and all images that I thought I would use were kindly provided by the Joint Research Centre of the European Union in Ispra, Italy. They did all the preparation of the images, so when I received them I could start using them right away.

Van het gevoel dat je bekruipt wanneer je als AIO een tijdje bezig bent met je onderzoek en je gaat vermoeden dat het niet allemaal (of allemaal niet) gaat lukken, heb ik nergens een betere beschrijving gevonden dan in 'The last continent' van Terry Pratchett. Ponder Stibbons is de jongste tovenaar aan de Unseen University in AnkhMorpork op de Discworld; Hex is zijn computer.

> "Ponder Stibbons was one of those unfortunate people cursed with the belief that if only he found out enough things about the universe it would all, somehow, make sense. The goal is the Theory of Everything, but Ponder would settle for the Theory of Something and, late at night, when Hex appeared to be sulking, he despaired of even a Theory of Anything."

En tja, dan blijven de belangrijkste mensen over om te bedanken. Mijn lieve ouders. Jullie probeerden me al vroeg te laten zien hoe de wereld in elkaar zat (ik werd als kleuter al meegenomen in een vliegtuig!) en vooral om het zelf te ontdekken en erover na te denken. Tijdens dit promotieonderzoek heb ik veel ontdekt en nog veel meer nagedacht, en hoewel het niet altijd meeviel, heb ik zelfs een proefschrift bij elkaar geschreven. En altijd waren jullie bereid in te springen of voor een ontspannen weekend te zorgen.

En Hein, hoe kan ik nou in een paar woorden genoeg zeggen om jou te bedanken? Samen promoveren viel niet altijd mee, regelmatig kwamen de discussies van het werk mee naar huis. Maar jij bent er een held in om ook van de niet-wetenschappelijke wereld te willen genieten, zodat we de afgelopen 7 jaar veel meer hebben gedaan dan alleen maar werken. Er waren prachtige reizen naar Zuid-Amerika, heerlijke weekenden naar de Wadden, lekkere Oud-en-Nieuw weekjes, gezellige avonden in Utrecht, thuis of in de stad, met of zonder spelletjes, kortom genoeg om een volwaardig niet-promotieleven te leiden.

Sinds twee jaar heb je de volledige steun van Manou, die ook volop van de niet-wetenschappelijke wereld wil genieten. Zij overtuigt ons dagelijks van het genot van een tocht naar de zandbak, de schommel of de glijbaan, en daar, naast die zandbak, schommel of glijbaan, lijkt het belang van een proefschrift ook wel heel erg klein. Lieve Hein en Manou, jullie hebben er voor gezorgd dat het leven naast en na het proefschrift meer dan de moeite waard is. En of we nou in Utrecht, Ann Arbor of Yellowstone zijn, het leven met jullie is prachtig.

Ann Arbor, augustus 2001

INTRODUCTION 1

1.1 Background

In October 1999 the world population reached 6 billion people (UN, 1999). Despite current and historic predictions that population growth would diminish due to limitations of food production capacity, there is still sufficient food to feed the people currently inhabiting our planet (Bennett, 2000). Through extension of the agricultural area and intensification of agricultural practices, production kept pace with the growing population. Associated with the increasing production, however, environmental degradation rose worldwide to serious levels of concern.

In Europe, the area in use for agriculture showed periods of expansion alternating with contraction. Since the end of the 18th century the area expanded as productivity could not keep up with the European population increase (Rabbinge and Van Diepen, 2000). This continued until the '50s, when there was a sudden intensification leading to increased productivity due to a combination of factors: new varieties with a high harvest index, better-used fertilisers, improved water management and appropriate crop protection led to a synergism that resulted in a strong increase of land productivity.

Simultaneous to this intensification, the environmental impact of agriculture showed a strong increase and environmental problems are now common throughout Europe (EEA, 1995b). Productivity is believed to increase even further since the majority of agricultural area is still sub-optimally used (Rabbinge et al., 1994) and the environmental impact accompanying its rise during the last five decades, might continue to increase as well. However, the general increase of environmental problems also raised the awareness that environmental impact must be limited in order to keep a liveable world (e.g. UN, 1992).

1

Consequently, continuing major changes in land use can be anticipated in Europe in the coming decades such as production increase and area reduction (Bouma *et al.*, 1998).

From its very start, agriculture has had environmental impact by its mere existence. Man adapt the environment in favour of crop growth or cattle raising, and consequently soil properties will change, some plants disappear, light conditions change, etc. When these practices are extensive the impact will be limited to the direct environment and nature could recover within some years, i.e. both the spatial and the temporal effects are limited. However, when this adaptation crosses a certain threshold, a wide range of environmental problems may arise.

Two types of ecosystems can be distinguished when considering environmental impact of agriculture: agricultural ecosystems and non-agricultural ecosystems, where the non-agricultural systems include natural, semi-natural and built-up areas. Environmental problems resulting from agriculture occur in both types of systems, but they show themselves in different ways. In agricultural ecosystems, they lead to reduced production and consequently to higher investments to retain the production level. Few data on production losses resulting from e.g. soil degradation exist, but available data indicate that for some countries these losses may be over 5% of total production (OECD, 1997a). Environmental problems in natural ecosystems result in reduced quality of soil, water, air, flora and fauna.

The European Environmental Agency produced a concise overview of environmental processes caused by agricultural activities (table 1.1; EEA, 1995b). The most widespread problem in Europe is soil erosion, which is the removal of soil particles from the topsoil at a rate that exceeds their replacement by weathering. It is a natural process, although human activities, especially agriculture, have considerably deteriorated the process (EEA, 1995a; Mannion, 1995). About 12% of all European territory is affected by water erosion and a further 4% by wind erosion (EEA, 1995b). Activities giving rise to erosion are specialisation and concentration, and mechanisation.

Other widespread problems in Europe are eutrophication, pesticide application, acidification, water stress, desiccation and salinisation. Eutrophication is the natural process of nutrient enrichment of lakes, rivers, coastal areas and groundwater. Fertilisation with animal manure or commercial fertilisers is the major cause of the widespread acceleration of these processes (Mannion, 1995; OECD, 1997a).

The environmental effects of pesticides mainly affect non-agricultural ecosystems. They accumulate in food chains with consequent indirect impacts down the food chain, while they also may directly eradicate, remove or reduce food sources for birds and mammals. The leaching of pesticides into rivers, lakes and coastal waters is known to cause damage to aquatic bio-diversity (OECD, 1997a), although the knowledge on effects of pesticides and their residuals in ecosystems is far from complete (EEA, 1995b).

2

Acidification is the process of ammonia from agriculture undergoing chemical conversion in the atmosphere into acid substances, which lead to changes in the chemical composition of soil and water and which are a serious threat to bio-diversity and ecosystems in general. They also cause material damage and lead to enhanced fluxes of nitrates and heavy metals in ground water (EEA, 1995a). In some countries 90% of ammonia emissions into the air result from agricultural activity (OECD, 1997a). Of the European Union territory 9% is threatened by acidification (EEA, 1995b).

Soil water conditions can be improved by installation of drainage and/or irrigation systems. Drainage accelerates water transport from the soil to surface waters. Irrigation applies water to crops, using either surface or ground water. Both systems can deplete ground water resources. In areas with deep ground water, this may lead to water stress (OECD, 1997a). In areas with high ground water tables (e.g. wetlands), this may result in desiccation (Brouwer, 1995). Desiccation is the decline of nature due to falling water tables, decreasing intensities of upward seepage, and the inlet of alloctonous surface water to the extent that it is used to compensate the negative effects of groundwater shortages (Witte, 1998). An unfavourable side effect of irrigation is salinisation. In areas subject to low precipitation combined with high temperatures and many hours of sunshine, irrigation may lead to levels of salt concentrations in soil and water harmful to agriculture (EEA, 1995b).

In contrast agricultural practices can also help to prevent environmental problems. Some practices like terracing in hilly and mountainous areas, can help minimise soil erosion and prevent landslides (OECD, 1997a). In addition, Avery (1999) argues that the intensification of agriculture can be used and is needed to limit the extension of agricultural areas, thus preventing the loss of habitats and wildlife.

During the last 10 to 20 years the focus of environmental policy and research shifted from a local / national perspective to a more international or even continental approach. In 1992 the United Nations organised a conference on global issues in Rio de Janeiro, where they proclaimed, that *in order to achieve sustainable development, environmental protection shall constitute an integral part of the development process and cannot be considered in isolation from it* (UN, 1992).

The various policies in the European Union now always account for environmental aspects (Treaty of Maastricht, 1992), although the aims of the Common Agricultural Policy still do not include explicit protection of the environment. The European Union did take several agricultural measures in favour of the environment (Brouwer and Berkum, 1996; EU, 1999a), but the effects are still limited since most of their programmes were only launched with farmers in 1995 and 1996 (EU, 1999b).

Table 1.1 Overview of significant environmental impacts from agricultural practices (EEA, 1995) (reprinted with permission)

Agricultural practice		*Environmental media*	
		Air	*Water*
Specialisation and concentration	Increasing field sizes, land consolidation , removal of vegetation cover		•Removal of vegetation cover → increased surface runoff and sediment load → sedimentation, contamination, eutrophication
	Intensive animal husbandry	•emissions of methane, ammonia	•silage effluent → organic matter and nutrients in waterbodies (see fertilisation)
	Intensive cropping		•soil erosion → increased sediment runoff → water pollution (see Fertilisation)
Fertilisation	Animal manure (slurry or solid)	•ammonia and nitrous oxide volatilisation •unpleasant odours	•spills of organic matter and nutrients to waterbodies → eutrophication → oxygen depletion → excess algae and water plants, fewer fish •leaching to groundwater → pollution of drinking water supply
	Commercial (nitrogen, phosphorus)	•ammonia and nitrous oxide release	•nitrate leaching and phosphate runoff → elevated nutrient levels → eutrophication of fresh and coastal waters, and contamination of aquifers
	Sewage sludge		•leaching of nutrients and other chemicals to aquifers
Pesticides application (insecticides, fungicides, herbicides)		•evaporation and pesticide drift → adverse effects in nearby ecosystems → long-range transport of pesticides in rainwater	•leaching of mobile residues and degradation products → groundwater → possible impacts on wildlife and fish and drinking water resources

4

Soil	*Nature and wildlife/Landscapes*
•removal of vegetation cover → soil erosion •inadequate management → soil degradation	•loss of hedgerows, woodlands, small watercourses and ponds → decrease in landscape variety and reduction in species diversity •land degradation if activity not suited to site
•spreading of manure high in heavy metal content → elevation of soil concentrations	•construction of storage silos → changed landscape
•loss of organic matter in soil → deterioration of soil structure, soil biological activity → decline in soil fertility and adsorption capacity → increased erosion and runoff	•increasing field sizes and land consolidation possibly required → changed landscapes
•accumulation of heavy metals and phosphates in soil (may enter food-chain) •overapplication → local soil acidification possible	•potential loss of nutrient-poor habitats
•accumulation of heavy metals → effects on soil microflora and entry into food-chain •overapplication → local acidification → deterioration of soil structure, imbalance in nutrients	
•accumulation of heavy metals and organic micro-pollutants (may enter food-chain)	•direct contamination of fauna and flora with microbial agents and chemicals
•accumulation of persistent pesticides and degradation products → contamination and leach into groundwater •use of broad spectrum pesticides → impacts on soil microflora and may affect or eradicate non-target organisms	•possible wildlife poisoning incidents (non-target-organisms) •loss of habitat and food source for non-target species •resistance on some target organisms

Continued on next pages

5

Table 1.1 *continued*

Agricultural practice		Environmental media	
		Air	Water
Irrigation/water abstraction		•increase of nitrous oxide and methane emissions (greenhouse gases)	•lowering of the water table → soil salinisation/alkalinisation → impacts on surface and groundwater quality → drinking water •high abstraction required for some crops → strain on resources in some areas
Drainage		•chemical changes in soil → greenhouse gases	•channelisation → hydrological changes → possible decrease in aquatic biodiversity •water abstraction → lowering of water table
Mechanisation	Tillage, ploughing	•increase in dust and particulate matter in air	•increased surface water runoff, sediment load and associated particles → sedimentation, contamination, eutrophication
	Use of heavy machinery		•soil compaction → increased surface runoff and sediment load → sedimentation, contamination, eutrophication

There is a need for information that is up-to-date and internationally standardised and comparable in order to evaluate the effectiveness of these programmes. A similar need for standardised land cover and land use information over large areas exists for environmental modelling, research and policy (Van de Velde *et al.*, 1994). Currently, information on agriculture and its environmental impact are mainly retrieved from statistical data. For example, the OECD (Organisation for Economic Co-operation and Development) developed environmental indicators for agriculture based on the analysis of statistical data that were collected at national level (OECD, 1997b). Major drawbacks of this approach are related to the thematic, spatial and temporal incompatibility. Each country collects its own data with different variables at different scales and at different timespans, which prohibits the construction of a complete overview of the environmental impact of agriculture at one specific point in time.

Remote sensing offers a powerful alternative as a data collection approach. Satellite images cover large areas and show reflectance and emission characteristics of land cover throughout the image in a standardised way. For studies at the continental scale, NOAA-AVHRR images (National Oceanic and Atmospheric Administration-Advanced Very High Resolution Radiometer) (USGS, 2000) are a valuable information source. Each scene covers an area of 2800 * 2800 km², thus

Soil	Nature and wildlife/ Landscapes
•waterlogging → salinisation/alkalinisation of soils •use of saline or brackish waters for irrigation in hot climates (high evaporation) → increased salt precipitation and carbonates → possible salinisation /alkalinisation	•soil salinisation/ alkalinisation → losses of species, desertification •drying out of natural elements affecting river ecosystems
•oxidation of organic soils → reduction in organic content, acidification and changes in soil structure	•potential loss of wetlands and changes in botanical composition of grassland, fens and other habitats
•ploughing up and down slopes → soil erosion (water and wind)	
•compaction and erosion of topsoil	

covering continental Europe with two scenes. The pixel size measures 1.2 km² at nadir. The AVHRR sensor is mounted on the Polar Orbiting Environmental Satellites, which pass over each area twice a day. Although originally designed for meteorological purposes, the sensor characteristics allow for distinction between different land cover types (table 1.2). AVHRR images are currently used for land cover mapping and monitoring (Belward *et al.*, 1999; Defries and Townshend, 1994; Gutman and Ignatov, 1995; Lambin and Ehrlich, 1996; Mücher *et al.*, 2000; Prince and Goward, 1996).

However, there are problems associated with the use of satellite images for monitoring. Classification accuracies seldom rise over 85% (pers.comm. Prof.Dr. G.M. Foody, University of Southampton). For the comparison of two classified images one has therefore to cope with a propagating uncertainty of 15%. Besides, the spatial accuracy can be less than desired. Images are generally geometrically corrected and geocoded after acquisition, so for each pixel the geographical position is known. The precision of this process can be as high as half a pixel, but for monitoring (multi-temporal comparison of images) this implies that possibly different pixels are compared. So, one could argue that we should not monitor individual pixels but some type of pixel aggregates.

7

Table 1.2 Spatial and spectral characteristics of NOAA-AVHRR

Pixel size at nadir	1100m
Band Number	Spectral coverage (in nm)
1	580-680
2	725-1100
3	3550-3930
4	10300-11300
5	11500-12500

An important disturbing factor for remote sensing observations is the atmosphere. Satellites are in orbit at a distance of about 800km above the Earth's surface, so the radiation registered by the satellite sensor and captured in the images has to pass through the atmosphere first. Absorption and scattering are common problems resulting in reduced data quality. Clouds prohibit the view of the surface completely and result in missing values for the land cover data. Other factors introducing variation in the data are the sun elevation, the sensor's scan angle and sensor instability. Variation in sun elevation causes more or less shadow and also influences reflection. Scan angle determines which side of objects is looked at and particularly with large variation in angle this can result in strong differences in reflection and emission. Due to sensor instability equal incoming radiation is registered as different values in the image.

The environmental impact of agriculture changes as a result from changes in intensity and/or changes in area used for agriculture. Environmental problems resulting from agriculture are currently widespread in Europe and policymakers seek to reduce those problems. To take relevant measures there is a need for up-to-date, internationally standardised and comparable information. Current indicators cannot provide this information.

NOAA-AVHRR images could offer a valuable information source. They cover large areas, they are frequently available, they have been recorded for two decades so significant time series exist and they have two relevant bands for vegetation and crop studies. If the gap between indicators describing environmental problems and land cover radiation shown in the images is bridged, NOAA-AVHRR images could prove to be a reliable basis for a monitoring method providing up-to-date information on environmental impact of agriculture to policymakers.

1.2   Objectives and research questions

In 1995 the RIVM (the National Institute of Public Health and Environment of The Netherlands) started a project on surveying pollution from agriculture at the European scale. Two partners were involved, the Department of Physical Geography at Utrecht University and the Laboratory of Geo-information

and Remote Sensing at Wageningen University. In Utrecht attention was focussed on the development of a spatial model of diffuse pollution at the European level, published as the Ph.D. thesis by De Wit (1999). In Wageningen the possible role of remote sensing to provide data on agriculture and its environmental impact in the European Union was investigated, resulting in the current thesis.

The aim of the study presented in this thesis is to develop a method to provide policymakers with up-to-date information on changes in environmental impact of agriculture using NOAA-AVHRR images. This method requires new indicators and new spatial observation units, since current descriptions of environmental problems are incompatible with the thematic and spatial characteristics of AVHRR images. The possibilities and limitations of remote sensing for monitoring agriculture at the European scale are investigated and some new procedures to use remote sensing data for monitoring agriculture are proposed and tested. The following research questions are addressed:

- **Which aspects of agriculture characterise the environmental impact it provokes and are possibly observable by NOAA-AVHRR?**
  Environmental impact of agriculture is mostly described in terms of problems resulting from it, like those presented in table 1.1. NOAA-AVHRR images do not reflect these problems, but merely show radiation characteristics of land cover. When NOAA-AVHRR is to be used for monitoring environmental impact, indicators bridging the gap between current descriptions of environmental impact and radiation of land cover are required.

- **Which methods can quickly detect changes in environmental impact of agriculture when applied to NOAA-AVHRR images?**
  Many different change detection methods are available in the remote sensing literature, but few have been applied to NOAA-AVHRR data. With its pixel size and frequent revisit time, NOAA-AVHRR provides a unique data source, but it is at the same time quite sensitive to radiometric distortions and misregistration. This requires meticulous consideration of existing techniques and might ask for a new approach. Changes should be detected in time, so that policy can be based on the actual situation.

- **Which spatial observation units match both agriculture and NOAA-AVHRR?**
  The size of agricultural fields in Western Europe, and most other parts of the world, is such that they are not recognisable in AVHRR images. Besides, their number is too large to deal with in a study at the continental scale. To describe agriculture, or its environmental impact, in a sensitive manner, spatial units related to agriculture must be defined. Next, to detect changes in those units using NOAA-AVHRR imagery, these spatial units must be observable in the images.

9

- **How can missing values in NOAA-AVHRR images due to cloud contamination be best replaced by estimated land cover radiation data?**
  The size of AVHRR images is such that they will, at least in Western Europe, always contain some degree of cloud contamination. When an image of the desired area is found with very limited cloud cover, small clouds will still hamper its utility. Replacing those clouds by estimated radiation values will significantly increase the availability of cloud-free images.

- **What could future imagery offer to change detection at the European scale?**
  At the start of this study, the NOAA-AVHRR sensor was the most promising system to collect information on agriculture at the European level. Currently, new sensors with spatial resolutions of 300-500m are available or will soon be launched. This spatial resolution fills the long-existing gap between the high resolution of SPOT-HRV and Landsat-TM and the low resolution of NOAA-AVHRR. These images might be of great value to studies at the continental scale by offering an overview without all the detail visible in high-resolution images, but showing more spatial aspects than AVHRR. No actual data were available yet, but by comparing sensors with a range of resolutions, the improvements that can be expected from the 300m-MERIS pixel compared to AVHRR, are estimated.

1.3   Study area

For a study aiming at the development of a change detection method, it is important to select a study area where actual changes occurred and where sufficient data are available to calibrate and validate the method. Originally, this study was intended to cover two study areas: one with agricultural changes in a data poor environment, and one with sufficient data availability, but possibly without significant changes. Hungary and the Rhine Basin seemed ideal to serve as study areas. In Hungary considerable agricultural changes followed the political changes of the late 80's and data provision was well organised compared to other East-European countries. The Rhine Basin was selected as study area together with De Wit at Utrecht University, because of its intensive agriculture. Environmental problems in the area are widespread and all problems mentioned in table 1.1 are present, except desertification and soil salinisation. In the Rhine Basin changes were not as profound as in Hungary, although EU policy changes in the early '90s (section 2.1.2) caused at least some changes. The major advantage of the Rhine Basin study area is the abundance of statistical data on agriculture at a detailed level.

Data collection in Hungary proved very complicated, unrealistically expensive, and finally an insuperable obstacle. As a result, the Rhine Basin

remained as the only study area. Since this study aims at the development and demonstration of a change detection method, a smaller area than the entire Rhine Basin is sufficient and more practical. Therefore, the study area was limited to the German part of a rectangular area of about 200*300 km² in size, located within the basin (figure 1.1). The Rhine valley occupies the central part of the area. In the southeast the Black Forest is located, in the north the Eiffel. Both the soils and the continental climate are favourable for agriculture.

The area overlaps with six states: Bayern, Baden-Württemberg, Hessen, Nordrhein-Westfalen, Rheinland-Pfalz, and Saarland. The main economic centres are Stuttgart and Frankfurt. Almost 50% of the area is used for agriculture and about 35% of the area is covered by forest (GIC, 2000).

1.4   Structure of the thesis

After setting the framework and describing the objectives of this study in chapter 1, chapter 2 gives some theoretical background to agriculture and the available sources providing information on agriculture and the environmental impact it provokes. It concludes with the theoretical framework and conditions of the required method.

The following chapters each cover a part of the procedure to come to the final method. In chapter 3 the spatial observation units to which the method should be applied are defined. For that, two alternative polygon sets are compared to land cover units derived from NOAA-AVHRR imagery using a geometric similarity index. This index is also developed and tested in this chapter.

Chapter 4 compares several methods to clean up cloud contaminated NOAA-AVHRR scenes. Conventional methods use pixel values from previous or following days to replace the clouded pixels. Here geostatistical methods using values from surrounding pixels sometimes in combination with an image of the following day are compared to the conventional methods. In total seven methods are tested against four validation sets.

Chapter 5 discusses variables to characterise environmental impact of agriculture. Variables should be observable in NOAA-AVHRR images, which basically means that they should describe changes in environmental impact in terms of land cover.

Chapter 6 combines the findings of the previous chapters and incorporates them in the procedure to test three alternative change detection methods. The new methods are expected to be less sensitive to misregistration and radiometric effects than conventional pixel-based change detection methods, because they operate on a region-base.

In July 2001 ENVISAT-MERIS will be launched. This sensor provides images with 300m pixels and 15 high-resolution bands. The added value of MERIS' spatial resolution is investigated in chapter 7. Actual MERIS data are not available yet, but by using images with pixel sizes ranging from 25 to 1100m, the expected performance of MERIS' 300m pixel in relation to AVHRR's 1100m pixel can be
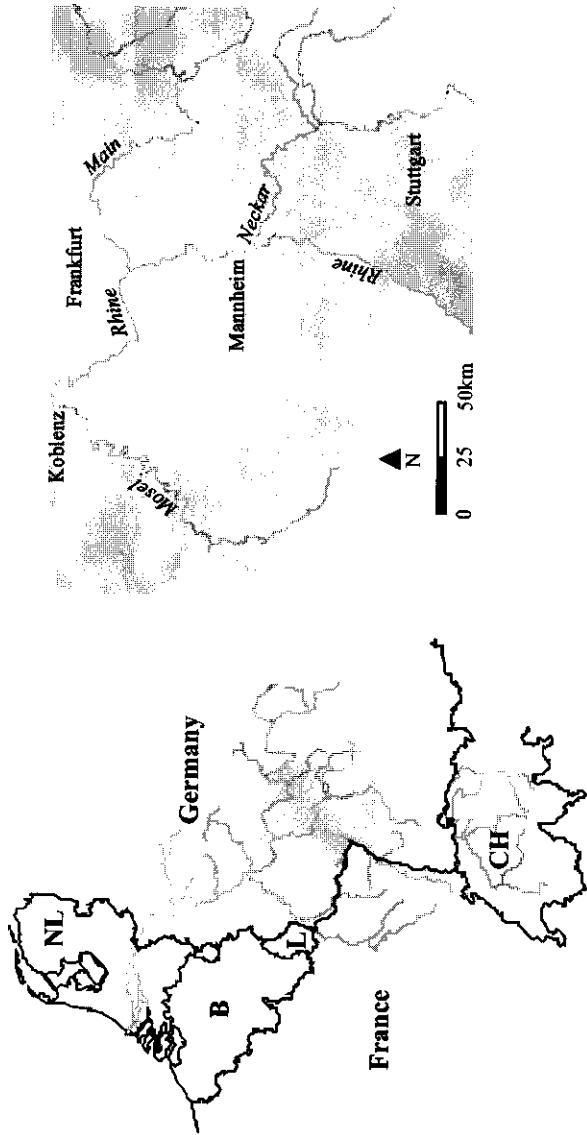
Figure 1.1 Location of the study area (on the left) and topography of the study area (on the right). In the left image black lines show country borders and grey lines show the river Rhine and its tributaries. NL stands for the Netherlands, B for Belgium, L for Luxembourg, and CH for Switzerland.

estimated. For this, the Stained Glass Procedure, which is described in chapter 7 as well, is developed.

Chapter 8 gives concluding remarks on all findings of the previous chapters and ends with recommendations for further research.

AGRICULTURE AND ITS MONITORING

2

This chapter provides specific background information on agriculture, the existing monitoring practices and the available information sources, before different aspects of the required method will be studied and defined in the following chapters. It explains why agriculture cannot exist without affecting the original environment and describes theoretical production levels. It gives an inventory of existing, international monitoring attempts and of different types of information sources with their respective (dis-)advantages. Combination of these sections leads to the final section which gives an overview of the requirements to be met and an outline of the method to be developed within this study.

2.1   Agriculture

Agriculture is the production of crop plants through cultivating the soil and the rearing of animals (Mannion, 1995). Grigg (1995) defines it as the purposive raising of livestock and crops for human needs. The addition of 'purposive' excludes hunters and gatherers who have not domesticated the plants and animals they use for food. Both definitions indicate a man-induced change of the ecosystem in favour of agriculture.

In a natural environment the major land cover types are vegetation, surface water, glaciers and bare rock or soil. The presence and type of vegetation is determined by the bio-physical environment and the availability of species. Every species can grow within a range of conditions set by environmental factors like temperature, solar radiation, and nutrient availability. Each factor has related variables like minimum and maximum daily temperatures, length of the growing season and day-length, etc. A species has a specific range of values for every variable in which it can function, from the minimally required to the maximally tolerated conditions. Together these ranges form the ecological amplitude, which

indicates under which circumstances the species can appear (Klijn, 1995).

All variables influencing the appearance of a certain plant can be put along axes to compose an imaginary multidimensional space. By outlining the specific ranges on the axes a sub-space is created which represents the requirements on the environment of a specific species. Within ecology this sub-space is called the fundamental niche (Pianka, 1976; Hutchinson, 1957) or habitat (Whittaker *et al.*, 1973); here it will be indicated by fundamental niche. It is entirely defined by the requirements of a species and has no geographic component. A species could grow anywhere where the environment meets the criteria of this fundamental niche.

In practice its area of possible settlement will be limited by competition. When two species are present in one location and their fundamental niches overlap, competition will arise. Unless one of the species expels the other, they will have to share available resources. As a result they cannot fully exploit their fundamental niches, reducing their area of possible settlement to the realised niche (Klijn, 1995; Hutchinson, 1957).

The extent of the realised niche depends on the natural environment and the presence of other species. If the natural environment corresponds to some part of the fundamental niche, which indicates the tolerance of a species for all variables, a species can grow there. But although a species can grow in all locations situated within the fundamental niche, it does not grow equally well throughout the range. There will usually be an optimum part of the niche and suboptimum conditions will prevail near the boundaries (figure 2.1) (Hutchinson, 1957; Whittaker *et al.*, 1973). A bell-shaped curve often indicates the species abundance in relation to a variable (Jongman *et al.*, 1987); the closer variable values at a certain location resemble the optimum values, the better the species will perform and the larger the realised niche will remain during competition.

In agriculture humans try to widen the realised niche of a desired crop to resemble its fundamental niche as much as possible. All agricultural practices performed out in the field before harvest can be considered as the widening of the realised niche. Fields are cleared and weeded to eliminate competition from undesired species. Besides, the bio-physical variables are adapted: fertilisers are applied to improve the nutritional state of the soil, irrigation or drainage is applied to improve the moisture content of the soil, tillage aims to improve the soil structure, etc. All practices aim to increase the resemblance of the environment to the optimum of the fundamental niche and thus to improve the production.

The actual degree of production improvement results from both the bio-physical and the socio-economic potential (Skole, 1996). The natural environment can indicate a very high potential level but in order to reach a high actual level the socio-economic environment should be such that sufficient yield-increasing and -protecting measures are taken. I.e., the socio-economic situation determines if and to what degree the natural environment is adapted to optimise the production level.
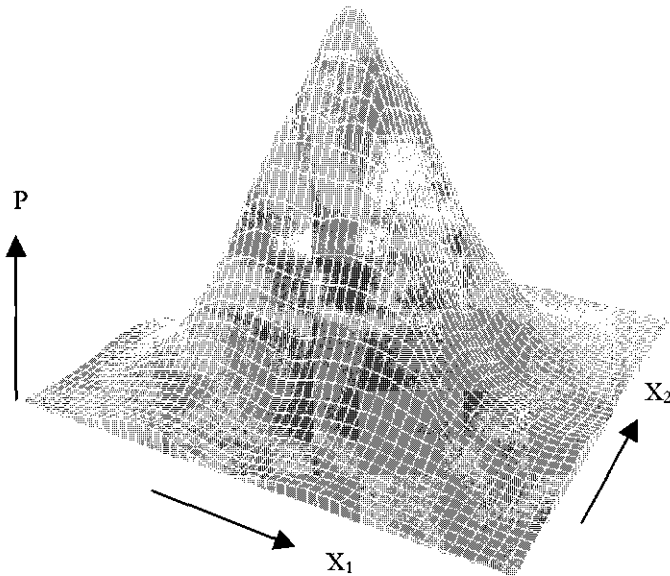
Figure 2.1 Example of a three dimensional view of a bivariate normally distributed surface. Vertically the occurrence probability (P) is plotted. In the horizontal plane two environmental variables (X_1 and X_2) are plotted (after Jongman *et al.* 1987).

2.1.1 Production levels

Three theoretical production levels can be distinguished (Penning de Vries and Van Laar, 1982): potential, attainable and actual (figure 2.2). The potential level is determined by CO_2 concentrations, the amount of radiation, temperature and crop characteristics. It is comparable to the fundamental niche of natural vegetation. The attainable level is lower than the potential level. It is determined by environmental conditions, more specifically by the effect of two limiting factors, water and nutrient stress. The actual level, finally, is lower than the attainable level, due to additional reducing factors. Competition with weeds, the outbreak of pests and diseases, pollution, and poor management practices all prohibit the actual level to reach the attainable level.

The potential level is the highest level that possibly can be obtained. Its value is determined by model simulation (Penning de Vries and Van Laar, 1982). No measures can be taken out in the field to raise this level. The attainable and the actual levels, however, can be increased by applying yield-increasing and yield-protecting measures, respectively. Examples of yield-increasing measures are fertilisation, irrigation, and drainage; examples of yield-protecting measures are weeding, and the use of pesticides and insecticides. Although the mere presence of agriculture will have an environmental impact, in Europe the main impact is caused

17

An important difference between the CAP and the Environmental Policy of the EU is their nature of competence. While the CAP is exclusive, the Environmental Policy is subsidiary, meaning that the EU only intervenes when its action will be more efficient than the one of the Member state (EU, 1999a). As a result environmental policies differ strongly between countries, and sometimes, when measures are introduced at a regional level (like in Germany), even within countries.

2.1.3 Changes in agricultural land use

Before actually concentrating on changes in agricultural land use, it is important to define the concepts of land use and land cover. Land cover refers to attributes at or directly below the Earth's land surface, including vegetation, soil and man-made structures, etc. Land use refers to the purpose for which humans exploit land cover. Grass, e.g., can be used for agriculture and for recreation (Turner *et al.*, 1993). Land cover is a resultant of land use. Agriculture is a form of land use, while the crops out on the fields form the resulting land cover.

Changes in agriculture may result from changes of both bio-physical and socio-economic factors (figure 2.3). As socio-economic factors are more dynamic than bio-physical factors, they are mostly responsible for agricultural changes (Mannion, 1995; OECD, 1998). Socio-economic factors depend on social aspects like demography, population density and knowledge level, and economic aspects like capital availability, level of mechanisation and political incentives. In the European Union policy instruments force the major changes.

Since agriculture is a type of land use, it will as such result in a specific type of land cover. And changes in agriculture will therefore cause either qualitative or quantitative changes in land cover, indicated by land-cover conversion or land-cover modification, respectively (Turner *et al.*, 1993). Land-cover conversion refers to the situation where a new land cover type replaces the old one, e.g. maize is replaced by potatoes. Land-cover modification refers to changes in intensity, i.e. the maize yield will change. Three types of changes can be identified:

- the area used for agriculture might change (*conversion*).
- the crop type might change (*conversion*).
- the intensity might change (*modification*).

Most fields are sowed according to rotation schemes. These cause annual changes of crop type on fields inherent to the system but do not indicate a change of agriculture. In larger regions the different stages of the rotation schemes each have an equal spatial extent with annually rotating locations. Relevant changes of crop type are those resulting from change of rotation scheme.
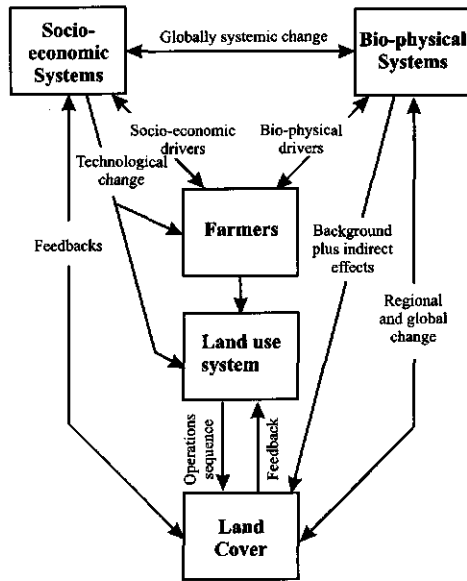
Figure 2.3 Fundamental structure of agricultural land use and land cover change. Farmers are influenced by both socio-economic and bio-physical factors, which results in a specific land use system. This system is reflected in specific land cover. (after Skole, 1996)

2.2   Monitoring agri-environmental developments

The agri-environmental policy aims to reduce the negative impact of agriculture on the environment and to maintain its positive effects. Evaluating the policy and inventorying the environmental impact of agriculture is essential for three reasons:

- to see whether the current policy is effective, i.e. whether the measures lead to the expected results,
- to check whether the countries or regions fulfil the requirements imposed by the regulations,
- and to determine the state of the environment in order to decide whether more measures are required.

When any of these three reasons give cause for concern, policy needs to be adapted (EU, 1999b).

21

2.2.1   Existing monitoring

Three different organisations are known to monitor the (agri-)environment of Europe on a more or less regular base: the Organisation for Economic Co-operation and Development (OECD), the European Environmental Agency (EEA), and the European Union. They follow different approaches.

The OECD, in which the Commission of the European Communities takes part, is working on definitions of agri-environmental indicators (OECD, 1997a), which can be based both on agricultural practices and on environmental parameters. Their aim is to support the evaluation of the agri-environmental policy at national level, to examine the response by the agricultural sector to the environmental policy, and to investigate available options for the agricultural sector to meet environmental targets (Brouwer, 1995).

Examples of indicators (OECD, 1997a) are the soil surface balance and the farm gate balance to monitor nutrients, the pesticide use indicator, and the agricultural water use indicator. The soil surface balance and the farm gate balance both require coefficients to determine the nutrient content of in- and outputs. The pesticide use indicator measures the trends in pesticide use classified by risk according to related environmental and health impacts. No universal risk ranking system associated with agricultural pesticides exists. The agricultural water use indicator measures the possible shortage of water resulting from agricultural activities. There is no internationally accepted standardised classification of the types of soil degradation that may be encountered.

The EEA produces both the evaluation of the Environmental Action Programmes (EAP), covering the environment in the European Union, so far produced in 1977, 1979, 1986, 1992 and 1995 (e.g. EEA, 1995a), and an overview of the Pan-European environment (EEA, 1995b and 1998). The EEA combines two approaches: they use observations out in the field to determine the state of the environment and agricultural statistics to monitor the agricultural influence.

The Directorate General VI (DG VI) of the European Commission, responsible for agriculture, lets the individual Member States develop measures to evaluate their agri-environmental policy. They consider it more important to have some evaluation than to have internationally comparable measures. Besides, indicators cannot easily be used in national or regional comparisons, because changes in the state of the environment do not have a constant universal significance. Given the diversity in agricultural and environmental conditions, universal definitions are neither realistic nor desirable. Although evaluation is not considered optional, it is not conditional yet for financing the programmes. So far, evaluation of the agri-environmental programmes is still at an early stage. Few reports are supplied, in many regions and some Member States less efforts have been made, and in some cases efforts have not been sufficient (EU, 1999b).

There is still a range of problems associated with monitoring the agri-environment in Europe. Even though the above mentioned organisations apply different approaches, they encounter similar inconveniences:

- there is no universal relation between agricultural inputs and environmental impact
- data are not available for all countries
- there is a lack of standardisation, which hampers international comparison
- data are often not up-to-date
- it is expensive to collect data with a sufficient spatial resolution
- it is expensive to collect data with a sufficient temporal resolution
- spatial variation of the environment complicates interpretation of data

Part of those problems are overcome in the new, not operational yet, monitoring system defined in the Global Terrestrial Observing System (GTOS) (ISCU *et al.*, 1995). Together with the Global Oceanic Observing System (GOOS) and the Global Climate Observing System (GCOS) this should form a world-wide system including observations on different time and spatial scales according to a both spatially and temporally standardised pattern. This would solve the problems of international comparison and the differences of data availability between countries, although the issue of labour-intensive and hence expensive data collection remains.

2.2.2 Alternative approach to monitoring

The method to be developed in this study should provide information on changes in environmental impact of agriculture. All of the problems mentioned above can have impact on the performance of this method. And even with the standardised GTOS approach, the issue of labour-intensive and hence expensive data collection remains. Part of this problem can be overcome when only a fraction of the area involved would be subject to the inventory at a certain moment. Instead of sampling the entire region, only those parts where changes occurred can be sampled intensively, saving all efforts for those regions where nothing changed. This implies a division of the monitoring process into two steps: change detection and change identification. The procedures for change identification are those currently used, the procedure for change detection needs to be developed.

Changes of interest concern the environmental impact of agriculture. When agriculture changes, this will affect the environmental impact, but moreover land cover will change as well, as discussed in 2.1.3. So, a less expensive system for monitoring agri-environmental developments would be a system that first determines where changes of land cover occurred. These are inevitably caused by changes of agriculture, which will at the same time have caused changes in the environmental impact. By locating the changes first, the labour-intensive procedures need to be applied to the relevant regions only.

2.3 Spatial information on agriculture

To create a spatial overview of environmental impact from agricultural land use, a link between the agricultural processes responsible for the impact and spatial data needs to be created. The process of agriculture is earth-bound and the characteristic spatial units are agricultural fields. Changes in the agricultural system will show on the fields, whether it is a change of crop, change of management intensity or a change between agriculture and another land use class. So the fields are the basic spatial unit. However, when large areas are involved the observations are preferably at a higher aggregation level, because of the amount of data involved and the level of information one is interested in. Crop change at one field is not relevant, but a change of the main rotation scheme in a region certainly is.

Information sources will have their own characteristic spatial units. The spatial observation units of a monitoring system should match the characteristic spatial units of both the process studied and the information source used. So when the units do not match at the lowest level, aggregates have to be formed which are relevant to both the process and the observation system.

No explicit information sources on environmental impact exist, so indirect sources should be converted. Besides the spatial component of the information important requirements are that it should be updated on a regular base to allow for monitoring and that the information should represent at most one growing season. The latter two requirements exclude: -the use of maps, because they represent one moment and are often not updated or only after long irregular time spans, and -the use of the European CORINE database on land cover (CEC, 1993), because the included data represent a period of about 10 years.

An overview of possible data sources, giving a short overview of their characteristics, and their advantages and disadvantages in respect to monitoring the environmental impact of agriculture, will follow next.

2.3.1 Statistical data sets

Statistical data sets show a summary of variables usually for administrative areas, so the spatial detail is reduced. Often they are provided at a regular base, mostly once per year. The size of the represented area varies strongly for different themes, but especially for different countries. They are mostly collected and distributed by the national and local authorities. The European Union introduced the so-called NUTS-regions (Nomenclature Utilisée Territoriale Statistiques). Four levels are distinguished, NUTS-0 to NUTS-3, where NUTS-0 represents entire countries, NUTS-1 large regions, NUTS-2 groups of communities and NUTS-3 individual communities.

Advantages

A major advantage of statistics is that they are available on a regular basis, mostly including the same variables for different periods, thus making the

comparison between different years relatively easy. National statistics, either on regions or the entire country, mostly cover the entire area. Eurostat, the statistical office of the EU, collects and publishes yearly statistics for all member-states on NUTS-0, -1 and -2 regions (Eurostat, 2000). A wide range of themes is included covering both socio-economic and bio-physical subjects. International institutes like FAO yearly collect national statistics in an international compatible format for many different countries (FAO, 2000). They cover subjects related to agricultural production and indices on the production, and are provided for all EU countries. These FAO data are on-line available and are rather up-to-date.

Disadvantages
The main disadvantage of statistics is that they often, particularly when sub-national levels are involved, cannot be compared between different countries, because of thematic, spatial and temporal discrepancies. Variables are defined by the institute collecting the data and are often specific for a region. While statistics are available on community level in one country, the national data may be the most detailed available in another country (Van de Velde *et al.*, 1994). Furthermore, statistics are not collected with the same frequency for all countries or regions, forcing comparison between different years.

Another important drawback of most statistical data sets is that publication takes at least several months and often over a year, which hampers up-to-date information supply.

2.3.2 Crop growth models
Crop growth models can be used to simulate crop production (Penning de Vries and Van Laar, 1982; Bouman *et al.*, 1996). Theoretical yields like discussed in section 2.1 can be calculated using their respective conditions as input. They reveal information on the potential of agriculture, not on its actual state. In the models relevant processes, like photosynthesis, transpiration and growth, are simulated for different phenological stages. Input variables are crop characteristics, meteorological data and soil parameters (if limiting factors are included) and pest and plague data (if reducing factors are included). Biomass accumulation of the entire crop or of specific organs is given as output. When spatial variation from meteorological data and soil parameters is entered in the models, the outcome shows the spatial distribution of biomass. By aggregating the input data to the desired resolution the outcome can be calculated for different aggregation levels. The models can calculate yields for one year or mean yields for several years.

Originally, crop growth models focussed on one plant, including no spatial information at all (Bouman *et al*, 1996). Later models predicting yields per hectare were developed and since 10-15 years yields are predicted and validated for the European Union using a 50*50 km^2 grid (Hooijer and Van der Wal, 1994). Within each grid cell meteorological circumstances are considered homogenous and for

25

each different soil type from the European soil map present in the cell, yields per hectare are calculated. The outcome for the entire cell is determined by a weighted average according to the areas covered by the respective soil types.

Advantages

Crop growth models can provide internationally comparable information. National borders should not influence the outcome, unless they influence the input data. They run per area which is homogenous in soil and meteorological aspects, and by selecting the input data at the appropriate scale they can thus even be applied to large areas like Europe without having to consider variation at the square meter. When the input data are provided with total coverage, the outcome will have total coverage as well. The time delay due to data collecting and publishing is little. As soon as the meteorological data of the growing season are available, the models can be run.

Disadvantages

The crop characteristics are species and variety dependent and in most cases different varieties will be used in vicinity of each other. So when working at areas including several varieties of one species, one should either have different runs for every variety or a generalisation error will be introduced. When working on higher aggregation levels, the environment is assumed to be homogenous, although the process of the actual plant growth takes place at a much lower aggregation level. The conditions for individual plants or even fields vary therefore more than can be captured in the crop growth model. On the other hand, aggregation of the outcome will level out these errors. Crop growth models are like all models simplifications of reality. Information not included in the model, like management practices or yield reducing influences, does not affect the outcome. The outcome of the models provides theoretical yields. For the translation into real figures, additional information from for example statistics or remote sensing is needed.

2.3.3   Remote sensing/Satellite images

Satellite images show reflection and/or emission characteristics of the Earth's surface. Images are recorded using sensors that are mounted on satellites. Many different sensors exist and each has its own spectral (e.g. wavelengths and bandwidths), spatial (e.g. pixel size) and temporal (e.g. recording frequency) characteristics (Lillesand and Kiefer 2000).

In contrast to statistics and crop growth models, which provide direct information on the variable of interest, satellite images provide radiation data that are indirectly related to agricultural variables. There is just one way to retrieve information on agricultural changes from statistics and crop growth models and that is by comparing the status of the variables at different moments. For satellite images there are several alternatives, because the satellite data have to be translated

into relevant information. Generally speaking, there are two options: comparing the reflectance data or comparing the classified images (Singh, 1989; Coppin and Bauer, 1996). Both options include several procedures.

Advantages

Satellite images provide standardised information over large areas, which allows for uniform data interpretation. Images are available at high frequencies and with short delivery times. And many different sensors are available, so one can select the appropriate spectral and spatial characteristics. When working with large areas, NOAA-AVHRR images seem to be very useful. They are recorded twice a day for every area around the world, their spectral characteristics allow for distinction between different land cover classes and their spatial resolution of 1.2 km^2 is such that local features are smoothed out and the larger features are clearly visible. Furthermore, NOAA-AVHRR data have been recorded since two decades, resulting in substantial time series. An alternative could be found in SPOT-VEGETATION, which has a comparable pixel size. However, VEGETATION images have been recorded since 1998 so time series are very limited yet.

Disadvantages

Classification of satellite images mostly results in accuracies of at best 85% (pers.comm. Prof.Dr. G.M. Foody, University of Southampton), indicating that 15% of the pixels got assigned the wrong class label. This hampers change detection because one has to cope with two classifications which both have their limited accuracy. For NOAA-AVHRR images the classification accuracy is even lower, due to their large pixel sizes and their limited number of spectral bands. The International Geosphere Biosphere Data and Information System (IGBP-DIS) Global 1-Kilometer Land-Cover Data Set (DISCover) including 16 broadly defined classes, has a mean accuracy of only 54.5% (Scepan *et al.*, 1999). Mücher *et al.* (2000) obtained a classification accuracy of 69% by combining NOAA-AVHRR data with additional information sources.

Satellite images need to be geo-rectified and geo-coded to know the exact location of each pixel. Accuracies that can be reached lie around half a pixel. When comparing two images that are both rectified with an accuracy of half a pixel, this may result in comparison of a pixel at t_0 with its neighbour at t_1.

Radiometric effects caused by atmospheric conditions, sensor instability, scan angle, and sun elevation can reduce the quality of satellite images (Stow, 1999).

A problem specific to monitoring is that the growing season develops at a different rate each year. This complicates comparison between different years, because phenological stages of vegetation will be reached at different moments.

Spectral information available in satellite images reveals only information on land cover, not on land use. Additional analysis or additional data are needed to translate the land cover data into land use data.

2.4 Conclusions

The aim of this study is to develop a method to provide policymakers with up-to-date information on changes in environmental impact of agriculture at the European scale using NOAA-AVHRR. As described in section 2.2.3 a more cost and time efficient monitoring method will first detect where changes occurred before identifying the changes. This study focuses on the first part of such a method, the change detection.

The method to be developed should provide information useful for the monitoring of environmental impact of agriculture in the European Union. Several conditions are to be met:

- It is supposed to be an information source for policymakers and for environmental models, which often aim to provide information for policymakers. Therefore it should be up-to-date.
- The outcome should be univocal; interpretation should not be location-dependent.
- It should detect regional changes. Since the European Union or even entire Europe should be covered by the method, local changes should not be included. Therefore it is determined that detected changes should occur in areas of at least 250 km².

In section 2.1.3 three types of changes affecting the environmental impact were mentioned: change of agricultural area, change of crop type or rotation scheme and change of intensity. The method to be developed will focus on the first and the third changes, thus leaving out changes of rotation scheme because no spatial information is available at this scale to validate candidate methods.

Section 2.3 described three sources that provide information on changing environmental impact of agriculture: statistics, crop growth models, and remote sensing. No spatial data on environmental impact from agriculture are readily available, only indirectly related data can be obtained. Each of the three sources contains information on different aspects and has its own (dis-)advantages. Statistical data sets on agriculture are most informative on environmental impact because variables related to land use practices are often included. Crop growth models reveal what is possible for agriculture under theoretical conditions and provide thus constraining information on agriculture. Remote sensing offers both thematic and spatial information on land cover, the result of land use, in a standardised way and with a high frequency.

The foundation of the method will be formed by remote sensing since it is the only source providing information on an almost real-time base, which is necessary in order to be up-to-date. Satellite images provide spectral information on land cover over large areas; national borders do not cause changes in data collection; and the images are available with a high frequency. However, there are several problems associated with the use of satellite images in general, which can take serious proportions for change detection/monitoring (section 2.3.3):

- thematic classification inaccuracies, which are especially problematic with post-classification change detection
- spatial inaccuracies, which have a severe influence when monitoring on a per-pixel base
- atmospheric variability, causing spectral changes which are not caused by land cover or land use changes
- spectral variations due to differences in scan angle and sun elevation and because of sensor instability
- seasonal year-to-year variability, causing spectral variation while land cover may remain unchanged

The latter three issues, all associated with spectral variability not related to land cover, will probably remain problematic. Atmospheric correction procedures are complex and are largely hampered by a lack of sufficient and useful data. For large areas the number of observation points needed is unrealistically large. The influence of scan angle and sun elevation can be limited by using images recorded with comparable scan angles and at comparable moments, but cannot be ruled out completely. Variation in growing season will cause vegetation to grow at different rates in different years. When concentrating on agriculture, it might be possible to take the shift of the growing season between the two observation moments into account. This will be very difficult, however, when larger areas are involved because of the spatial variation coming on top of it.

The aim here is to develop a method for change detection that avoids the first two problems, classification and spatial inaccuracies, as much as possible. Instead of post-classification change detection, the reflectance data will form the basis. Several methods already exist, but they all work on a pixel basis and thus experience the full influence of the spatial inaccuracies. Instead of considering individual pixels, here an integrated measure over the entire observation unit is developed. So, the change detection procedure to be developed is to indicate whether agriculture changed based on an **integral consideration of the reflectance data within a region**. The next step of identifying the detected change lies beyond the scope of this study.

SPATIAL OBSERVATION UNITS 3

In the previous chapter the requirements for an 'agricultural-change detection method' were discussed. Such a method can only be applied successfully when the geographical units match the units of both the topic studied and the observation system. The units commonly used are either administrative regions or cells from a regular grid. Administrative regions are related to socio-economic conditions, whereas regular grid cells are not related to agriculture at all. Biophysical units are not encountered, although they determine the conditions under which agricultural land use can develop. In this chapter a comparison will be made between a biophysical and a socio-economic zoning factor; for both the geometric similarity to land cover units as observed in a NOAA-AVHRR image is determined. The outcome of this chapter will yield the geographical units that will be used further during this study. No suitable method to characterise similarity between polygon sets existed, so a new method is proposed and tested here.

3.1   Introduction

The performance of the change detection method is not just determined by the procedures used to detect and identify changes, but also by the observation units, or regions, to which the procedures are applied. Those regions should be defined with the relevant spatial variability. When they are very large, e.g. when Europe is considered as one region, changes that can be detected need to be excessive. On the other hand, when they are very small, e.g. every pixel is used as one unit, the slightest shift in land cover will be marked as a change. Furthermore, change detection in small regions is more sensitive to the geometric inaccuracy of image registration. Besides the size, the type of region influences the performance of the method. When large differences exist within one region, e.g. half of it is in use for very intensive agriculture, while the other half is used for some extensive grazing, changes in the one half can be camouflaged by changes in the other. To

avoid false or missed/failed alarms, it is important to define regions that match both the observed and the observing system, i.e. agriculture and NOAA-AVHRR.

The regions currently used in studies covering large areas are either administrative units (e.g. Brouwer, 1995) or regular cells from a grid (e.g. RIVM, 1992). The former represent the socio-economic factors, which determine the state of agriculture, as discussed in chapter 2. The latter are not related to whatever factor.

For this monitoring study/method a zoning factor is desired that results in units which:

1. represent agricultural activities. The relation to agriculture is a prerequisite as the units form the basis for detecting changes in agricultural activities. The regions should be homogenous in terms of land use to assure that changed land cover patterns do indeed indicate changed land use.
2. have a stable geometry. Comparison for different years should not be hampered by changed borders. Geometric characteristics of the zoning factor should remain unchanged for at least several decades.
3. should match spatial units observable in NOAA-AVHRR images.
4. have a size such that regional changes are detected, excluding local changes and such that the method remains manageable, considering the $10 \cdot 10^6$ km^2 that Europe comprises and to which the method should be applied.
5. have no irregularly shaped appendices as these hamper the use of remote sensing for monitoring by increasing the sensitivity to spatial inaccuracies.

Individual fields form the basic spatial unit in agriculture, which is not perceptible in NOAA-AVHRR images due to its size. To find units that are detectable, aggregates are needed which relate agriculture and NOAA-AVHRR. They can be retrieved from biophysical and/or socio-economic factors, which together control the potential and actual state of agriculture.

Biophysical factors determine the appearance of landscapes, from small to large scales. There are seven factors that together are responsible for the characteristics of landscapes, each having its own spatial variability. They are in declining hierarchical order: climate, lithology, relief, hydrology, soil, flora and fauna (Bakker *et al.*, 1981). The factors higher up the hierarchy condition the lower ones, whereas the lower ones have some influence upward through feedback mechanisms. A region homogenous with regard to for example lithology will have characteristic types of relief, hydrology, etcetera.

Socio-economic circumstances strongly influence land use, as discussed in chapter 2. Unfortunately, administrative regions form the only possibility at the EU-scale to define socio-economic mapping units. In the European Union they are defined by NUTS-regions ("Nomenclature Utilisée Territorial Statistique") at four different levels: NUTS-0, NUTS-1, NUTS-2 and NUTS-3 (from the entire country down to groupings of communities). For Germany they correspond to *Bundesrepublik Deutschland (NUTS-0)*, *Bundesländer (NUTS-1)*, *Regierungsbezirke (NUTS-2)* and *Kreise (NUTS-3)*. In contrast to the agricultural policy of the EU

which is identical throughout the Union, the agri-environmental policy is implemented at national and regional levels and thus varies for different NUTS-regions and -levels (EU, 1999a).

In this chapter aggregates retrieved from bio-physical and socio-economic zoning are compared to spatial units observed in NOAA-AVHRR images. No existing method proved to be suitable to perform this comparison, therefore a method to determine the geometric similarity of two polygon sets was developed and demonstrated in the context of this study as well.

3.2   Materials and Methods

6.2.1   Data

This section describes and discusses what kind of zonation can best be used as a basis for agricultural land use changes. Zonations are either based on biophysical or socio-economic data. Next, a new geometric similarity test is proposed to determine which zonation corresponds best to the information derived from NOAA-AVHRR imagery.

A bio-physical and a socio-economic factor will be used to zone the German test site into regions, which will be compared to 40 land cover units in order to determine their applicability. These units were delineated by visual interpretation of all five bands of a NOAA-AVHRR image recorded at 27 April 1993 (figure 3.1). They can be observed in images obtained throughout the year. The land cover units cannot form the desired units, because their borders can change from year to year, thus forming dynamic regions which complicates a multi-year comparison. Delineation in the image was based on the following rules:

- units should show either homogenous reflection or a distinct pattern of reflection. This means that a large forest area as well as an agricultural area with patches of forest will be distinguished as a separate unit.
- units should have a minimum size of 250 km² in order to focus on regional changes and to keep the method manageable (condition 4 for the zoning factor, section 3.1).

Small details of landscapes are not visible in NOAA-AVHRR images, because of the 1.2-km² pixel size. Although this prohibits the recognition of individual crops, it facilitates the recognition of larger landscape structures.
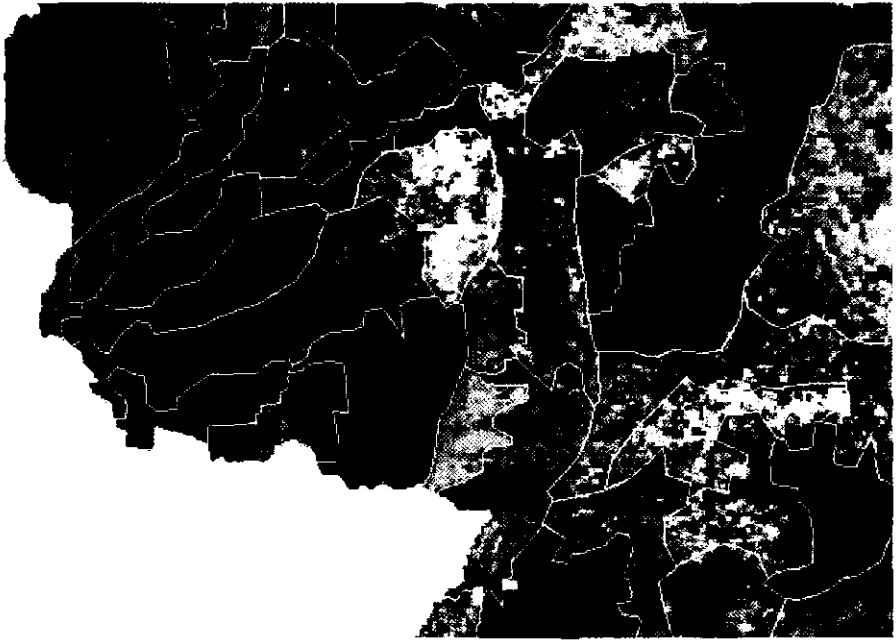
Figure 3.1 Land cover units delineated in NOAA-AVHRR image (1,2,4) recorded at 27 April 1993

Bio-physical zoning factor

Parent material from the European soil map (CEC, 1985) was chosen as biophysical factor. Parent material is here in fact a substitute for lithology, as no Europe-covering digital map data are available for lithology. Parent material is the material in which soils develop and is an indicator for soil texture and fertility. As such, it strongly determines the potential for agricultural land use. Usually it consists of weathered remains of underlying rocks, unless soils are formed in unconsolidated materials deposited during Quaternary, such as loess or alluvium. Lithology describes the underlying rocks and is the second highest factor from the hierarchy after climate. Climate has an unmistakable impact on landscapes, which is clearly illustrated by, for example, the differences between glacial and tropical regions. It is, however, difficult to contour climatic units, since they appear in gradual fields rather than in crisp regions. In contrast, parent material does show clear borders, data describing large parts of Europe in sufficient detail are available and it significantly controls agricultural land use activities.

Within the test site 450 polygons for parent material (figure 3.2) are found with a mean size of 93 km² (table 3.1). To fulfil the fourth condition of the method (focus on regional changes and keep the method manageable) the minimum size of polygons was set at 250 km². Therefore, the 450 polygons were aggregated into 27 polygons (figure 3.3) following these hierarchical rules:
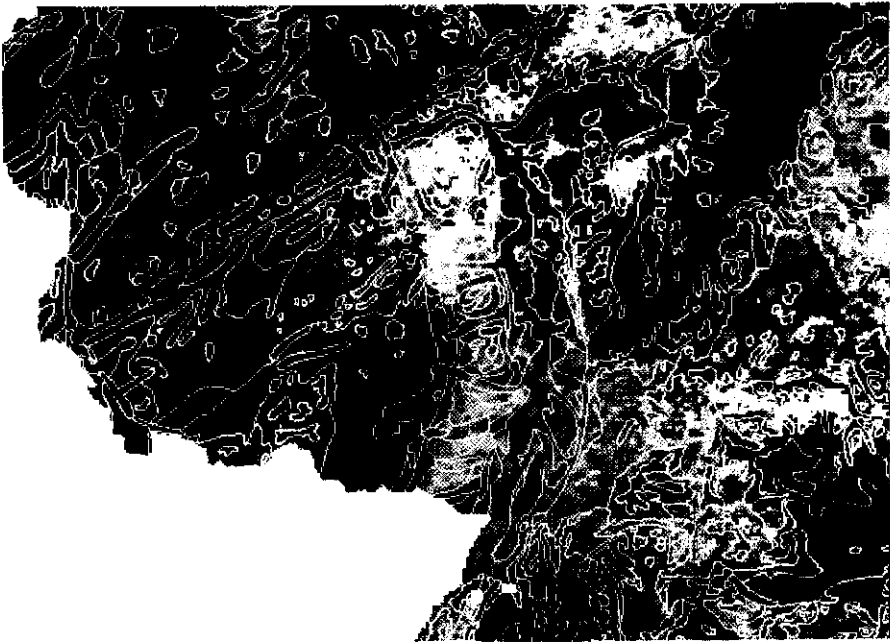
34

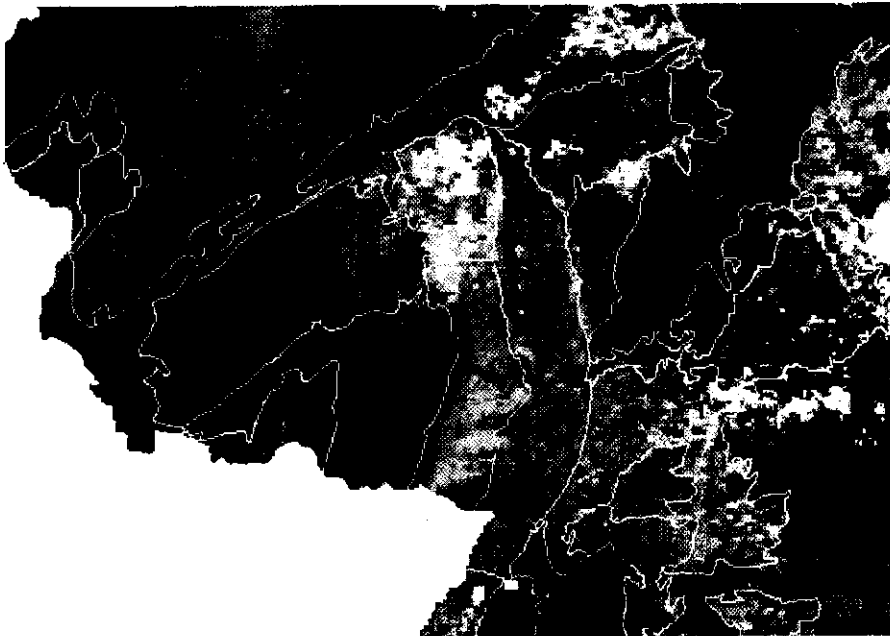**Figure 3.2** NOAA-AVHRR image (1,2,4) overlaid with original parent material polygons

Figure 3.3 NOAA-AVHRR image (1,2,4) overlaid with aggregated parent material polygons

35

Table 3.1 Statistics of the zoning variables

variable	number of polygons	mean area (km^2)	standard deviation (km^2)	coefficient of variation of area	minimum area (km^2)	maximum area (km^2)
parent material	450	93	341	3.67	1	5875
aggregated parent material	27	1541	1544	1.00	286	7155
NUTS-3	84	495	351	0.71	33	1387
NUTS-2	8	5200	1594	0.31	2489	7375

- if a polygon is smaller than 250 km^2 it should be merged.
- if a polygon can be merged with two or more aggregates, the one whose parent material resembles that of the polygon best is preferred.
- if a polygon can be merged with two or more aggregates none of which shows any similarity in parent material to the polygon, the aggregate with which it shares the longest border is selected. The alternatives of selecting the largest aggregate or the least homogenous aggregate were rejected, because they will easily result in irregularly shaped aggregates. These should be avoided because of increased sensitivity to geometric inaccuracies (condition 5, section 3.1).

In some exceptional cases polygons were split to be merged with different aggregates to avoid irregular shapes. The resolution of AVHRR allows for some contamination, since not all spatial structures are visible in the images. This is the case e.g. for the alluvium deposited by a tributary of the Main (figure 3.5), where the width of this tributary is such that it is not detectable in AVHRR images.

The original polygon set contains many polygons that do not fulfil the requirement of the minimum size of 250 km^2. Nevertheless both the original and the aggregated sets were used for zoning the test site in order to gain insight in the effect of polygon size on the outcome of the applied method.

<u>Socio-economic zoning factor</u>
For the socio-economic zoning factor NUTS-regions form the only alternative. They are organised in a fixed, nested hierarchy; a NUTS-3 region can only be merged into a predetermined NUTS-2 region, which belongs to one NUTS-1 region. The test area contains 84 *Kreisen* (the German NUTS-3 regions) (figure 3.6) the smallest of which measures only 33 km^2 (table 3.1), and 8 *Regierungsbezirke* (the German NUTS-2 regions) (figure 3.7) the smallest of which
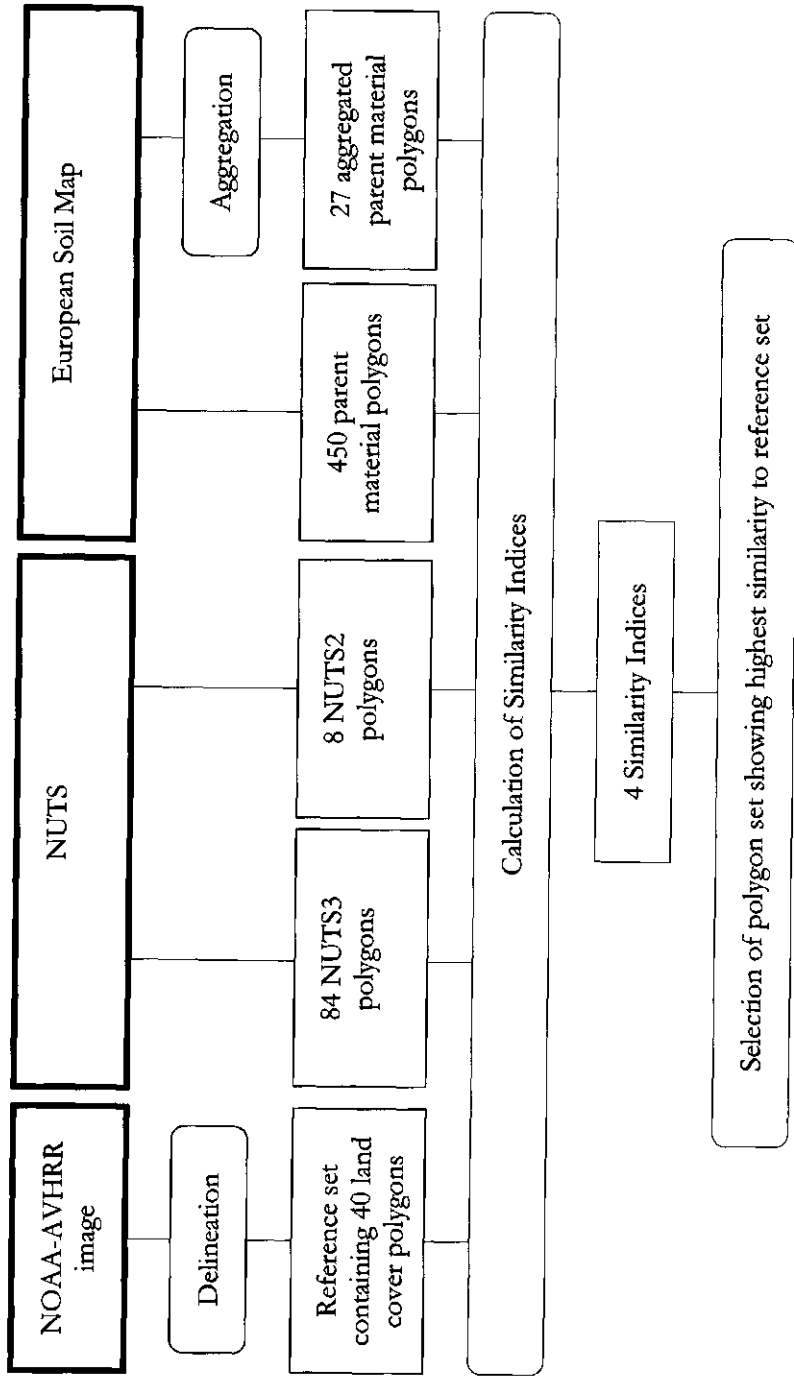
Figure 3.4 Data flow during the selection of the spatial observation units
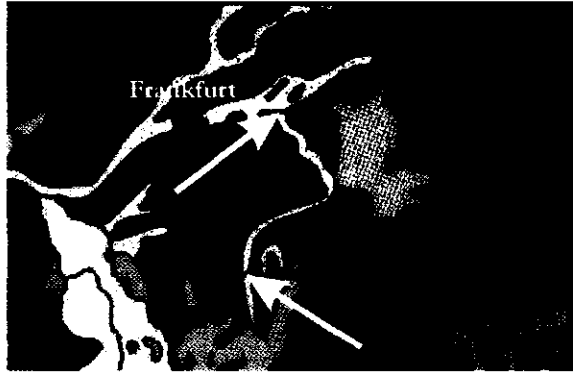
Figure 3.5 Subset of the European soil map (CEC, 1985). The white arrows indicate where the tributary of the river Main was split to avoid too irregular polygons.

measures 2489 km². Just the latter set meets the condition of the minimum size, but to gain insight into the response of the applied method to polygon size both the *Kreise* and the *Regierungsbezirke* were used, just like both aggregated and unaggregated parent material polygons were used for the bio-physical zoning factor.

6.2.2   Methodology

Figure 3.4 gives a schematic representation of the data flow. The reference set contains the polygons delineated in the NOAA-AVHRR image (figure 3.1). The four alternative polygon sets are derived either directly from the original data sets, NUTS-regions and the European Soil Map, or after aggregation. For each of four sets the geometric similarity to the reference set was determined. Considering the requirements defined in section 3.1 and the geometric similarity indices, the best zoning factor can subsequently be determined and applied in the change detection procedures.

Methods to determine geometric similarity

Winter (2000) gives a concise overview of location-based similarity between regions, and he concludes that there is only a limited number of properties that can be compared. His regions, however, are individual polygons that can coincide completely, can partly overlap, or can be disjoint. In this study not the individual polygons, but partitions of an area into different polygon sets are to be compared. By definition they will coincide completely, whereas the overall correspondence between the individual polygons is the matter of interest. For this purpose the measures provided by Winter are not qualified.

Figure 3.6 NOAA-AVHRR image (1,2,4) overlaid with NUTS-3 regions

Figure 3.7 NOAA-AVHRR image (1,2,4) overlaid with NUTS-2 regions

39

In literature two methods to define similarity between polygon sets were found: 1) Uitermark *et al.* (1998) aim at improving a topographical database using a less detailed, b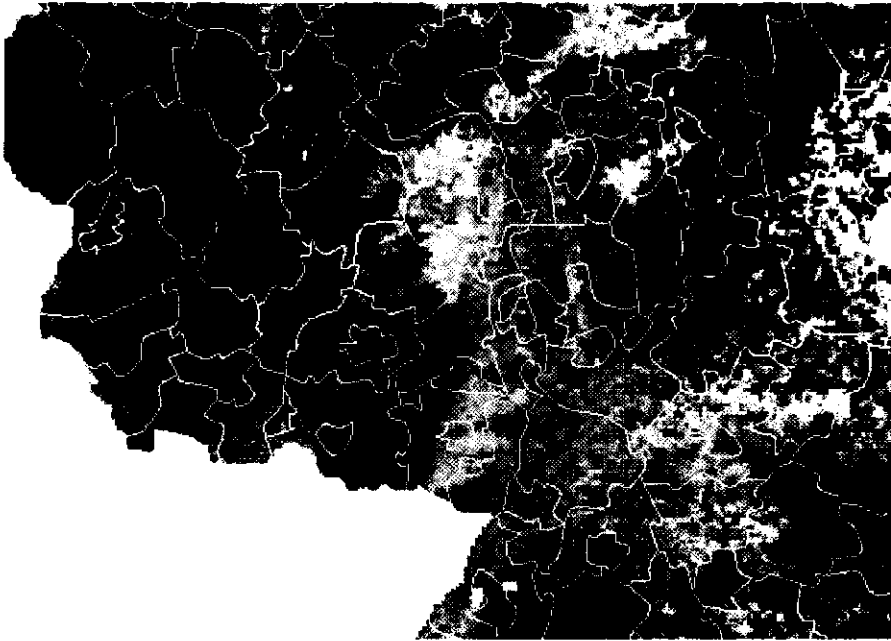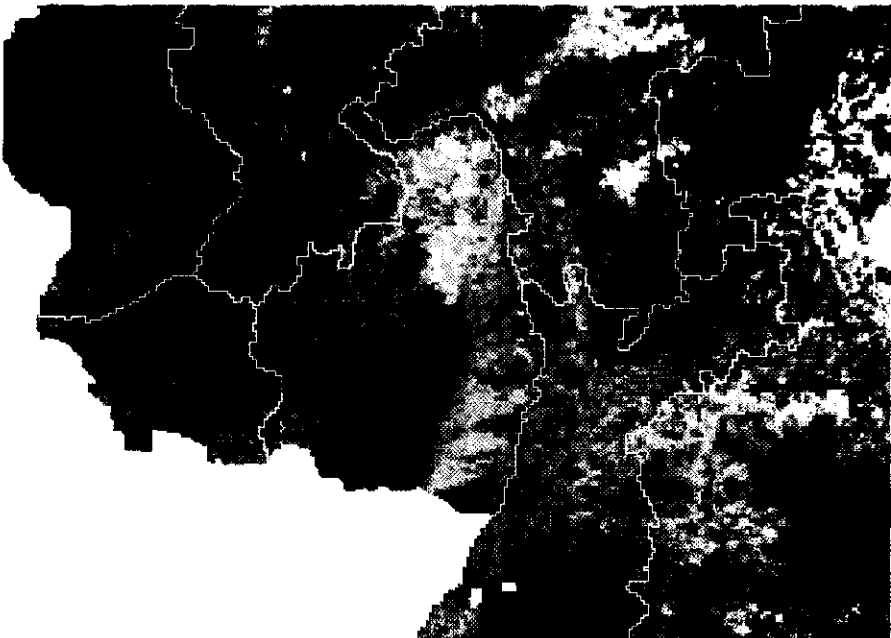ut more frequently updated database. First, the thematic descriptions of the objects in both sets are linked, second the correspondence in geometry is determined. The percentage of overlap determines to what extent correspondence exists between different objects. Relevant combinations can be used to improve the more detailed data sets, although part of them needs field checks first. 2) The second method is described by Molenaar and Cheng (2000), who aim at monitoring dynamic objects in coastal zones such as beaches. A classification is performed for two different moments and through a comparison in overlap the spatial development of the objects is determined.

Both methods perform a classification after which the correspondence between objects of the same (or similar) classes is determined. In the current study no thematic information is available and the similarity or correspondence between objects can only be based on geometric characteristics. Therefore, the two mentioned methods are not suitable for this specific problem and a new method had to be defined.

The new method should identify how well a polygon set corresponds with the reference set, when both sets cover the same area. Perfect similarity should equal 1, total dissimilarity should equal 0, and the outcome should be symmetric, i.e. similarity between A and B should equal similarity between B and A.

When a polygon from one set coincides well, but not perfectly, with a polygon from another set, the intersection polygons will show large variation in size (figure 3.8a). The difference between the area of the largest intersection and the area of the next largest intersection will be relatively large, as will the ratio between the two. The same applies to figure 3.8c where two polygons of one set largely cover one polygon of the other set. The ratio will be large again. When the two polygons from *(a)* are moved from each other, resulting in a smaller overlap (figure 3.8b), the relative difference in size of the intersections is reduced and the ratio will decline.

The developed method compares two sets of polygons covering the same area and determines their geometric similarity by calculating an index. The basic assumption is that in two similar polygon sets the individual polygons will have a large overlap and some smaller remaining intersections with other polygons. The mean ratio of the largest to the next largest intersection of one polygon will hence be larger for similar than for non-similar polygon sets.

Two polygon sets A and B contain n and m polygons respectively, indicated by $A_{1..n}$ and $B_{1..m}$. The areas of all intersections I between $A_{1..n}$ and $B_{1..m}$ are determined. For every single polygon from A and B its intersections are ordered according to their area. The geometric similarity of a polygon from A to a polygon from B is determined by dividing the area of its next largest intersection by the area of its largest intersection. According to the size of the polygons a weighted average

(a)   (b)   (c)
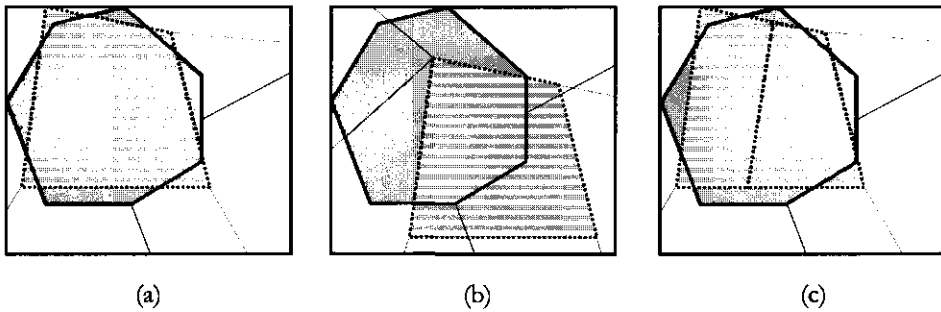
Figure 3.8a, b and c Intersection of polygons. Two polygon sets covering the same area are overlaid. One set is drawn with continuous lines, the other set with dotted lines. The shaded polygons in (a) show a good coincidence; the largest intersection of the striped polygon forms a large part of the entire polygon. In (b) they show some overlap, but not a very large one. The largest intersection of the striped polygon contains about half of the entire polygon. In (c) two striped polygons together coincide well with the plain one. For either of them the largest intersection forms a large part of the entire polygon.

is calculated for both A and B. By subtracting the average for A from 1 the geometric similarity S_{A_B} of polygon set A to set B is obtained:

$$S_{A_B} = 1 - \sum_{x=1}^{n} \left(\frac{area\left(I_{A_x B}(2)\right)}{area\left(I_{A_x B}(1)\right)} \cdot \frac{area(A_x)}{area(A)} \right) \tag{3.1}$$

and similarly for B:

$$S_{B_A} = 1 - \sum_{x=1}^{m} \left(\frac{area\left(I_{B_x A}(2)\right)}{area\left(I_{B_x A}(1)\right)} \cdot \frac{area(B_x)}{area(B)} \right) \tag{3.2}$$

where $I_{A_x B}(1)$ indicates the largest intersection of polygon A_x with B, and $I_{A_x B}(2)$ indicates its next largest intersection.

The geometric similarity S_{AB} between polygon sets A and B is indicated by:

$$S_{AB} = \frac{S_{A_B} + S_{B_A}}{2} \tag{3.3}$$

The values of S_{AB} can range from 0 to 1, where 1 indicates 100% similarity and 0 indicates no similarity. In figure 3.9 four regularly shaped polygon sets, A to D are combined to give some insight in the meaning of the value of the geometric
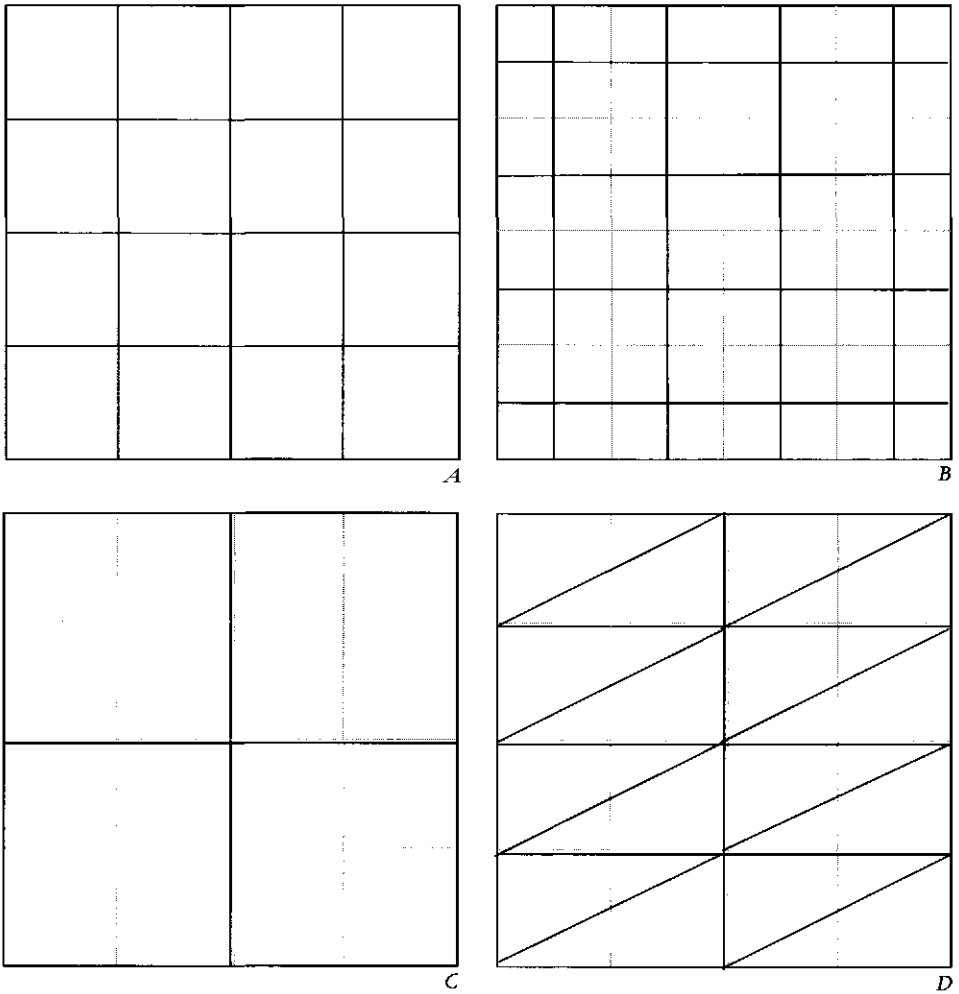
Figure 3.9 Examples of the Geometric Similarity Index for four polygon sets, where A is combined with B, C and D, respectively. In A the original set is displayed. In B the location of the polygons changed, while the size remained equal (except for the border polygons). In C the size of the polygons changed and in D the shape changed, while the size remained equal. In B, C, and D the polygons from A are indicated by grey lines. The area of a single polygon in A equals 4, while the total area equals 64.

$$S_{A_B} = 1 - \sum_{x=1}^{n} \left(\frac{area\left(I_{A_x B}(2)\right)}{area\left(I_{A_x B}(1)\right)} \cdot \frac{area(A_x)}{area(A)} \right) = 1 - 16 \cdot \left(\frac{1}{1} \cdot \frac{4}{64} \right) = 1 - 1 = 0$$

$$S_{B_A} = 1 - \sum_{x=1}^{m} \left(\frac{area\left(I_{B_x A}(2)\right)}{area\left(I_{B_x A}(1)\right)} \cdot \frac{area(B_x)}{area(B)} \right) = 1 - \left(4 \cdot \left(\frac{0}{1} \cdot \frac{1}{64} \right) + 12 \cdot \left(\frac{1}{1} \cdot \frac{2}{64} \right) + 9 \cdot \left(\frac{1}{1} \cdot \frac{4}{64} \right) \right) =$$

$$1 - 0.94 = 0.06$$

$$S_{AB} = \frac{S_{A_B} + S_{B_A}}{2} = \frac{0 + 0.06}{2} = 0.03$$

$$S_{A_C} = 1 - \sum_{x=1}^{n} \left(\frac{area\left(I_{A_x C}(2)\right)}{area\left(I_{A_x C}(1)\right)} \cdot \frac{area(A_x)}{area(A)} \right) = 1 - 16 \cdot \left(\frac{0}{4} \cdot \frac{16}{64} \right) = 1 - 0 = 1$$

$$S_{C_A} = 1 - \sum_{x=1}^{m} \left(\frac{area\left(I_{C_x A}(2)\right)}{area\left(I_{C_x A}(1)\right)} \cdot \frac{area(C_x)}{area(C)} \right) = 1 - 4 \cdot \left(\frac{4}{4} \cdot \frac{16}{64} \right) = 1 - 1 = 0$$

$$S_{AC} = \frac{S_{A_C} + S_{C_A}}{2} = \frac{1 + 0}{2} = 0.5$$

$$S_{C_D} = 1 - \sum_{x=1}^{n} \left(\frac{area\left(I_{C_x D}(2)\right)}{area\left(I_{C_x D}(1)\right)} \cdot \frac{area(C_x)}{area(C)} \right) = 1 - 16 \cdot \left(\frac{1}{3} \cdot \frac{4}{64} \right) = 1 - 0.33 = 0.67$$

$$S_{D_C} = 1 - \sum_{x=1}^{m} \left(\frac{area\left(I_{D_x C}(2)\right)}{area\left(I_{D_x C}(1)\right)} \cdot \frac{area(D_x)}{area(D)} \right) = 1 - 16 \cdot \left(\frac{1}{3} \cdot \frac{4}{64} \right) = 1 - 0.33 = 0.67$$

$$S_{AD} = \frac{S_{A_D} + S_{D_A}}{2} = \frac{0.67 + 0.67}{2} = 0.67$$

Figure 3.9 continued

similarity index. Set *A* contains sixteen squares, which change in location (set *B*), in size (set *C*), or in shape (set *D*). Similarity values increase from 0.04 to 0.5 to 0.67 for A combined with B, C, and D respectively. These values are just an illustration for the four polygon sets shown here. They do not implicate that similarities will always remain higher for changes in shape than for changes in location. If the location change had been smaller, the geometric similarity would have been higher. And if the change of size had been smaller, the geometric similarity would have been higher too.

Method to select the spatial observation units

The Geometric Similarity Index is calculated for the four polygon sets, two parent material and two NUTS sets, combined with the land cover units delineated in the NOAA-AVHRR image (figure 3.1). Only the aggregated parent material polygons and the NUTS-2 regions meet the requirements defined for the regions, but to gain some insight in the developed geometric similarity method the other two sets are taken along as well.

Besides the application of the geometric similarity method, the NOAA-AVHRR image overlaid with the four polygon sets is visually interpreted (figure 3.2, 3.3, 3.6 and 3.7). Like the geometric similarity index this interpretation reveals how well the polygons explain the land cover patterns which can be observed in the image, but in a qualitative way. This reduces objectivity, but has the advantage it is not hampered by uncertainties introduced during the delineation of the land cover units. The results of the index and the visual interpretation will be compared to assess the performance of the newly developed method.

3.3   Results

The rows of table 3.2 refer to the pair wise comparison of the polygons with the land cover units. The last column provides the final similarity value. The polygon sets representing aggregated parent material and NUTS-2 regions, the two possible candidates to which the change detection procedures can be applied, show similarities of 0.62 and 0.44 respectively with the land cover units.

In figure 3.9 the combination of set *A* and *C* shows that the set containing smaller polygons fits easier into the set containing larger polygons, i.e. that $S_{small_{large}}$ will yield a higher outcome than $S_{large_{small}}$. Three out of the four combinations with land cover confirm this. The 40 land cover units fit better into the 27 aggregated parent material polygons and the 8 NUTS-2 regions than the other way around, and the 84 NUTS-3 regions fit better in the 40 land cover units than the land cover units in the NUTS-3 regions. Only the unaggregated parent material set shows a higher geometric similarity of the 40 land cover units to the 450 parent material polygons than vice versa, even though the two values of 0.66 and 0.65 are almost equal.

Table 3.2 Geometric similarities of the land cover units derived from NOAA-AVHRR to the four polygon sets, and vice versa. The third column, $S_{A-land\,cover}$, indicates the geometric similarity between the land cover units and the polygon sets.

variable A	$S_{land\,cover_A}$	$S_{A_{land\,cover}}$	$S_{A-land\,cover}$
parent material	0.66	0.65	**0.65**
aggregated parent material	0.67	0.56	**0.62**
NUTS-3	0.35	0.51	**0.43**
NUTS-2	0.64	0.24	**0.44**

The effect of the difference in number of polygons on the geometric similarity index is ambiguous (figure 3.9). Sets A and B contain an equal number of polygons and have a geometric similarity of 0.04. Sets A and D also contain an equal number of polygons, but they have a similarity of 0.67. Set A contains four times as many polygons as set C and their geometric similarity is 0.5. The ratio between the number of polygons alone clearly does not explain the outcome. The similarities of the four combinations with land cover confirm this: the parent material sets containing 450 and 27 polygons show similarities to the 40 land cover polygons of 0.65 and 0.62, respectively, while the NUTS-regions containing 84 and 8 polygons have similarities of 0.43 and 0.44. Here the ratio of the number of polygons does not explain a higher or lower geometric similarity, either.

The visual interpretation shows comparable results. The polygons from the aggregated parent material set correspond well to the boundaries between land cover types observed in the image. The Rhine valley is outlined by the polygons, the wooded areas are delineated, and several cultivated regions are clearly recognisable. Worse performance can be observed in the north-western corner which is not subdivided and in the east/south-eastern corner where borders appear which cannot be found in the image. The non-aggregated parent material set contains some polygons which coincide well with homogenous areas in the image, though in general this set contains too many small polygons which do not correspond to image patterns. The two sets containing the NUTS-regions do not show any relation to the patterns in the image with one exception: the river Rhine forms a border. This is a clear indication that the administrative boundaries are not related to land cover.

3.4   Discussion

This chapter aimed at defining the best type of zonation to be used as a basis for further land use change detection. Four different polygon sets were tested, of which aggregated parent material and NUTS-2 regions fulfil the requirements of the desired polygon set (section 3.1). The geometric similarity values in table 3.2 clearly indicate the aggregated parent material set as the better choice. Without the

minimum size requirement the geometric similarity index suggests the unaggregated parent material set as an even better option.

Visual interpretation of the aggregated parent material polygons as an overlay over an 1989 image (figure 3.10) reveals that they show a good geometric similarity to this image as well, even though the land cover patterns are different.

As shown in this analysis, parent material more strongly regulates land cover patterns than the administrative NUTS-regions. Although agri-environmental measures are implemented at NUTS-level, borders in land cover patterns are determined by transitions in parent material rather than in NUTS-region. Veldkamp and Fresco (1997) came to the same conclusion. They performed a study to land use drivers and their spatial scale in Costa Rica. They found that for large areas the biophysical situation determines which regions are favourable for agriculture. Within these regions the presence of people determines where it is practised.

In this study just one socio-economic factor and one biophysical factor are considered. For the NUTS-regions currently no alternative polygon data set providing total EU coverage is available, but alternatives for parent material do exist. It might be expected that biophysical factors other than lithology would generally perform better than socio-economic factors regarding the geometric similarity index.
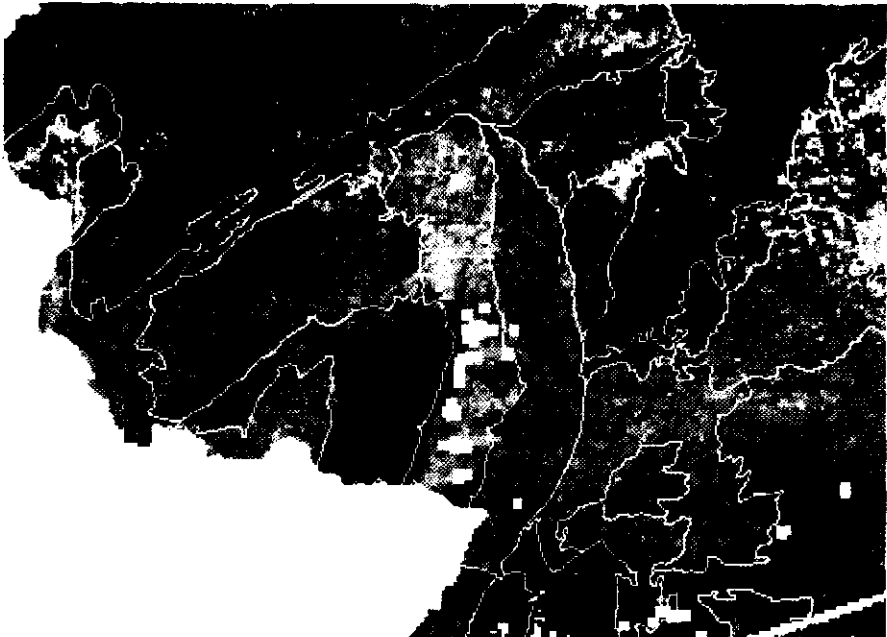

Figure 3.10 NOAA-AVHRR image (1,2,4) recorded at 16 May 1989 overlaid with aggregated parent material polygons

One aspect not taken into account in this study is the effect of international borders on land cover patterns, because just one country is involved. Although the monitoring method is intended to cover entire Europe, it might be interesting to allow monitoring at national level as well. This requires zoning not only after parent material but also after national borders.

Besides determining which factor is most suitable for change detection units, this chapter described a method that was developed to calculate geometric similarity between two polygon sets covering the same area. No thematic information could be included, so all information should be derived from the geometry of the polygons. The index that is produced is based on the intersections that evolve after overlaying two polygon sets. For each individual polygon from both sets, its largest and next largest intersections are determined and the ratio between the two is calculated. For each polygon set the average ratio is computed, weighting the scores by the individual polygon area. The averages of the two sets are added, divided by two and subsequently subtracted from one as to get higher values indicating better similarities.

To get some insight in the performance of the geometric similarity index four polygon sets were included in the study, while only two met the conditions of the desired set. Furthermore a visual interpretation of the correspondence between these four sets and the NOAA-AVHRR land cover patterns was performed. Visual interpretation confirmed that parent material is the best option and the aggregated set is the better of the two. The land cover units which are easily identified in the image coincide more or less with the aggregates, whereas the unaggregated parent material set contains many small polygons which cannot be identified in the image.

With the new method, the two parent material sets obtained much higher geometric similarity values than the two NUTS sets. Here, however, the unaggregated parent material set obtained the highest score. This is probably caused by the skew distribution of the polygon size of the latter set. There are many small polygons, but also rather large ones in which the land cover polygons apparently fit rather well. This suggests that a correction factor should be added to the geometric similarity index. This factor could be based on, for example, the coefficients of variation of the polygon sizes (table 3.1) which is 3.7 for the unaggregated parent material set and ranges from 0.3 to 1.0 for the other three sets. The coefficient of 3.7 reflects the many small polygons that fit perfectly within a land cover polygon, and the large one that is so large that it fits entire land cover polygons.

Uncertainties in the geometric similarity values are raised by inaccuracies in the geometry of the polygons. Five types of uncertainty can be responsible for this, namely: 1) data or value, 2) space, 3) time, 4) consistency, and 5) completeness (Gahegan and Ehlers, 2000). For satellite images these categories show in: digital numbers or spectral characterisation, spatial accuracy, temporal errors (can be neglected within one image), atmospheric distortions, and missing values due to cloud cover, respectively. For the parent material data and the NUTS-regions all five categories apply and they can show in: labelling uncertainty, spatial accuracy,

temporal mismatch when data from different moments are combined, incomparable classification legends, and missing values. Unfortunately, no uncertainty data were available for the data sets used within this study, and although there certainly is some uncertainty, it cannot be quantified.

The land cover units were digitised by hand and even though the conditions to delineate units were clearly defined, this will have introduced some subjective boundaries as discussed by Middelkoop (1990). Furthermore they were digitised in the NOAA-AVHRR image which will have some geometric inaccuracy. The four polygon sets will include some digitalisation and, the soil map, some classification errors as well. Besides, they needed to be re-projected in order to fit the image, which will have introduced some additional errors.

It is not possible to connect a level of significance to the outcomes of the method, because it considers complete data sets rather than samples. So, even though it is obvious that geometric uncertainties are present in the polygon sets, no level of significance can be tied to the outcome.

The geometric similarity index is here calculated for continuous polygons. In principle, it is also applicable to fragmented polygons, although the geometric inaccuracies will play a stronger disturbing role. An example of such an application is to test the performance of unsupervised classification, where the resulting clusters can be compared to known patterns or where the optimal number of clusters should be assessed.

3.5 Conclusions

The spatial observation units of the change detection method should match both agriculture and NOAA-AVHRR. In this chapter a comparison was made between bio-physical and socio-economic partitions to determine which can serve best as observation units. Parent material was selected as bio-physical factor and the administrative regions of the European Union, the so-called NUTS-regions, served as socio-economic factor. Parent material showed a much better correspondence to land cover units delineated in a NOAA-AVHRR image than the NUTS-regions. Consequently, parent material polygons, merged into manageable aggregates, will serve as spatial observation units for the change detection method.

To allow for monitoring at national level besides monitoring entire Europe, national borders should be taken into account during polygon definition, because agri-environmental policies are implemented at national or even lower levels. This does not apply here, because the study area is located in just one country.

To compare the two polygon sets a method was developed, which compares two partitions of the same area and calculates a Geometric Similarity Index. The method is based on the observation that when two polygon sets show a good correspondence, the difference in size of the largest and the next largest intersection of one polygon with polygons from the other sets is quite large.

Consequently, the ratio between these intersections will be quite large too. When the two sets do not correspond well, intersections will show less difference in size and the ratio will be small. In the Geometric Similarity Index the ratios of all polygons are combined and weighted according to their area.

Visual interpretation confirmed the outcome of this new method, that parent material polygons better match land cover units visible in NOAA-AVHRR images.

Possibly a correction factor should be included in the method to correct for large differences between the two partitions concerning the number of polygons. Particularly when one of the sets shows a high coefficient of variation for polygon size, this might be necessary.

49

classified. If missing values are ignored, the combination of several masked images results in increasingly less data and eventually in white spots on the map. Partitioning the area into smaller regions that can be classified independently could solve this problem, by using images of varying dates for the different regions. The number of regions should be as low as possible, because each needs its own time-consuming classification procedure. Reducing the number of missing values can be achieved by replacing them with estimated values.

The aim of this chapter is to compare various methods to replace missing values of clouded pixels by values which best resemble the values of those pixels under cloud-free conditions. They are intended for images that are almost free of clouds and where only a small percentage of the pixels require an estimated value. Seven methods, ranging from simple replacement of pixel values to calculation of values with geostatistics, were applied to all five bands and the NDVI of NOAA-AVHRR images recorded at the end of April 1993. Data from images of succeeding days as well as from pixels surrounding the clouds were used. Introducing four different cloud patterns in an actually (almost) cloud-free image yielded four validation sets on which the different methods could be tested.

4.2 Methods and Materials

4.2.1 Materials

Ten daily NOAA-AVHRR mosaics, recorded at 21-30 April 1993, were obtained from the SPACE database at the Joint Research Centre of the European Union (JRC) in Ispra, Italy (Millot and Loopuyt, 1997). NOAA-AVHRR images consist of two optical bands, two thermal infrared bands and one mid-infrared band (table 4.1). The images were radiometrically and geometrically corrected when we received them (Kerdiles, 1998).

The images were provided with a separate cloud mask. Pixels covering the edges of clouds are often not included in the masks, because both the clouds and the surface determine their spectral characteristics. Therefore we buffered all clouds in the masks by an additional pixel to improve their coverage before applying them to the images.

Table 4.1 Statistics on NOAA-AVHRR image of 27 April 1993. Wavelengths are between brackets and are expressed in μm.

	Band1 (0.58-0.68)	Band2 (0.73-1.1)	Band3 (3.55-3.93)	Band4 (10.3-11.3)	Band5 (11.5-12.5)
mean	91	266	547	650	633
sd	19	44	54	19	18
minimum	47	129	42	539	508
maximum	263	438	678	727	709

The image of 27 April is of good quality and could therefore be selected for classification. It is almost free of clouds (< 0.2%) and only in north-eastern corner traces of haze can be detected. Mean values of bands 1 to 5 and their corresponding standard deviations are shown in table 4.1. The minimum and maximum values are separated from the mean more than twice the standard deviation. Those extreme values occur only for few pixels, whereas 95% of the pixels show values between the mean ± 2·standard deviations.

Because of its quality we used the image of 27 April to compare the procedures. Some of them require a second image recorded at the previous or following day. We selected the image of 28 April because it is less clouded (26%) than the image of 26 April (60%). In case a procedure requires stratification, the aggregated parent material polygons from chapter 3 serve as strata.

4.2.2 Seven interpolation procedures

Seven procedures to replace clouded pixels were tested. Three of them are entirely based on temporal information, two on spatial information and two on both temporal and spatial information (figure 4.1). The seven procedures can briefly be described as follows. We consider the pixel values in one specific band $z(p,t)$, where p is a pixel and t is the time of measurement. The pixels are uniquely determined by the co-ordinates according to an arbitrary origin. As such, they show a correspondence to regionalised variables, taking values in space and time (Matheron, 1965; Christakos, 1992). Images are collected at a range of instances for example once every day, hence at t_i, $i = 1, ..., 365$. We will therefore consider images $z(p,t_i)$ for $p \in P$, where P represents the area.

In the presence of clouds, $z(p,t)$ can be a missing value for pixel p_0 at time t_i. The actual land cover is not recorded, but merely the reflectance of a cloud. If this is the case, an estimate $\hat{z}(p_0,t_i)$ is required using data from earlier or later days and/or neighbouring pixels. We will discuss seven different procedures, which are all applicable to optical and thermal bands, except for ii and iii, Maximum and Minimum Value Composites (*MaxVC* and *MinVC*). *MaxVC* is applicable to thermal bands, while *MinVC* can be used to replace missing values in optical bands. The seven procedures are:

i Simple Replacement (*SR*): $\hat{z}(p_0,t_i) = z(p_0,t_{i+1})$ (or $\hat{z}(p_0,t_i) = z(p_0,t_{i-1})$). The pixel is replaced by the pixel value at the same location obtained one day later (or earlier). When images of two subsequent days are geometrically and radiometrically corrected, the day-to-day variance of pixel values will be minimal. Pixel values from one image can thus be used to replace the missing values of corresponding pixels in the other image.
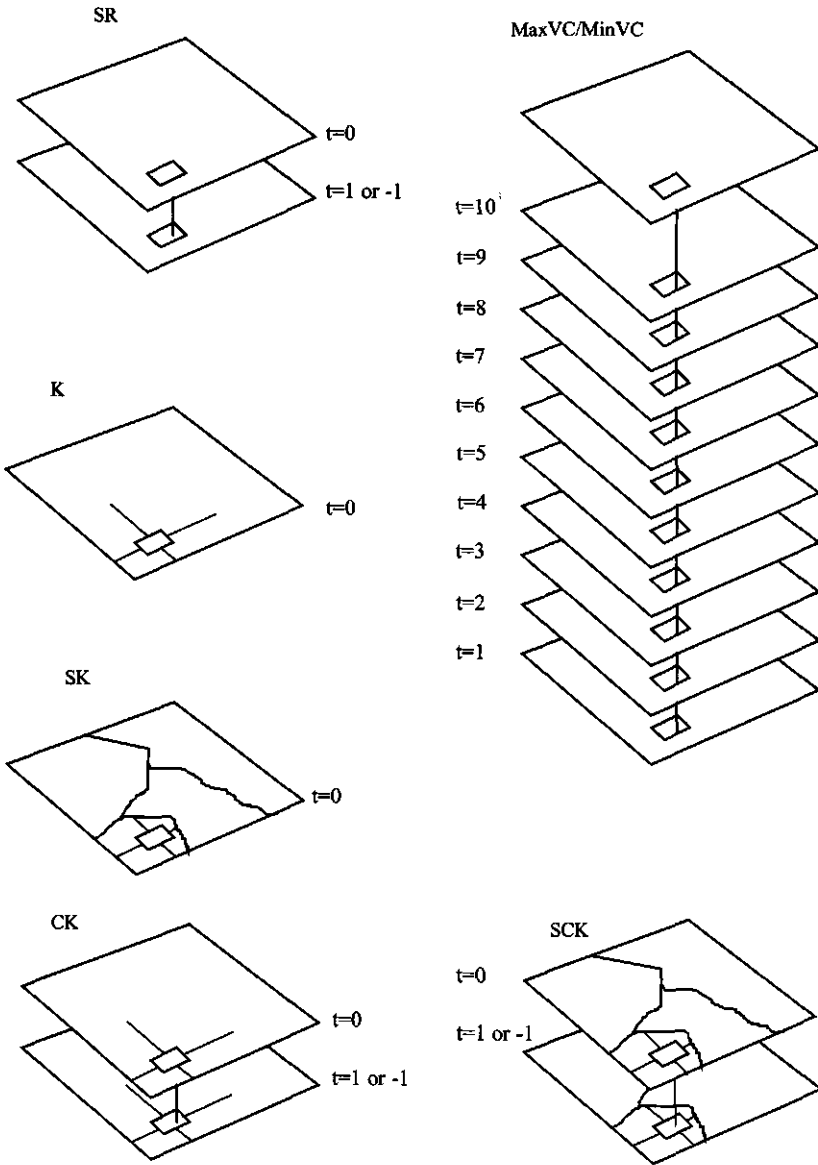
Figure 4.1 Overview of the seven methods included in the comparison. Vertical lines indicate temporal relations, all other lines indicate spatial relations. Abbreviations are explained in the text.

ii. Maximum Value Composite (*MaxVC*): $\hat{z}\ (p_0,t_i) = \max_{1 \leq j \leq 10} z(p_0,t_{i+j})$.
Atmospheric influences such as haze will reduce the signal in the thermal domain. Therefore pixel values will be largest when atmospheric disturbance is minimal. For every individual pixel the maximum value out of ten images of successive days is used in the composite.

iii. Minimum Value Composite (*MinVC*): $\hat{z}\ (p_0,t_i) = \min_{1 \leq j \leq 10} z(p_0,t_{i+j})$.
The *MaxVC* approach is valid for the thermal bands and the NDVI, but it is invalid for the visible, near- and mid-infrared bands, for which pixel values are lowest when atmospheric disturbance is minimal. The pixel value in this composite image is obtained by selecting the minimum value for one pixel out of ten images of successive days.

iv. Ordinary kriging (*K*). Ordinary kriging interpolates pixel values spatially (Journel and Huijbregts, 1978). The spatial dependence of pixels in an image is expressed by the variogram (Woodcock *et al.*, 1988a and 1988b; Curran, 1988; Atkinson *et al.*, 1994), which is characterised by three parameters, nugget, range, and sill (figure 4.2). Variogram values $\gamma_i(h)$ at t_i are calculated for any distance h as

$$\gamma_i(h) = \frac{\sum_{j=1}^{N(h)} \left(z(p_j + h,t_i) - z(p_j,t_i) \right)^2}{2 \cdot N(h)} \tag{4.1}$$

where $z(p_i+h,t_i)$ and $z(p_j,t_i)$ is the jth pair of pixel values measured at a distance h apart at time t_i. The total number of these pairs equals $N_i(h)$. The variogram can be used in ordinary kriging, which is the best linear interpolator (predictor) with weights λ_j based upon the variogram:
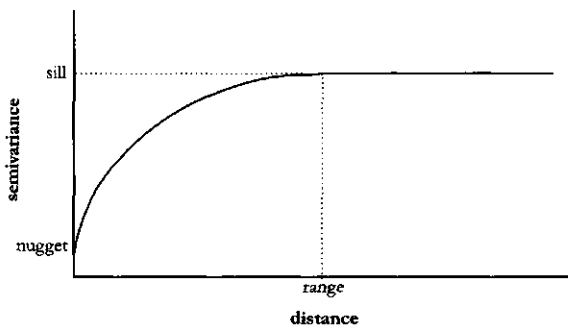
Figure 4.2 The three characteristic parameters of a variogram

$$\hat{z}(p_0, t_i) = \sum_{j \in \Omega_i(r)} \lambda_j z(p_j, t_i) \qquad (4.2)$$

where $\Omega_i(r)$ is a neighbourhood of pixels observed at t_i within a distance r of the missing value to be predicted.

v. Ordinary co-kriging (*CK*). When a second variable is available, co-kriging extends kriging by using this second variable. Co-kriging was originally developed to save cost and sampling time (Stein *et al.*, 1988b; McBratney and Webster, 1983). Here we applied co-kriging by using the pixel values at t_i as the variable and those at t_{i+1} (or t_{i-1}) as the co-variable. Three variograms are necessary: the variograms for t_i and for t_{i+1} (or t_{i-1}) and the cross-variogram to model the spatial cross-dependence, e.g. between t_i and t_{i+1} as

$$\gamma_{i,i+1}(h) = \frac{\sum_{j=1}^{M(h)} \left(z(p_j + h, t_i) - z(p_j, t_i) \right) \left(z(p_j + h, t_{i+1}) - z(p_j, t_{i+1}) \right)}{2 \cdot M(h)} \qquad (4.3)$$

where the total number of pairs available on t_i and t_{i+1} is equal to $M(h)$. A similar expression applies for the cross-variogram between t_i and t_{i-1}. The missing value is predicted by

$$\hat{z}(p_0, t_i) = \sum_{j \in \Omega_i(r)} \lambda_j z(p_j, t_i) + \sum_{j \in \Omega_{i+1}(r)} \eta_j z(p_j, t_{i+1}) \qquad (4.4)$$

using a linear combination of observations measured at t_i and at t_{i+1} with weights λ_j and η_j, respectively.

vi. Stratified kriging (*SK*). In *K* the entire image is used to estimate the variogram and every pixel may be used to predict a missing value. This may be unrealistic because remotely sensed images are well known to display structural differences in pixel values caused by different semi-natural conditions. To take this into account, the area P may be stratified into homogeneous strata, e.g. on the basis of hydrological, geological or land cover units (Stein *et al.*, 1988a). A variogram is then calculated for each stratum and only pixels belonging to the same stratum as that in which the pixel with the missing value is located, are used for interpolation. For the *k*th stratum the variogram is calculated as

$$\gamma_i^k(h) = \frac{\sum_{j=1}^{N_k(h)} \left(z_k(p_j + h, t_i) - z_k(p_j, t_i) \right)^2}{2 \cdot N_k(h)} \qquad (4.5)$$

where $z_k(.,.)$ indicates the pixel value within the kth stratum. The predictor of the missing value is equal to

$$\hat{z}_0(p, t_i \mid k) = \sum_{j \in \Omega_{i,k}(r)} \lambda_j z_k(p_j, t_i) \qquad (4.6)$$

where $\Omega_{i,k}(r)$ is the neighbourhood of pixels within the kth stratum not further than distance r removed from the prediction location at time t_i.

vii. Stratified co-kriging (SCK). Stratified co-kriging combines both the use of a co-variable and the presence of strata. A stratified cross-variogram between pixels at t_i and t_{i+1} is defined as

$$\gamma_{i,i+1}^k(h) = \frac{\sum_{j=1}^{M_k(h)} \big(z_k(p_j + h, t_i) - z_k(p_j, t_i)\big)\big(z_k(p_j + h, t_{i+1}) - z_k(p_j, t_{i+1})\big)}{2 \cdot M_k(h)} \qquad (4.7)$$

where the pairs of pixels $z_k(p_j+h,t_i)$, $z_k(p_j,t_i)$ and $z_k(p_j+h,t_{i+1})$, $z_k(p_j,t_{i+1})$ form the jth pair of pixel pairs in the kth stratum, separated by a distance h, on which observations are available at t_i and at t_{i+1}, the total number of these being equal to $M_k(h)$. Stratified co-kriging uses observations from the two images:

$$\hat{z}(p_0, t_i \mid k) = \sum_{j \in \Omega_{i,k}(r)} \lambda_j z_k(p_j, t_i) + \sum_{j \in \Omega_{i+1,k}(r)} \eta_j z_k(p_j, t_{i+1}) \qquad (4.8)$$

where $\Omega_{i+1,k}(r)$ is the neighbourhood of pixels within the kth stratum not further than distance r removed from the prediction location at time t_{i+1}.

Several models can be used to fit through the variogram values (Cressie, 1991) of which the Exponential, the Gaussian and the Bessel model were applied here. The variograms are all based on distances up to 11 km, which equals 10 pixels in the image. The maximum interpolation distance was set at 10 km and an optimal fit over this distance was preferred to a complete variogram. Calculation of the cross-variograms was based on those points where both images are free of clouds. The number of interpolators was set at 10 pixels, both for the variable and the co-variable.

4.2.3   Validation

To compare the seven replacement procedures four validation sets were created (figure 4.3 and table 4.2). The first validation set ($V1$) consists of 3619
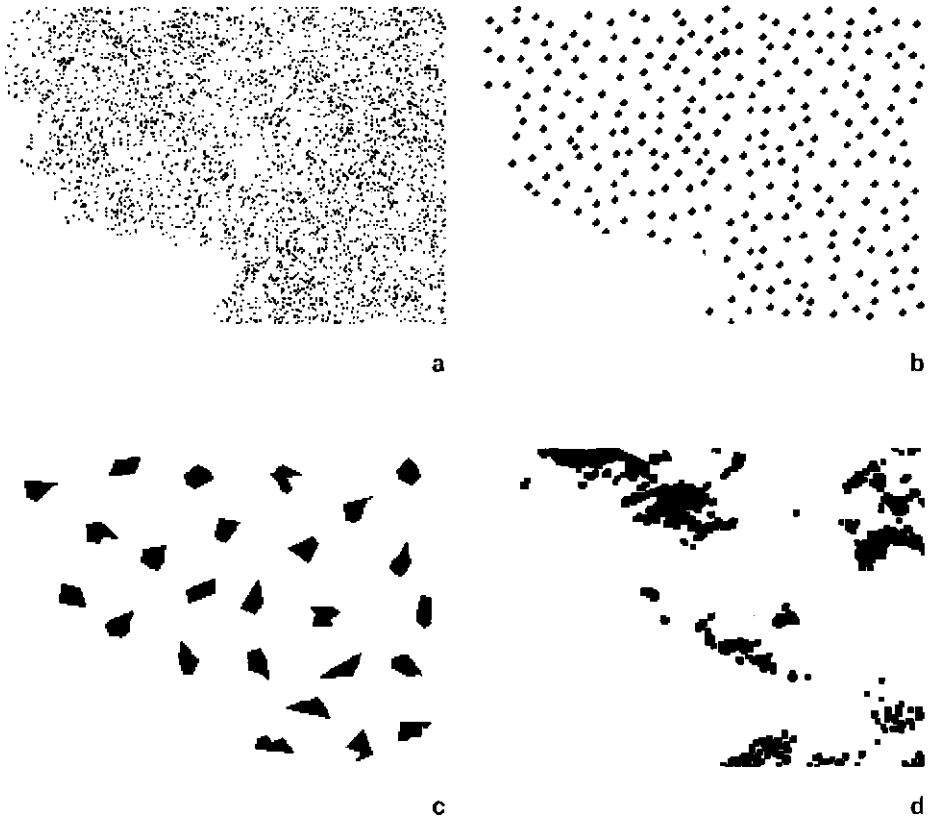
Figure 4.3 Validationsets *V1* (a), *V10* (b), *V100* (c), and *Vreal* (d)

single pixels that are randomly distributed over the area. The second set (*V10*) consists of 277 identical polygons of 10 pixels. The polygons are manually placed on the map, such that they are evenly distributed. The third validation set (*V100*) consists of 25 polygons of about 120 pixels with sizes ranging from 113 to 132 pixels, which are also manually located. The fourth set (*Vreal*) consists of 50 polygons with a mean size of 84 pixels obtained from an existing cloud mask. The latter set, representing real cloud patterns, contains 4284 pixels. After marking these pixels as missing values their values were estimated by the seven methods.

For each method the root mean square errors (rmse) were calculated for the four validation sets for the entire area as well as for the individual strata by:

$$rmse = \sqrt{\frac{\sum_{p=1}^{N}(\hat{z}_{p,t_i} - z_{p,t_i})^2}{N}} \qquad (4.9)$$

Table 4.2 Number of NOAA-AVHRR pixels in each region in total and in each validation set ($V1$, $V10$, $V100$ and $Vreal$)

	total area	$V1$	$V10$	$V100$	$Vreal$
region 1	545	51	44	3	0
region 2	1750	168	155	128	56
region 3	2576	247	225	380	52
region 4	5921	617	474	532	1193
region 5	3172	385	263	228	542
region 6	691	88	52	92	155
region 7	1034	123	64	2	410
region 8	1551	212	119	187	34
region 9	3107	334	235	319	378
region 10	269	26	23	53	35
region 11	320	30	22	74	14
region 12	604	79	54	107	16
region 13	635	101	58	80	293
region 14	237	21	16	43	59
region 15	261	27	10	0	0
region 16	1878	221	135	80	45
region 17	1226	103	81	66	157
region 18	245	22	22	76	0
region 19	1123	112	89	6	16
region 20	581	40	53	114	0
region 21	309	24	25	21	0
region 22	327	33	21	12	0
region 24	244	25	22	0	0
region 25	1039	91	79	98	0
region 27	858	50	72	111	225
region 28	1732	164	173	117	396
region 29	2149	225	173	179	208
total	34384	3619	2759	3108	4284

To enable mutual comparison between bands the rmse was normalised by division by the standard deviation of the respective bands; the value thus obtained is indicated by $rmse_{cor}$. Only those pixels for which estimates by all methods were available were included.

4.3   Results

Several causes prohibited validation of all pixels by each method. SR cannot provide values when the corresponding pixel value in the second image is missing. $MaxVC$ and $MinVC$ result in unreplaceable pixels when all 10 images

59

show a missing value. Kriging procedures result in unreplaceable pixels when insufficient points are available within the search radius. K is not restricted by strata, nor by missing values in the second image. Only in $Vreal$ some pixels could not be replaced, because some polygons were too large compared to the search radius. With CK replacements are only made when sufficient pixels are available in both images. With SK only those points located in the same stratum as the clouded pixel are available for interpolation. When interpolating with SCK sufficient points must be present within the right stratum in both images. In conclusion 3392 points in $V1$, 2612 points in $V10$, 2956 points in $V100$, and 4154 points in $Vreal$ were estimated for all methods.

The $rmse_{cor}$ values of the seven procedures for the entire image are shown in table 4.3. For each combination of validation set and spectral band the best method is marked. The procedures incorporating spatial information perform better than the temporal methods in all cases. Spatial information improves the reliability of the replacements. The values of the spatial methods do not show much difference. CK results in the best estimates in most cases, SCK is selected as best method in five cases, while K produces best results in three cases. Including temporal information in addition to spatial information results in better estimates. More precise spatial information obtained by stratification does not yield further improvements. In conclusion, a combination of temporal and spatial information results in best replacements.

Mutual comparison of the bands reveals that for the kriging procedures none of the bands produces systematically better or worse than the other bands. Bands 4 and 5 show low values for $V1$ and $Vreal$, but high values for $V10$ and $V100$. Band 1 shows best estimates with $V10$ and $V100$. Estimates for the NDVI are intermediate for all validation sets, although they are lower for $V1$ than for the other three sets. The $MaxVC$, which is the most common used method to fill gaps in NDVI images, results in worse estimates than the kriging methods for all validation sets.

We conclude that spatial information is more important to estimate land reflection values of clouded pixels than temporal information. A combination of spatial and temporal information yields even better estimates, whereas the sole use of temporal information produces far worse estimates. Stratification of the area does not lead to improvements. CK thus produces best results to replace clouded pixels.

4.4 Discussion

Geostatistical methods perform better than conventional methods that are of a purely temporal nature. Spatial patterns as observed in the image are apparently more consistent than the temporal behaviour of individual pixels. Variation in solar and satellite angles and geometric or radiometric inaccuracies could provoke this.

Table 4.3 Root mean square errors of the four validation sets for the seven methods tested. Each value is divided by the standard deviation of its respective band. The best value per validation set for each band is indicated by a shaded figure.

	Band 1	Band 2	Band 3	Band 4	Band 5	NDVI
V1						
SR	0.724	0.738	0.947	2.066	2.198	0.879
MaxVC				0.963	1.046	0.776
MinVC	1.213	1.924	0.703			
K	0.405	0.445	0.413	0.276	0.313	0.421
SK	0.407	0.446	0.416	0.282	0.320	0.425
CK	0.401	0.437	0.412	0.277	0.315	0.421
SCK	0.409	0.456	0.418	0.286	0.324	0.425
V10						
SR	0.760	0.776	0.995	2.218	2.349	1.057
MaxVC				1.212	1.283	0.939
MinVC	1.105	1.797	0.697			
K	0.511	0.558	0.557	0.772	0.806	0.725
SK	0.512	0.555	0.564	0.775	0.811	0.732
CK	0.488	0.529	0.528	0.764	0.799	0.702
SCK	0.494	0.533	0.540	0.766	0.802	0.704
V100						
SR	0.746	0.755	0.946	2.012	2.129	1.008
MaxVC				1.028	1.096	0.921
MinVC	1.069	1.810	0.644			
K	0.604	0.657	0.640	0.806	0.835	0.800
SK	0.606	0.656	0.640	0.809	0.837	0.797
CK	0.580	0.618	0.599	0.790	0.822	0.777
SCK	0.577	0.617	0.599	0.795	0.826	0.773
Vreal						
SR	0.726	0.761	0.873	1.576	1.635	0.794
MaxVC				0.813	0.846	0.854
MinVC	1.211	1.909	0.645			
K	0.614	0.650	0.596	0.497	0.523	0.624
SK	0.625	0.644	0.607	0.500	0.529	0.635
CK	0.582	0.611	0.559	0.476	0.508	0.593
SCK	0.592	0.598	0.570	0.489	0.521	0.602

61

the lowest distance to the boundaries. However, from the behaviour of individual pixels for *V100* (figure 4.5) no clear pattern is apparent, although one can say that pixels near boundaries between strata with strongly different statistics profit more from stratification than those near boundaries between similar strata. The most encountered solution to clouded images is the maximum value composite of NDVI values (Holben, 1986; Moody and Strahler, 1994). The NDVI shows an unambiguous reaction when atmospheric disturbance is present: its value will decrease. It was shown here that kriging improves the NDVI estimates by 20 to 70% compared to MaxVC. Besides, the MaxVC offers a solution to clouded pixels when the NDVI contains sufficient information, i.e. when the information from bands 3, 4 and 5 is not needed. With the presented kriging procedures, estimates can be made for the original bands and no information is excluded, which is advantageous for LUC classifications.

The quality of the images used for interpolation needs to be quite good. The presence of (slightly) clouded pixels among the interpolators has a detrimental effect on the outcome and thus introduces uncertainty. A manual adjustment of the
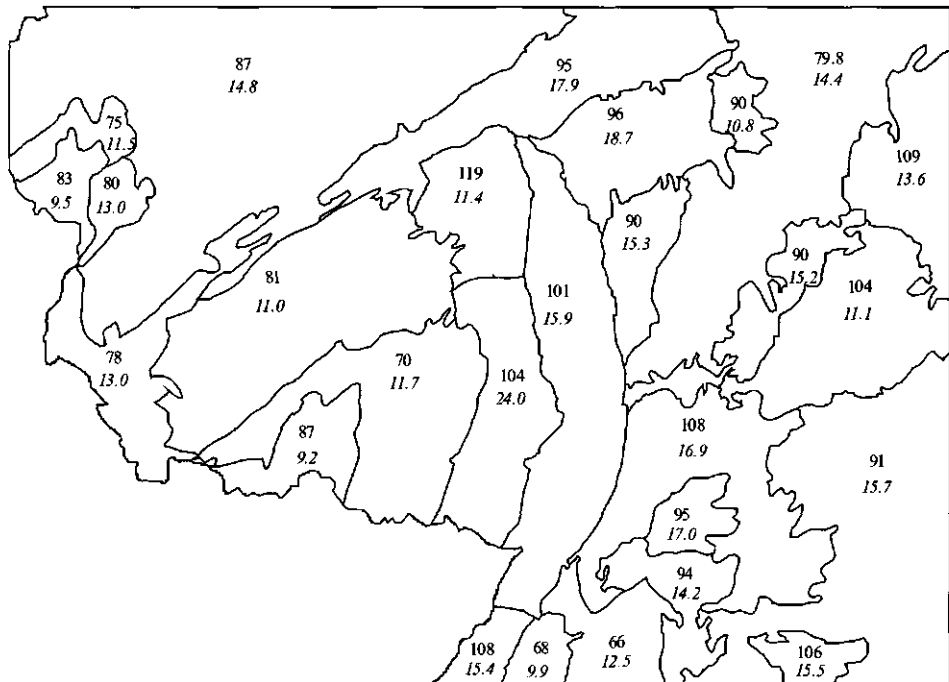

Figure 4.6 Mean and standard deviation (in italics) of band 1 for individual strata.

Table 4.4 Mean distance (in pixels) to nearest region boundary of method leading to best results. Per pixel the method with the lowest prediction error is determined, after which the mean distance is calculated for those pixels where stratified methods led to best results and for those where the unstratified methods resulted in best estimates. Only pixels within 10 pixels from the boundaries are considered.

	K				CK			
	$V1$	$V10$	$V100$	V_{real}	$V1$	$V10$	$V100$	V_{real}
Stratification	3.7	3.5	3.3	3.4	3.8	3.6	3.7	3.6
No stratification	3.8	3.6	3.6	3.6	4.0	3.9	3.8	3.8

cloud masks may be necessary. When too many pixels in the second image have to be marked as clouded, the number of missing values among the replacements will increase to an undesirable number. To obtain estimates for more pixels unstratified kriging forms an acceptable alternative. The estimates show only a minor decrease of reliability compared to co-kriging, although the difference increases for larger polygons. Unstratified is also a good alternative when daily images are not available.

Currently, kriging options are not available in image processing packages. As a result we used four software packages for interpolation. If kriging were included in image processing software, interpolation of the clouded pixels, including calculation of the variograms process, could be performed in one run.

The seven methods tested on an area in Central Europe can be assumed to have similar results for other areas as well. World-wide, changing atmospheric conditions rather than changing land cover causes day-to-day variance of pixel values. Co-kriging uses this optimally by retaining the pattern of the other-day image. Patterns remain fairly constant, although pixel values may change.

4.5   Conclusions

Seven different methods to replace clouded pixels were applied to NOAA-AVHRR images. As unstratified co-kriging showed the lowest $rmse_{cor}$ values in this study, it is recommended as the most reliable method for replacing clouds at a sub-continental level. The $rmse_{cor}$ values of the validation sets for unstratified co-kriging were reduced by 20 to 70% as compared to the conventional replacement procedures. The spatial arrangement of radiation values apparently shows less day-to-day variation than the reflectance value of a single pixel.

A good alternative to co-kriging is found in ordinary kriging. Rmse-values are somewhat higher, but it has the advantage of not needing a second image as co-variable. With the rare availability of high quality images this is a very positive characteristic.

Stratification did not result in improved estimates. Rmse-values were slightly better without stratification. Apparently, none of the three stratification effects, local

65

variograms, better interpolation points and increased interpolation distances, dominated the interpolation process.

Once kriging options have been implemented in existing image processing packages, co-kriging will form an easy-to-use solution to missing values, provided that images of subsequent days with low cloud coverage are available. Otherwise, unstratified kriging offers a good alternative.

CHARACTERISING CHANGES
IN ENVIRONMENTAL IMPACT

5

In chapter 3 the spatial observation units to be used for change detection in environmental impact of agriculture were discussed and defined. This chapter focuses on the question which variables are suitable to characterise changes in environmental impact. Within the context of this study they should be related to agriculture and observable with NOAA-AVHRR. Two types of changes are of relevance here: land use conversions between the major land use classes (in particular changes from or towards 'agriculture'), and land use modifications due to in- or extensification. Conversions will result in changes of area used for agriculture, whereas modifications will result in changed intensities. While changes in area can be clearly expressed, it is not clear yet which variable, observable with NOAA-AVHRR, can be used to describe intensity changes.

5.1   Introduction

Change detection methods always comprise two components with each its own characteristics. One component, in this case NOAA-AVHRR, is used to observe changes in a second component, in this case environmental impact of agriculture. For effective change detection, relevant agricultural variables must be observable with NOAA-AVHRR. Currently, environmental impact of agriculture is described in terms of environmental problems resulting from it, such as declining biodiversity, eutrophication and land degradation (e.g. EEA, 1995b) (see also section 2.2.2). These problems, however, cannot be observed in NOAA-AVHRR images directly. Hence, the new change detection method must be based on variables that can be derived from satellite images and that are relevant to environmental impact of agriculture.

Such variables should meet several criteria. Firstly, since the method will consider entire regions (chapter 3), the variable should provide a measure

representing a region. It should reflect the situation in an entire region, not in single spots. Secondly, the method is supposed to provide quick insight in locations where changes occurred, so comparison of the variable over time should reveal directly whether the situation changed or not. This decision should preferably be reached without additional information, because of the huge number of regions involved. Thirdly, the variable should be related to environmental impact and to the information in NOAA-AVHRR images. And fourthly, the method should yield valid results throughout the European Union, irrespective of the exact location.

The information that NOAA-AVHRR provides is emitted thermal energy and reflected solar radiance. Per pixel the AVHRR sensor registers an average values of emitted or reflected radiance of all land cover surfaces within the $1.2km^2$ represented by that pixel. Although the pixel size is such that it is difficult to delineate individual patches of forest or agriculture, land cover composition is reflected in the pixel values. Significant changes in land cover should therefore be detectable in the images, whether they are qualitative, i.e. the land cover type changes, or quantitative, i.e. the amount of biomass changes.

Two types of agricultural changes that lead to more or less environmental impact are considered here; conversion between agriculture and other major land use classes, and modification of existing agriculture due to in- or extensification. Conversion will lead to changes in the area used for agriculture and can be characterised as a qualitative land use change, which will result in land cover change. For example, agriculture is converted into built-up area, or forest is cleared to practice agriculture.

Intensification of agriculture is the process of increasing input variables, such as labour, capital, skills, chemical fertilisers, and pesticides, in order to raise production (Turner and Doolittle, 1978). As a secondary result, given the increase of input variables, it will also give rise to larger environmental impact (e.g. De Wit, 1999). There is general consensus in literature, that higher intensity leads to higher production and therefore that production level is the best measure to characterise intensity (e.g. Lambin *et al.*, 2000; Shriar, 2000; Turner and Doolittle, 1978). So, intensification does not bring about a qualitative change, since the type of land cover remains unchanged, but it does result in a quantitative land cover change, since the amount of biomass does change.

The area used for agriculture is a functional measure to characterise some aspect of its environmental impact. The larger the agricultural area, the more impact it will have on the environment (with comparable management practices). Changes in agricultural area are therefore a clear indicator for changes in environmental impact. For intensity changes yields are not as straightforward an indicator as area is for modifications, because yields can show large annual variations due to meteorological differences. Besides, different crops have different yields (in tons per ha), which should be accounted for before defining a suitable measure to characterise changes of intensity.

It must be concluded from the previous, that change in agricultural area is a suitable variable to indicate land use conversion, and that a second variable is required to indicate changes due to modifications of agricultural practices. Therefore, this chapter will present and study two measures to characterise changing agricultural intensity and it will consider whether NOAA-AVHRR can yield suitable information on these measures.

5.2   Data and Methodology

5.2.1   Theory

The Food and Agricultural Organisation (FAO, 1993) defines sustainable land use and management by five areas of attention: 'Sustainable land management combines technologies, policies and activities aimed at integrating socio-economic principles with environmental concerns, so as to simultaneously:
    -maintain and enhance production and services;
    -reduce the level of production risk;
    -protect the potential of natural resources and prevent degradation of soil and water quality;
    -be economically viable and
    -socially acceptable'.
Consequently, when agriculture is sustainable, it can be practised for a long period without nutrient depletion of the soil, eutrophication of surface and groundwater, etc. Following these FAO guidelines, sustainable agriculture is expected to have limited environmental impact resulting in a negative correlation between sustainability and environmental impact.

Bouma and Droogers (1998) propose the ratio of actual and potential yield as basis of a measure for sustainability of agriculture. They simulated 30 years of wheat production on one soil type with different land use scenarios. From these simulations they deduced cumulative probabilities of threshold exceedance of nitrate leaching with different percentages. By accepting a risk level, indicators for land quality, as they called the ratio, can be derived. This procedure leads to a crop and soil specific result. For the change detection method to be developed in this study, this is currently no feasible option, because many crops and many soils are involved and it would require determining the exceedance probabilities for each relevant combination.

Instead of using the ratio between actual and potential yield for determining the exceedance probabilities it is suggested here to use the ratio for change detection. This ratio, here further indicated as actpot-yield ratio, corrects the yield figures for annual fluctuations due to meteorological variation, because the potential yield is calculated on a yearly basis. Therefore, comparison over time is allowed for one crop in one region.

This ratio allows for comparison over time, but comparison between regions does not make sense, as the measure does not account for differences in the regions' original capacity, which shows quite some variation throughout the European Union. For some regions, little effort is needed to obtain yields close to the potential yield, whereas for other regions the same effort would hardly raise the yields. These efforts might cause comparable environmental impact, but the actual-potential yield ratio will show different values. To compensate for differences in original capacity, an extension of the ratio is proposed with a term to correct for nutrient limitation.

The extended ratio to characterise environmental impact due to agricultural intensity includes a third term indicating the theoretical nutrient limited yield. It is introduced as a lower limit, while the potential forms the upper limit. The value of the actual yield is determined relative to the nutrient limited and potential yield. The values this ratio can take lie between 0 and 1, when the actual yield exceeds the limited yield, while they are negative otherwise. This ratio will further be indicated as nutlim-yield ratio.

So, two ratios are proposed to be tested here. The actpot-yield ratio:

$$\text{actpot - yield ratio} = \frac{\text{actual yield}}{\text{potential yield}} \tag{5.1}$$

and the nutlim-yield ratio:

$$\text{nutlim - yield ratio} = \frac{\text{actual yield} - \text{nutrient limited yield}}{\text{potential yield} - \text{nutrient limited yield}} \tag{5.2}$$

Both ratios are crop specific, which can result in contradictory results for different crops within one region. Since no detailed crop information is available for the study area, the ratios should here show comparable behaviour for different crops within a region when they are to be used for characterisation of change in environmental impact.

5.2.2   Data

Yield data were available from two different sources. For 1989 and 1993 regional statistics were available, containing actual yield figures (BLSD, 1990a and 1994a; HSL, 1990a and 1994a; LDSN-W, 1990a and 1994a; SLB-W, 1990a and 1994a; SLR-P, 1990a and 1994a; SLS, 1990a and 1994a). Yields are expressed in tons/ha and figures are provided for each *Kreis* (NUTS-3 region).

Potential yield data were available from WOFOST (WOrld FOod STudies), a crop growth model which estimates the growth of an annual crop given a set of specific soil and weather conditions (Hijmans *et al.*, 1994; Supit *et al.*,

1994). The environmental data needed by the model are daily weather data, including solar radiation, minimum and maximum temperature, rainfall, air humidity and wind, and soil profile data including the available moisture holding capacity and maximum rootable depth. The growth driving process is photosynthesis, of which the maximum is determined by light interception and temperature. WOFOST is amongst others used for the Crop Growth Monitoring System (CGMS) for operational yield forecasting for the European Union (Van Diepen, 1991).

By application of WOFOST at the European scale, spatial units are defined by the intersection of a 50*50 km² grid containing weather conditions and polygons from the European soil map (CEC, 1985) holding soil conditions. Since potential yields depend entirely on radiation, temperature and crop characteristics, they were identical throughout each 50*50km² grid cell. Potential yield data were available for four crops: potato, sugar beet, winter wheat and maize.

Data to simulate nutrient-limited yield with WOFOST were not accessible. Instead nutrient-limited yield figures were deduced from the potential yield using a fertility reduction factor (Zobler, 1986 in Leemans and Van den Born, 1994). For each FAO soil type a multiplication factor between 0 and 1 is applied to the potential yield to retrieve the nutrient-limited yield.

All yield data, potential, nutrient-limited and actual, were aggregated into the regions defined in chapter 3 by taking the average value weighted according area.

5.2.3   Method

The main condition to be fulfilled here by the proposed measures of agricultural intensity is that changes in intensity within a region show comparable trends for all crops, or at least for the main crops. Alternatively, validation should be performed per crop with environmental impact data to see whether they show some correlation with the ratios. No crop-specific impact data are available, however, so this is no option within this study.

Both the actpot-yield ratio and the nutlim-yield ratio are calculated over the 27 regions for 1989 and 1993 for each of the four crops. Changes during the four years are determined and correlation coefficients between those changes of the four crops are calculated.

5.3   Results

Using the WOFOST yield data the actpot-yield and nutlim-yield ratios are calculated for each region in the study area. These ratios are thought to be indicators for agricultural intensity and a change in ratio value thus indicates a change in intensity. Changes in ratio differ quite strongly within a region for the different crops (figures 5.1 and 5.2). For two regions WOFOST considered the
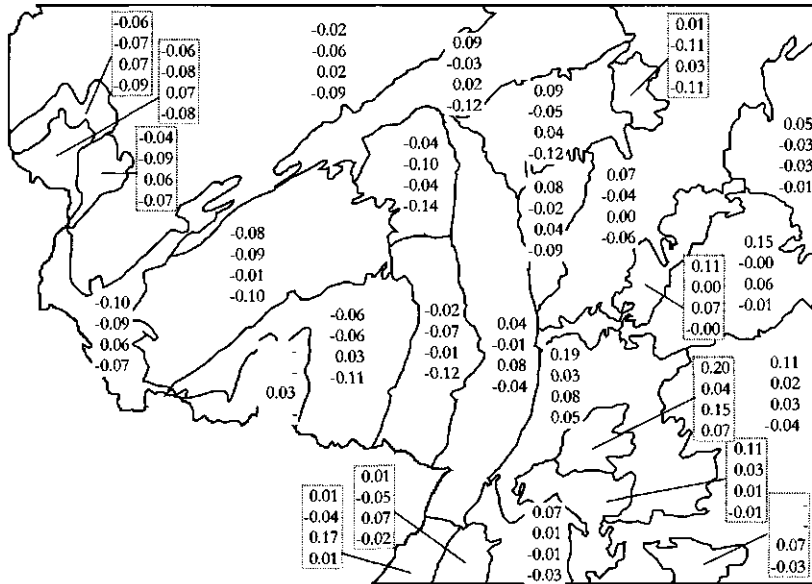
Figure 5.1 Differences in the actpot-yield ratio between 1989 and 1993. The upper most value shows the change for potato, the next one for sugar beet, the third for winter wheat, and the bottom one for maize. A '–' indicates that for at least one of the years WOFOST found circumstances unsuitable to this crop.

growing conditions in both 1989 and 1993 unfavourable for potato and sugar beet, and for one of the regions for maize as well. The statistics showed that those crops had been grown anyway in these regions and that yields were comparable to other regions in terms of tons per ha.

The ranges of the changes of the two ratios show quite some variation (table 5.1). While the minimum and maximum values for the actpot-yield ratio vary between -0.14 to 0.19, they range from -0.69 to 0.60 for the nutlim-yield ratio. A negative value indicates that intensity decreased, while positive values show increased intensity.

The mean values of the ratios for the different crops show similar trends. For potato and winter wheat the ratios increased, while they decreased for sugar beet and maize, although the nutlim-yield change for sugar beet was minimal with -0.004. Within regions the two ratios may show opposite behaviour.

Correlation coefficients of the crops for changes in the actpot-yield ratio are rather low (table 5.2), but for the nutlim-yield ratio they are even lower (table 5.3).
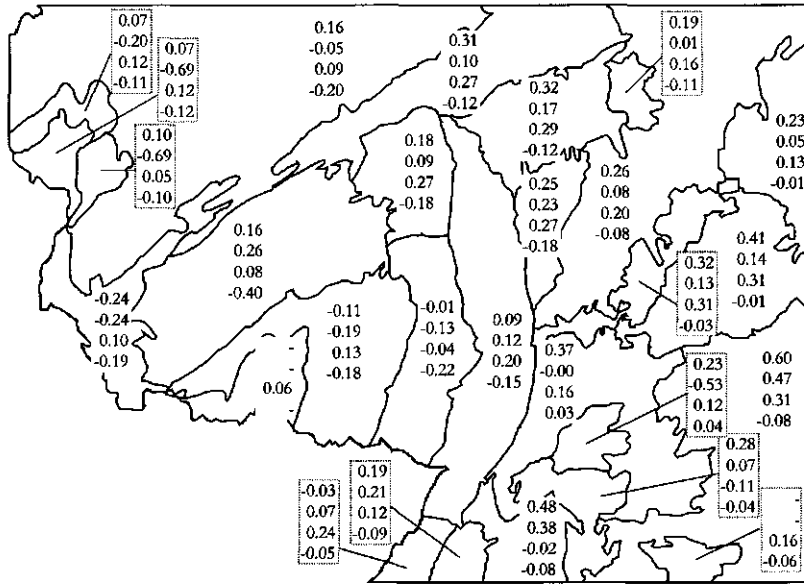
Figure 5.2 Differences in the nutlim-yield ratio between 1989 and 1993. The upper most value shows the change for potato, the next one for sugar beet, the third for winter wheat, and the bottom one for maize. A '–' indicates that for at least one of the years WOFOST found circumstances unsuitable to this crop.

Table 5.1 Statistics of the changes of the two ratios for the four crops between 1989 and 1993.

	Potato	Sugar beet	Winter wheat	Maize
Actpot-yield ratio				
Mean	0.03	-0.04	0.04	-0.05
Standard deviation	0.08	0.04	0.05	0.06
Minimum	-0.10	-0.11	-0.04	-0.14
Maximum	0.19	0.04	0.17	0.07
Nutlim-yield ratio				
Mean	0.20	-0.00	0.15	-0.11
Standard deviation	0.18	0.29	0.11	0.09
Minimum	-0.24	-0.69	-0.11	-0.40
Maximum	0.60	0.47	0.31	-0.04

Table 5.2 Squared correlation coefficients (r^2) of changes in the actpot-yield ratios between the four crops

	Potato	Sugar beet	Winter wheat	Maize
Potato	-	0.78	0.06	0.43
Sugar beet		-	0.13	0.56
Winter wheat			-	0.37
Maize				-

Table 5.3 Squared correlation coefficients (r^2) of changes in the nutlim-yield ratios between the four crops

	Potato	Sugar beet	Winter wheat	Maize
Potato	-	0.29	0.09	0.15
Sugar beet		-	0.10	0.01
Winter wheat			-	0.03
Maize				-

5.4   Discussion and conclusions

For two regions data from WOFOST indicated that conditions were unfavourable to grow potato, sugar beet and, for one region, maize as well. Three reasons are possible responsible for these contradictory findings. The first and most probable reason is that the scale of the soil map is responsible for missing some suitable areas. The second reason could be that requirements for crops formulated for WOFOST are too strict. And a third reason could be that despite unfavourable conditions, the level of agriculture is such that advanced agricultural practices result in acceptable yield levels anyway.

The values of the two ratios showed low correlation coefficients and opposite trends between crops. The ratios for potato and winter wheat increased, suggesting increased agricultural intensity. At the same time the ratios for sugar beet and maize decreased, suggesting decreasing agricultural intensity. These contradictory results complicate the definition of a useful measure to characterise environmental impact due to agricultural intensity.

The mean composition of the study area in terms of crop type is 24% winter wheat, 10% maize, 7% sugar beet, and 3% potato. So, the two largest crops in terms of covered area do show contradictory behaviour. The average percentage of the area cropland in the *Kreise* used for the four crops for which simulated yield data were available is 42%. This means that almost 60% is in use for other crops, the main one being spring barley with a mean coverage of 17%. Another important category not included is horticulture, which covers 10% on average. Given the contradictory behaviour found here, it is doubtful whether including all major crops would have led to useful results.

Of the two ratios, the actpot-yield ratio shows highest correlation figures between the crops. This is probably the better option of the two to validate with crop specific environmental impact data. For this study the results are nevertheless found too weak and, therefore, unsuitable to be used as validation data for the change detection methods. Consequently, the methods will be validated with just land use conversion data.

A new source for useful variables could be the area of yield predictions from remote sensing. Yields for individual crops should be estimated from images spanning the monitoring period. This requires reliable crop identification and reliable biomass estimation. Overall trends could then be used to account for annual fluctuations and when individual regions deviate from this trend this might be caused by changed intensities. With NOAA-AVHRR this is no realistic option, but with future imagery, like MERIS with its narrow spectral bands and 300m pixels (ESA, 2000), this might become feasible.

CHANGE DETECTION METHODS

6

In chapters 3 and 5 spatial and thematic aspects of change detection were discussed. In this chapter the methods for change detection of land cover are studied. Three new methods for regionwise change detection are compared and tested, which are believed to experience less influence of misregistration and atmospheric differences between images than the conventional pixelwise approach. The first method uses the Geometric Similarity Index presented in chapter 3 to compare the spatial correspondence between spectrally homogenous polygons in images of different dates. The second method compares probabilities of pixels belonging to spectral clusters for images of different acquisition dates. And the third method compares semivariances of radiation data of two images. The methods aim to indicate whether changes occurred or not. Identification in terms of land cover of the located changes is beyond this study. All three methods are tested in three phases. First the sensitivity to the disturbing factors of misregistration and radiometric effects is tested. Next, the methods are validated using real data, but this is hampered by the disturbing factors of radiometric effects and misregistration. To overcome these deteriorating effects, a third phase is included, where simulated images with artificial changes are created to test the methods under circumstances where disturbing factors are eliminated.

6.1 Introduction

Remote sensing is a valuable information source for change detection because of frequent revisit times, consistent image quality and a synoptic view of large areas (Coppin and Bauer, 1996; Singh, 1989). The basic assumption for land cover change detection with remote sensing is that a change of land cover results in a change of spectral properties that is significantly larger than changes of radiation resulting from disturbing sources like atmospheric variation and sensor noise. Many studies on change detection have been performed. Singh (1989) gives a general

overview of existing methods, Mas (1999) compares existing techniques, while Coppin and Bauer (1996) give a review of change detection for forest ecosystems (table 6.1).

Singh (1989) distinguishes two different approaches; the first is comparative analysis of independent classifications, and the second is simultaneous analysis of multi-temporal data such as image differencing, image ratioing and change vector analysis. He concludes that even over the same time span and in the same environment various techniques may yield different results. According to Singh geometric imprecision of the imagery used is an important source of uncertainty. Therefore Singh suggests that there is a need for methods which are less sensitive to misregistration.

Mas (1999) recognises three categories of change detection techniques. Like Singh, he identifies comparative analysis of independently classified images as one approach. He classifies Singh's second approach, simultaneous analysis of

Table 6.1 Overview of categories for remote sensing change detection techniques. Singh (1989) distinguishes two broad categories with seven techniques in the second one, Mas (1999) distinguishes three categories, and Coppin and Bauer (1996) recognise broader categories (indicated by dashed lines), but distinguish ten distinct types of change detection methods that are entirely based on remote sensing. The solid black lines indicate divisions between categories as indicated by the respective authors.

Singh	Mas	Coppin and Bauer
• Post-classification comparison	• Post-classification analysis	• Post-classification comparison
	• Multi-date data classification	• Multi-dimensional temporal feature space analysis
		• Composite analysis
• Image differencing • Vegetation index differencing	• Subtraction of bands	• Image differencing
• Image ratioing	• Image ratioing	• Image ratioing
• Principal Component Analysis (PCA)	• Principal Component Analysis	• Multitemporal linear data transformation (PCA and Tasselled cap)
• Change vector		• Change vector analysis
• Image regression	• Image regression	• Image regression
		• Multitemporal biomass index
		• Background subtraction
• Raw data		

multi-temporal data, as image enhancement. Besides he recognises a third category: multi-date classification, which he defines as a mathematical combination of two images. Mas concludes that post-classification techniques result in most reliable results.

Coppin and Bauer (1996) considered more than 75 change detection studies. They acknowledge the existence of two or three broader categories, but recognise eleven distinct approaches themselves (in table 6.1 only ten are shown, since their first approach, mono-temporal change delineation, does not concern comparison of imagery of different dates). The relation to each of the techniques mentioned by Singh and Mas is clear, except for the raw-data techniques of Singh. Coppin and Bauer conclude that accurate registration of multi-date imagery is a critical prerequisite of accurate change detection.

Two general conclusions are that there is no single best method: different methods may yield different results in the same situation. Furthermore, accurate registration of imagery is of utmost importance, and, as Singh states, there is a need for methods that are less sensitive to misregistration.

Most studies included in the overviews by Singh, Coppin and Bauer, and Mas use high-resolution images, mainly Landsat TM. Few papers are encountered on change detection based on low-resolution imagery, like NOAA-AVHRR. One of the few researchers working on this topic is Lambin. He publishes frequently on the development of change detection tools for sub-Saharan areas in West Africa (Borak *et al.*, 2000; Lambin and Ehrlich, 1996; Lambin and Strahler, 1994a; Lambin and Strahler, 1994b). In the latest publication, they compared several temporal metrics for change detection. Using 30-day maximum value composites, they demonstrated that a combination of surface temperature and NDVI yields the best change parameters for their study area. A multivariate combination of these parameters is subsequently shown to have the highest correlation with total change and with net vegetation gain. They emphasise that the results are valid for warm, water-limited environments. In Europe such areas are only found in selected parts of the Mediterranean. Moreover, the heterogeneity of west European landscapes is much larger than that of the sub-Saharan region, which will result in larger sensitivity to misregistration (Townshend *et al.*, 1992) and consequently in less reliable maximum value composites.

The general conclusion from the review/comparison studies is that although the use of satellite images seems promising, there are problems related to change detection with remote sensing. For NOAA-AVHRR these problems may be even more significant. The main problems are:

- **Classification uncertainty.** Classification accuracy of satellite images such as Landsat TM and SPOT-HRV, generally does not exceed 85% correctly classified (Foody 2000 keynote Accuracy2000 and pers.comm. Prof.Dr.

G.M. Foody, University of Southampton) due to the mixing of spectral reflectance of various objects within the pixels and other sources of uncertainties. Post-classification comparison should account for twice 15% or more inaccuracy. As already indicated in section 2.3.3 classification accuracy for NOAA-AVHRR imagery with pixels sizes of 1.2 km² is normally much lower. The International Geosphere Biosphere Data and Information System (IGBP-DIS) Global 1-Kilometer Land-Cover Data Set (DISCover) including 16 broadly defined classes, reached regional classification accuracies varying from 15.4% for Southeast Asia to 85.7% for North Africa (Scepan *et al.*, 1999). The mean accuracy was 54.5%, while the accuracy for Europe reached no further than 46.7%. By including ancillary information sources on locations of forest, urban, water and wetlands Mücher *et al.* (2000) reached an accuracy of 69% with fourteen classes for Pan-Europe. These sources of uncertainties largely hamper the comparison of multi-date images since error propagates and increases during the analysis process of multi-temporal images. Consequently, the conclusion of Mas (1999) that postclassification techniques result in the most reliable change detection results, is probably valid for his case but not valid for change detection based on NOAA-AVHRR images in Central Europe.

- **Spatial uncertainty.** Land cover change detection requires the comparison of images acquired at different dates and possibly by two types of satellite sensors in different orbits. An accurate change detection analysis requires an almost perfect geometric match of the images. Misregistration may result in identification of land cover change caused by non-matching pixels rather than real land cover change (Townshend *et al.*, 1992) and hence it reduces the reliability of change detection methods. The best obtainable accuracy of georeferencing of images lays normally around 0.5 pixel (Schowengerdt, 1997). NOAA-AVHRR is particularly sensitive to misregistration, because of the type of scanner. Radiation is registered using rotating mirrors (the so-called whiskbroom scanner) and the scan width is 2800km. The alternative to the whiskbroom scanner is the push-broom scanner, which is much less sensitive to geometric distortions (Loedeman, 2000 and pers.comm. Dr. Ch.K. Toth, Ohio State University). The large scan width introduces large distortions at the edge of a scene: while a pixel at nadir measures 1.2km², it reflects an area of 3*7km² at the edge. Limiting the used part of the scene to the central 1400km largely eliminates this latter effect, whereas distortions due to the whiskbroom principle can only be reduced by geometric corrections which will never completely remove them. Therefore, the conclusions of Coppin and Bauer (1996), that accurate registration is a critical prerequisite, and of Singh (1989) that there is a need for methods that are not or less sensitive to misregistration, are

probably even more valid for change detection using NOAA-AVHRR images.

- **Radiometric effects**. Multi-temporal satellite images used for change detection show different reflection values because of land surface changes, misregistration effects and/or radiometric effects caused by sensor noise, sensor calibration drift, and illumination and atmospheric differences (Stow, 1999). Misregistration and radiometric effects prohibit a direct comparison of reflectance data. Particularly when large areas are involved, correction for these radiometric effects is not or only limited possible due to lack of correction algorithms or the amount of data needed in order to obtain reliable results.

From the discussion above it follows that there are three types of factors complicating change detection: classification uncertainty, spatial uncertainty and radiometric effects. To improve the reliability of change detection a new methodology, as opposed to the conventional pixel-wise methods, is presented and discussed here and referred to as *region-wise change detection*. Integral assessment of reflection values within a region forms the basis of this methodology. Three alternative approaches are tested, which all eliminate at least one of the complicating factors:

1. Cluster patterns

   The assumption behind this approach is that, although it is not possible to reliably classify individual pixels, pixels with similar spectral characteristics have similar land cover characteristics. Consequently, spectrally similar clusters of pixels indicate groups of pixels with similar land cover composition, and changes of the spatial arrangement of the associated polygons over time will therefore indicate changes of land cover. As the new proposed analysis is performed on reflectance values, uncertainties originating from classification are avoided. The influence of spatial uncertainty is partly reduced due to the clustering of pixels with similar reflection values. Radiometric effects are partly reduced as well; effects that are homogenous throughout a region are eliminated, those that are not will influence the results.

2. Cluster signatures

   Instead of the spatial arrangement of the spectral clusters, their signatures can also form the base for change detection. Each cluster has its own signature and for every pixel the probability of belonging to them is calculated. These probabilities are summed per cluster and yield a basis for change detection. Classification uncertainties are avoided, again because the spectral values are used. Spatial uncertainties are almost completely excluded, because comparison is regionwise. Radiometric effects are not tackled by this approach.

81

3.   Semivariances
        A third approach is to describe the spatial arrangement of the reflectance
        values of the individual pixels, which can be summarised by semivariances.
        This approach excludes classification uncertainties, because it uses the
        reflectance values. Like the second approach, it avoids spatial uncertainties
        because comparison is regionwise. Finally, it reduces radiometric effects,
        because, as found in chapter 4, the spatial arrangement of reflectance values
        shows less day-to-day variation than the reflectance values of a single pixel.

6.2   Data and Methodology

6.2.1   Data

Several NOAA-AVHRR images covering the study area were retrieved
from the SPACE database of the Joint Research Centre of the European Union
(JRC) in Ispra, Italy (Millot and Loopuyt, 1997). AVHRR images of 31 August, 7
and 8 September 1989, and 11 August 1997 are used in this chapter (table 6.2). The
images had all been subjected to geometric and radiometric corrections (Kerdiles,
1998; Tanré *et al.*, 1990). Furthermore, they were provided with masks indicating
amongst others whether a pixel is clouded or not. The cloud masks did not cover all
affected pixels; especially pixels bordering the indicated cloud pixels still showed
cloud effects. Therefore, all cloud pixels in the masks were buffered by one pixel to
include those bordering pixels and to remove cloud effects from the image as much
as possible.

The images of 7 and 8 September 1989 were used to test the sensitivity of
the methods to radiometric effects and misregistration. The image of 7 September
is of high quality, with cloud coverage of 1.3%. The 8 September image is of high
quality, too, with 4.6% cloud cover and 1.5% missing values due to striping. The
combination of these two images allows for short-term comparison. The cloud
masks of 7 and 8 September were combined and applied to both images, leaving
only those pixels that are free of clouds on both days. In the analyses just bands 1
and 2 are used, because over land they show mainly vegetation characteristics which

Table 6.2 Statistics of four NOAA-AVHRR images. Values are expressed in reflectance percentages on a scale from 1 to 1024.

		7 September 1989	8 September 1989	31 August 1989	11 August 1997
Band 1	Mean	58	53	45	64.3
	Standard deviation	19.9	19.1	18.9	25.6
Band 2	Mean	179	171	147	215
	Standard deviation	21.9	22.6	23.2	34.6

have a strong seasonal development and which will therefore be very similar on two succeeding days. Band 3 is not calibrated (Tanré *et al.*, 1990) and therefore cannot be expected to remain constant over time, and bands 4 and 5 offer data on emissivity, which does not depend on seasonal developments but can instead show considerable day-to-day variation.

For the long-term comparison two images from the late growing season are available: 31 August 1989 and 11 August 1997 (table 6.2). The image of 1989 contains 1% clouds, whereas the 1997 image is completely free of clouds. The choice for two dates in August is based on image availability and the stage of the growing season, which is then coming to its end. Consequently most crops and forests will have reached maximum biomass for some time and comparison between different years will be less hampered by differences in the development of the growing season (Coppin and Bauer, 1996). To both images the combined cloud masks were applied, and just bands 1 and 2 were used.

Validation data are preferably obtained from field investigations, but they are scarcely available for change detection studies. Next best is manual interpretation of higher resolution images (Scepan *et al.*, 1999). Two high-resolution data sets were available: the CORINE database and a Landsat TM image. CORINE is a European land cover database, offering detailed land cover information with a hierarchical legend containing 44 classes, composed by visual interpretation of Landsat TM images (CEC, 1993). For Germany images from the late eighties were used and for the south-eastern part of the study area a TM image recorded at 7 September 1989 was used. The used data set has a pixel size of 100m. The 44 classes were generalised into five classes: forest, agriculture, built-up area, water and natural area.

A Landsat TM image recorded at 11 August 1997 served as high-resolution data for the end of the monitoring period. This image was co-registered to the CORINE data set with a root mean square error of 1.3 TM pixel. No clouds were present and visual inspection revealed no atmospheric disturbances like haze, either.

The polygons of the 1989 CORINE data were overlaid over the 1997 Landsat image. Visual interpretation of this combination produced the validation data of the land cover changes between 1989 and 1997. The percentage of the total area per region that changed is very low (table 6.3). Most changes concerned agriculture changing into forest or built-up areas and they occurred in concentrated spots, mostly in patches with a mean size of 20 ha.

6.2.2   Methodology

The methods will be tested following the procedure shown in figure 6.1. In the first phase the radiometric sensitivity of the three methods will be examined by applying them to the images of 7 and 8 September 1989. Differences in radiation between images can originate from land cover change, radiometric effects and
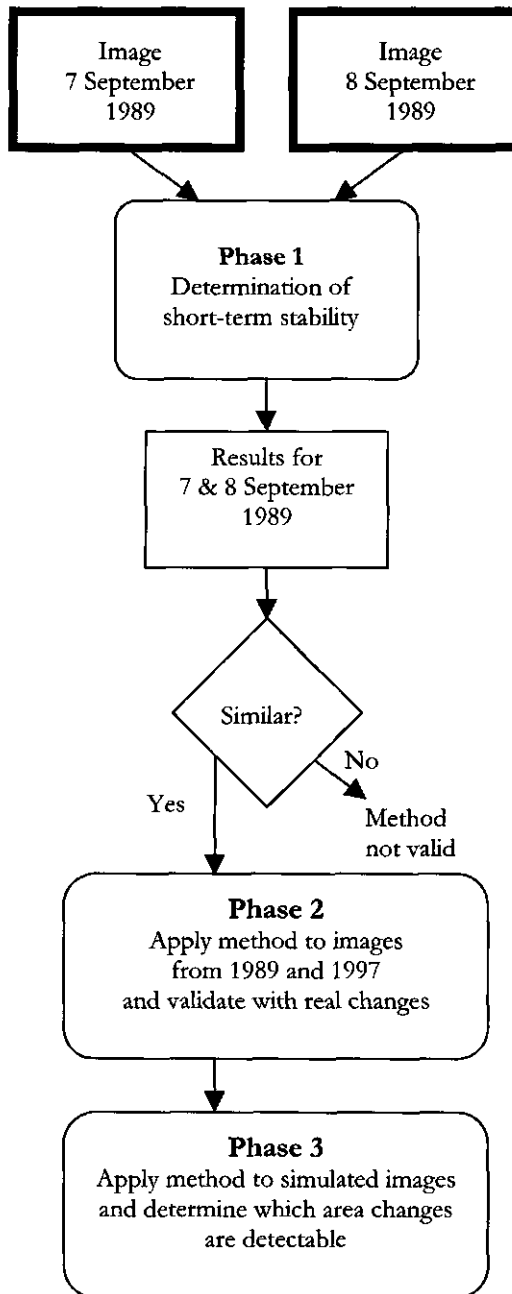
Figure 6.1 Procedure to test the methods

Table 6.3 Changes in land cover between 1989 and 1997 expressed as percentage of the total area. Region numbers refer to figure 6.2.

Region 11	1.2%	Region 15	0.3%
Region 12	0.4%	Region 16	0.2%
Region 13	0.3%	Region 17	0.1%
Region 14	0%	Region 29	0.4%

misregistration. Only changes in land cover are of interest here. Due to the short time span between acquisition of the two images (24 hours) it is assumed that no land cover changes occurred and hence no spectral change should be found. Consequently, all differences observed result from radiometric effects and/or misregistration. The sensitivity of a reliable change detection method to these detrimental effects should be minimal.

In the second phase only those methods showing little sensitivity to radiometric effects and misregistration are included. The methods are applied to the images of August 1989 and 1997 and evaluated.

As the changes observed were smaller than was anticipated based on the regional statistics, a third phase was included to validate the proposed methods. In this phase artificial changes are applied to an existing land cover pattern which is used to create simulated images. From these images is then deduced how large changes must be in order to be detectable with NOAA-AVHRR images.

Five sets of simulated pattern changes are applied to the CORINE land cover pattern of region 11 (figure 6.2) which contains 40% forest, 54% agriculture and 6% built-up areas. Each change set contains three stages. The first shows the situation after 5% of the area changed, the second after 10% and the third after 20% (figure 6.3). All change simulations concern polygons of agriculture changing into forest or built-up areas as comparison of 1989 and 1997 data revealed that these occur most frequently. The procedure to simulate the changes consisted of the following steps:

1. A data set containing random values was created for the region of interest and a selection was made containing 2.5% of the pixels that showed the lowest values within this set.
2. From these selected random pixels all corresponding pixels from CORINE pixels belonging to the class agriculture and bordering forest or built-up areas were selected as 'seed points' for change polygons.
3. If a seed point was located next to a built-up area it was a starting point for a built-up polygon, else it was a starting point for a forest polygon.
4. A new random set was created and a selection was made containing 20% of the pixels that showed the lowest values.
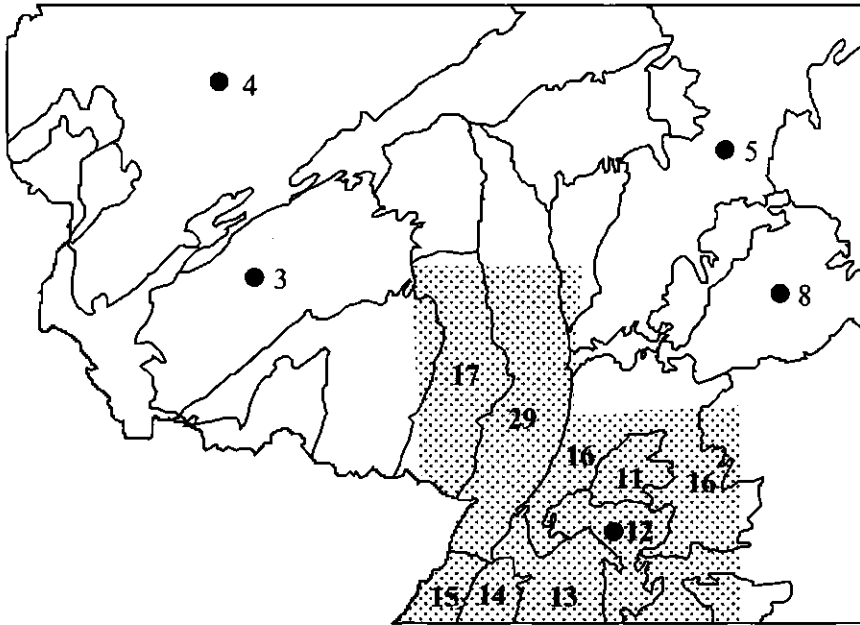
85

Figure 6.2 Regions used during testing procedure. Region numbers in the text refer to those in the map. The shaded area indicates the area for which validation data are available for 1989 and 1997. The first phase included all regions, except for the signature method which was applied only to the five regions marked with a ●. In the second phase all regions within the shaded area were used, but only those parts located within the shaded field. In the third phase the land cover pattern from region 11 served as reference situation.

5.   From these random pixels all corresponding agricultural CORINE pixels bordering a seed point (or later a change polygon) were selected and added to the polygon.

6.   Agricultural pixels that were surrounded by at least 6 (out of 8) built-up pixels of which at least one belongs to a built-up polygon are added to this polygon.

7.   Agricultural pixels that were surrounded by at least 6 forest pixels of which at least one belongs to a forest polygon are added to this polygon.

Steps 4 to 7 were repeated in an iterative manner until the number of pixels changed equalled the desired fraction of the area. The 10% change patterns include the changes of the 5% pattern, while the 20% change patterns include the changes
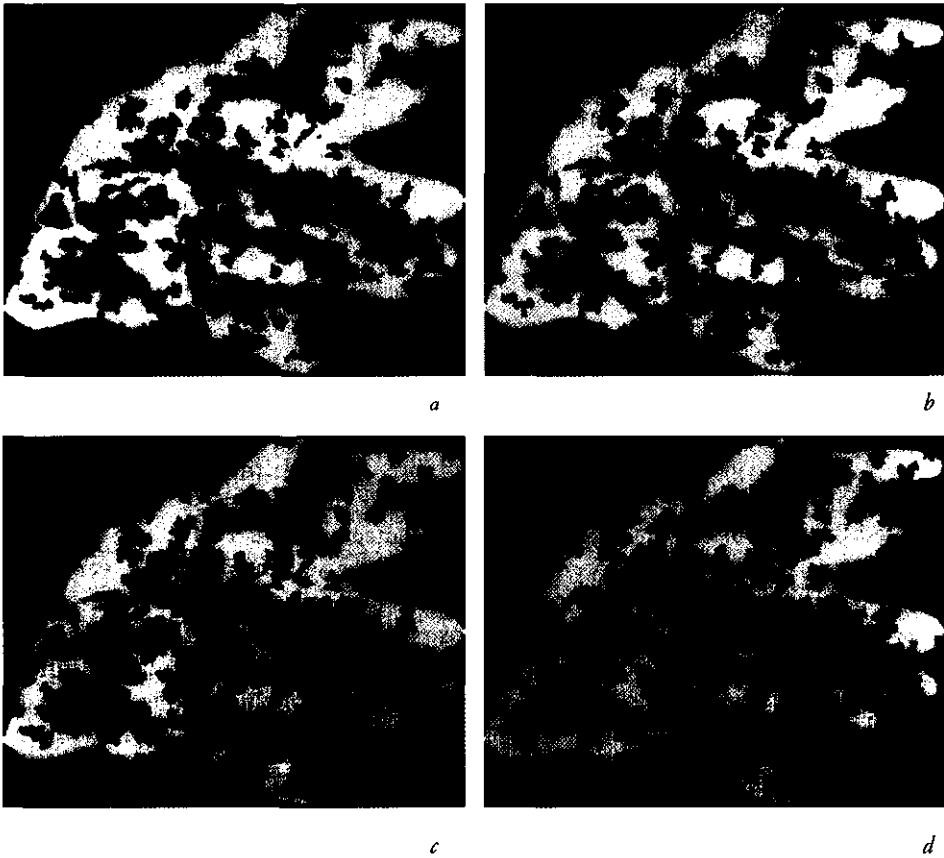
Figure 6.3 Example of a land cover change set. Green indicates forest, yellow agriculture, and red built-up areas. The original pattern is shown in *a*; in *b* 5% of the area changed from agriculture into forest or built-up area; in *c* 10% of the area changed; and in *d* 20% of the area changed.

from both the 5 and the 10% patterns. In each new pattern one third of the former agricultural pixels was converted into built-up and two-third into forest.

Homogenous areas were selected for the three land cover classes (agriculture, forest and built-up) and from the Landsat TM image their mean spectral characteristics were determined (table 6.4). To each pixel from the fifteen changed land cover patterns as well as from the original pattern the spectral values associated with its class were assigned. This resulted in a seven-band image data set with 100m pixels, resulting from the use of the CORINE data set as starting pattern. The pixels of each of the images were subsequently aggregated into 1100m pixels matching the spatial resolution of the AVHRR sensor. In absence of the point spread function, the mean spectral values of the original 100m pixels were assigned to the aggregated pixels following Van der Meer *et al.* (2000). In the

Table 6.4 Spectral characteristics of the three land cover types of Landsat TM bands 3 and 4 (corresponding to AVHRR bands 1 and 2) used to compose the simulated images.

	Forest	Agriculture	Built-up
Band 3	32	25	16
Band 4	63	98	75

subsequent analysis only those 1100m pixels that were composed from 121 (11*11) 100m pixels were used, so pixels at the edge of the area were excluded.

The aggregated parent material polygons from chapter 3 serve as spatial observation units for the methods (figure 6.2). In the first phase all regions are included for the cluster pattern and the semivariance method. The cluster signature method was applied to just five large regions, because the method is very time intensive and because the trend after those five regions was obvious. In the second phase the validation data were used and those are available for eight regions in the south-eastern part of the study area (cf. figure 6.2). In the third phase artificial changes were applied to the land cover pattern of one of the regions. Obviously, just this one region was included.

In the next sections the three approaches for change detection will be described and evaluated. Their results will be presented and carefully discussed.

6.3   Cluster patterns for change detection

Reliable classification of the available NOAA-AVHRR images is not possible, but clusters containing pixels with similar spectral characteristics do exist. These similar spectral properties suggest that the pixels have similar land cover compositions. The assumption is that, although these clusters cannot be linked to individual land cover classes, they do represent a combination of classes in a certain proportion. Without identifying the classes and their respective proportion involved, the geometric similarity (chapter 3) between the polygons associated to the spectral clusters from two images might be a functional change indicator in itself.

The geometric similarity index indicates the correspondence between two partitions of the same area. It is based on the ratio of the largest and next largest intersection of an individual polygon with polygons from the other partition (section 3.2.2). Clusters from two images for the same region here form the two partitions.

Table 6.5 Geometric similarities of the 27 regions for 7 and 8 September

	3 clusters	5 clusters	7 clusters
Mean	0.71	0.56	0.54
Standard deviation	0.13	0.16	0.11

The clusters for each region were determined independently for both images. They were obtained by iteratively clustering the data based on the spectral distance to the cluster means. After each iteration the new cluster means were calculated. The maximum number of iterations was set at 20, and the convergence level at 0.98. To determine the optimal number of clusters, the procedure was repeated for 3, 5, and 7 clusters.

When the polygons of 7 and 8 September show a high geometric similarity, this method appears to be little sensitive to radiometric effects and misregistration.

The Student's T test is used to determine whether the similarities differ significantly with different numbers of clusters.

The similarities between the images from 7 and 8 September 1989 decrease with increasing cluster numbers from 0.71 to 0.56 to 0.54 (table 6.5). The group of three clusters differs from the five and seven cluster groups at the significance level of 0.001. The value of 0.71 indicates that radiometric effects and misregistration can reduce similarities by almost 30% without actual changes taking place. In order to detect real changes similarities must therefore be lower than 0.71.

It is concluded that cluster patterns are relatively stable on short time spans and that grouping into three clusters yields the highest geometric similarity in this test. Next, the test whether changes of cluster patterns are related to the magnitude of land cover changes between 1989 and 1997 can be performed.

Validation data are available for eight regions, for which the geometric similarity index is calculated comparing the images of 31 August 1989 and 11 August 1997 (table 6.6). All similarities but one are lower than 0.71, the value found for the short-term comparison, indicating that land cover changes occurred. The actual changes, however, were very low and correlation between the index and the observed area changes is just 0.02.

Table 6.6 Geometric similarities of eight regions for 31 August 1989 and 11 August 1997

Region 11	0.57	Region 15	0.43
Region 12	0.53	Region 16	0.55
Region 13	0.66	Region 17	0.76
Region 14	0.56	Region 29	0.41

Table 6.7 Geometric similarities between a simulated image with an existing land cover pattern and simulated images with land cover changes

	5% area change	10% area change	20% area change
Mean	0.91	0.81	0.61
Standard deviation	0.02	0.06	0.09

The relation between changed area and similarity index is expected to show lower similarities for larger changes. For those changes smaller than 1% this is indeed true, but the one region with a larger change shows the second highest similarity. Explanations might be found in non-homogenous radiometric effects, in misregistration and in errors of the validation set.

In phase 3 the method is applied to simulated images with artificial land cover changes to determine which magnitude of change the method can detect. Five images with 5% change, five images with 10% and five images with 20% change are available. In this data set of simulated images there is no misregistration and there are no radiometric effects. Even the intra-class radiometric variation is excluded, since each pixel got assigned the mean signature of its class. The results are therefore comparable to those under ideal circumstances.

Similarities between the change images and the original image show a clear decline with increasing changes (table 6.7). The mean similarities decrease from 0.91, to 0.81, to 0.61 for the 5, 10 and 20% changes, respectively. Given the 0.71 similarity level due to radiometric effects, it must be concluded that changes of 20% are detectable, while radiometric effects would overshadow the effects of the 5 and 10% changes.

6.4 Cluster signatures for change detection

Instead of comparing spatial correspondence of the clusters, their spectral signatures might also be a reliable base for change detection. For every pixel the probabilities for the different composite classes can be determined, which can then be summed per class. When this ratio of summed probabilities changes, the land cover composition of the region will have changed.

A region is classified into three clusters for which the spectral signatures are determined. The same cluster procedure was followed as in 6.3. For each pixel the probabilities of belonging to each of the three clusters are calculated using the spectral distance (Gorte, 1999):

$$P(C_i \mid x_p) \sim e^{-\frac{1}{2}D_i(x_p)} \tag{6.1}$$

where $P(C_i \mid x_p)$ is the probability of pixel x_p belonging to class i, and $D_I(x_p)$ the Mahalanobis distance from pixel x_p to the spectral mean of class i. For every cluster the probabilities of all pixels are added, resulting in three summed probabilities. For the pixels of the second image the probabilities of belonging to the three clusters of the first image are calculated.

For the short-term stability, five regions (3, 4, 5, 8, and 12) were selected, containing 604 to 5921 pixels. The signatures of the clusters from the image of 7 September were determined, and the summed probabilities of the pixels belonging to them were calculated. Subsequently, for each cluster the summed probability of all pixels from the 8 September image was calculated. Finally, for each image the probabilities were normalised, so the sum of them equals 1.

The summed probabilities for 7 and 8 September show large differences (table 6.8). The maximum shift of the probabilities for the five regions varies from 13.4 to 50.5%, resulting from either radiometric effects or misregistration. The disturbing effect of misregistration is largely eliminated, since this method considers complete regions and misregistration can take some effect only at the borders. It is therefore concluded that this method is very sensitive to radiometric disturbances and consequently, it is not tested any further.

Table 6.8 Summed and changed probabilities of all pixels for three clusters derived from the image of 7 September 1989. Values are normalised and changes are in percentages.

	cluster1	cluster2	cluster3
Region 3 7 Sept	0.31	0.36	0.33
Region 3 8 Sept	0.24	0.29	0.47
Change region 3	**6.5**	**6.9**	**13.4**
Region 4 7 Sept	0.30	0.36	0.34
Region 4 8 Sept	0.11	0.05	0.84
Change region 4	**19.2**	**31.3**	**50.5**
Region 5 7 Sept	0.48	0.31	0.22
Region 5 8 Sept	0.26	0.41	0.33
Change region 5	**21.3**	**10.3**	**11.0**
Region 8 7 Sept	0.27	0.41	0.31
Region 8 8 Sept	0.10	0.56	0.34
Change region 8	**17.4**	**15.1**	**2.3**
Region 12 7 Sept	0.23	0.38	0.39
Region 12 8 Sept	0.07	0.39	0.54
Change region 12	**16.8**	**1.1**	**15.8**

6.5 Semivariances for change detection

The third method compares semivariances, computed from two images, to detect land cover changes. Semivariance stems from the regionalized variable theory, which was developed by Matheron (1965). He recognised that the spatial variation of a 'regionalized variable', i.e. a natural property with a geographical component, is too irregular to be modelled by a smooth mathematical function but can be described better by a stochastic surface (Burrough, 1986). Curran (1988) and Woodcock *et al.* (1988a, 1988b) introduced the concept of semivariances in remote sensing. They demonstrated that different land cover types show different spatial patterns captured by the semivariance values. The resulting semivariogram (the model fitted through the semivariance values) changes with different, but comparable compositions of spatial patterns in artificial images (De Jong and Burrough, 1995). The underlying assumption for this approach is that spatial patterns of reflectance values in satellite images will change when land cover changes, and that the associated semivariances change as well. Although different patterns can result in equal semivariances, different semivariances cannot result from equal patterns. So when a change in semivariance is observed, the pattern must have changed.

Comparison of the different images is based on the semivariance γ, calculated per lag h, a distance class. The lag distance here equals the pixel size. Semivariance is computed as (Isaaks and Srivastava, 1989):

$$\gamma(h) = \frac{1}{2n} \sum_{i=1}^{n} \{Z(x_i) - Z(x_i + h)\}^2 \tag{6.2}$$

where n indicates the number of pairs of pixels in lag h, x_i a certain pixel, $x_i + h$ a pixel at distance h from pixel x_i and Z the value of the respective pixels. Figure 6.4 shows that semivariances are quite comparable for the two NOAA-AVHRR images of 7 and 8 September 1989.

The Absolute Normalised Difference at lag h (*AND(h)*) is introduced to calculate differences between two sets of semivariances from images of days 0 and 1:

$$AND(h) = \frac{\frac{1}{2}|\gamma_1(h) - \gamma_0(h)|}{\frac{1}{2}(\gamma_1(h) + \gamma_0(h))} \tag{6.3}$$

where AND can take values ranging from 0 to 1, indicating no and total change, respectively. Analysis of differences between semivariances of the studied AVHRR images showed that largest changes occurred within the first five kilometres. Therefore, the *AND(h)* values are calculated for the first five lags only.
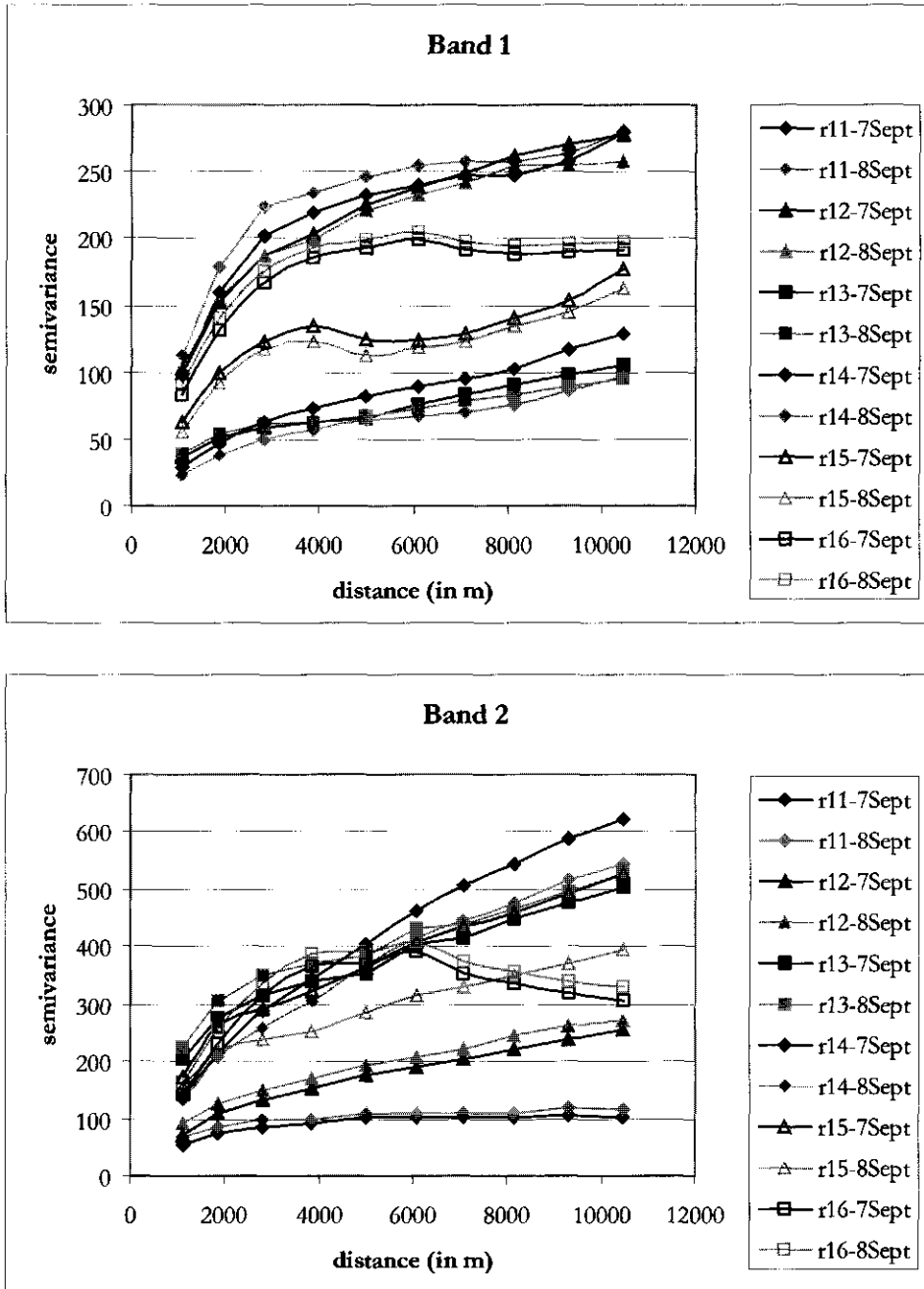
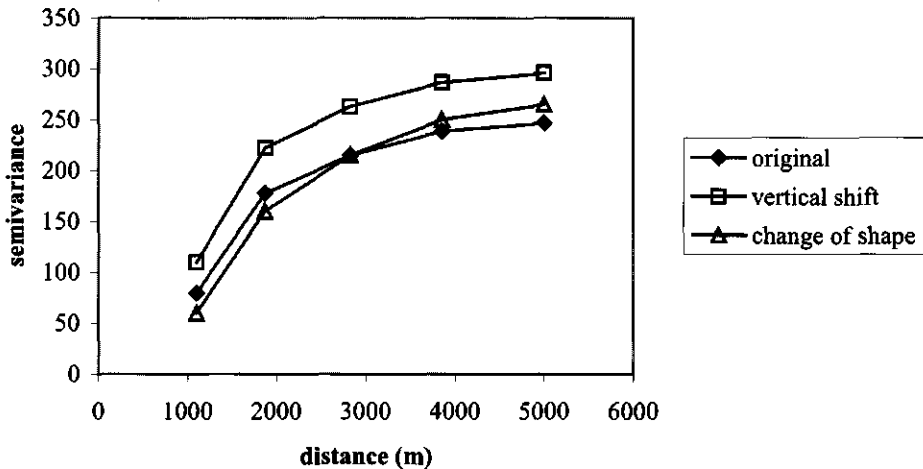**Figure 6.4** Semivariances of 7 and 8 September for six regions

Figure 6.5 Two types of changes of semivariances. The filled diamonds indicate the original semivariances and the open squares and triangles indicate two sets of semivariances after pattern changes occurred. The squares show a vertical shift, where the shape remained more or less the same but where the values changed substantially. The triangles show a change of shape, where the values remained comparable to the original values, but the overall shape of the curve connecting the semivariance values changed.

Differences between sets of semivariances may show as a vertical shift at all lags or as a change of shape of the variogram (figure 6.5). To account for both types of changes, the mean ($mean_{AND}$) and the standard deviation (sd_{AND}) of the five $AND(h)$ values per region are used to characterise the difference.

For all 27 regions, $AND(h)$ values were calculated for four different combinations of bands 1 and 2; the semivariances of the individual bands: γ_{b1} and γ_{b2}; the summed semivariances: $\gamma_{b1}+\gamma_{b2}$; and the semivariances of the two bands summed to each other: γ_{b1+b2}. Table 6.9 shows the statistics of the $AND(h)$ values for the four measures calculated over the 27 regions. As no land cover changes occurred from 7 to 8 September, the measure showing lowest difference values is least sensitive to radiometric effects and misregistration. The summed semivariances yield the lowest $mean_{AND}$ values with an average of 0.039. The average sd_{AND} value is 0.012, which is just somewhat higher than the minimum value. The summed semivariances were selected to serve as input to the $AND(h)$ for the next two phases.

For the eight validation regions the $mean_{AND}$ and sd_{AND} values were calculated (table 6.10). For $mean_{AND}$ values varied from 0.24 to 0.39, they all amply exceed the value of 0.039 found for radiometric effects, thus indicating change. For

Table 6.9 Statistics of the four possible band combinations for change detection. For each measure the average and the associated standard deviation for the $mean_{AND}$ and sd_{AND} are calculated over the 27 regions.

	γ_{b1}	γ_{b2}	$\gamma_{b1}+\gamma_{b2}$	γ_{b1+b2}
$mean_{AND(b)}$				
Average	0.041	0.051	0.039	0.044
Standard deviation	0.030	0.029	0.026	0.033
$sd_{AND(b)}$				
Average	0.011	0.015	0.012	0.011
Standard deviation	0.0070	0.0122	0.0093	0.0096

Table 6.10 Values of $mean_{AND}$ and sd_{AND} for the eight validation regions, based on images from 1989 and 1997

	$mean_{AND}$	sd_{AND}
Region 11	0.39	0.008
Region 12	0.24	0.015
Region 13	0.27	0.007
Region 14	0.37	0.020
Region 15	0.31	0.036
Region 16	0.35	0.008
Region 17	0.36	0.009
Region 29	0.36	0.003

Table 6.11 Statistics of $mean_{AND}$ and sd_{AND} values between a simulated image with an existing land cover pattern and simulated images with land cover changes

	5% area change	10% area change	20% area change
$mean_{AND(b)}$			
Average	0.004	0.018	0.074
Standard deviation	0.002	0.003	0.013
$sd_{AND(b)}$			
Average	0.003	0.007	0.016
Standard deviation	0.001	0.003	0.007

sd_{AND} values varied from 0.003 to 0.036, so part of them exceeds the radiometric effects, while part of them is overshadowed. Correlation between the actual changes and both $mean_{AND}$ and sd_{AND} values is 0.05.

The simulation results in the third phase show that the $mean_{AND}$ and sd_{AND} values for 5 and 10% changes do not exceed the outcomes of the radiometric effects (table 6.11). Changes of 20% do result in larger values, although the $mean_{AND}$ still shows a change of only 7.4%. Since values of the $AND(b)$ can range from 0 to 1, the sd_{AND} theoretically can take values between 0 and $\frac{1}{2}\sqrt{2}$. With five AND-values, like here, the maximum value is 0.55. The values exhibited in table 6.11 only occupy the very lowest part of this range.

6.6 Results and Discussion

In the previous sections three methods for change detection were presented and tested in the study area. This section focuses on comparison and discussion of the results.

Information on land cover changes between 1989 and 1997 was obtained from comparison of the CORINE data set and a Landsat TM image. Less change was detected by high-resolution remote sensing than was anticipated on the basis of regional statistics from 1989 and 1993 (BLSD, 1990b and 1994b; HSL, 1990b and 1994b; LDSN-W, 1990b and 1994b; SLB-W, 1990b and 1994b; SLR-P, 1990b and 1994b; SLS, 1990b and 1994b). Those statistics showed a mean change of 1.3% for the 27 regions, which was assumed to double for the eight-year period, also because of the environmental programmes implied within the Common Agricultural Policy of the European Union. This doubling apparently did not occur. The values retrieved from the visual interpretation will underestimate the actual change, because very small changes involving few pixels will not be observed. This is a result of the scale difference of the two sets with 30m and 100m pixels, and because of misregistration which forces the interpreter to assess whether differences are due to changes in or mismatch of the images. This might lead to erroneous decisions when small changes are concerned. However, this cannot explain the entire difference between the expected and the observed land cover change.

The land cover change validation set showed that the mean size of changed patches is 20ha, which is only 17% of a NOAA-AVHRR pixel reflecting an area of 1.2km^2 or 120ha. Spectral changes must therefore be considerable in order to remain detectable in the radiation values of the entire pixels. The largest change patch measured 40ha, still only 33% of an AVHRR pixel. Given this size of area changes, NOAA-AVHRR images do not seem the right means to detect them with regard to pixel size but also to spectral coverage. However, in absence of alternative imagery, they are currently the only means.

The validation set retrieved from the visual comparison of CORINE and Landsat shows just land cover conversions between 1989 and 1997. Differences between the associated NOAA-AHVRR images, however, are due to land cover conversions, differences in radiometric effects and misregistration, but are also caused by differences in growing season and land cover modifications. These additional differences might be partially responsible for the differences indicated by the methods, although it is assumed that radiometric effects still play a major role.

The influence of the radiometric effects and misregistration was determined using one image pair, recorded at 7 and 8 September 1989. A more reliable assessment of these effects would have been obtained when several image pairs were included. Analysis of daily images over 1989 and 1993 revealed that the occurrence of two high-quality images on succeeding days is extremely rare, and in effect occurred only once: on 7 and 8 September 1989. Radiometric effects that are not included when images of two succeeding days are compared are differences in

seasonal development, which will influence vegetation, and sensor deterioration. The values of the second phase, validation with images of 1989 and 1997, suggest, however, that these effects might play a role.

The decision whether a method is vulnerable to radiometric effects, and thus whether it would be included in the second phase, was a subjective one. The presented methods are all newly proposed techniques for change detection, so no reference data exist, as yet. For the similarity index of the cluster patterns, similarity index values computed in chapter 3 guided the decision. For the cluster signatures, the fact that the method does not reduce the influence of radiometric effects in any way, combined with the observation that radiometric effects are quite large, directed it. And for the semivariances, the low value of the mean Absolute Normalised Difference, which can take values between 0 and 1, led to the decision to continue.

The first method, using cluster patterns, produced reasonably stable results for 7 and 8 September. Three clusters offered the highest similarity compared to five and seven clusters.

Pixels from each region in the images of 1989 and 1997 were grouped into one of three clusters according to their spectral characteristics. Similarities of the associated polygons should be significant given the small changes observed with the high-resolution data, but they all showed values lower than what was expected due to, amongst others, radiometric effects. This suggests that actual land cover changes took place. Radiometric effects larger than expected from 7 and 8 September and misregistration are probably responsible for this. Of the three tested methods, this cluster pattern method is most sensitive to misregistration. The clusters contain pixels with similar spectral characteristics. These pixels do not necessarily form continuous polygons and their spatial arrangement can be scattered. Misregistration will then introduce errors in the estimates of the size of polygon intersections, which form the base to the geometric similarity index.

Results from the simulated changes show that reduced radiometric effects would offer improved change detection results. The outcomes for 5 and 10% change lie within the expected range due to radiometric effects and hence, those changes are currently not detectable. Only the 20% changes show detectable results. The similarity values of the 5 and 10% changes (0.91 and 0.81), however, are such, that with smaller radiometric effects and with better co-registration of the images, the cluster patterns might form a good means for change detection.

The second method, using cluster signatures, showed large differences between 7 and 8 September. For all pixels probabilities of belonging to either of three signatures from the clusters of 7 September were calculated. The summed probabilities for each cluster were compared. Differences are unlikely to result from misregistration, because the regionwise comparison does not include a spatial component. Instead radiometric effects are thought to be fully responsible for the disappointing performance of this method. The cluster signature method was not further considered in phase 2 and 3.

97

cluster signatures and uses changes of these sums as change indicator. The third method compares semivariances and for this method the Absolute Normalised Difference is introduced. Values are calculated for each lag and the mean and the standard deviation over five lags are used as change indicator. Three phases were defined to test these methods.

First the three methods were applied to two images of succeeding days. The time span between the acquisition of these images is so small that it is assumed that practically no land cover changes can have occurred and all changes observed will be caused by radiometric effects and misregistration. The methods are supposed to be little sensitive to radiometric variation resulting from other sources than land cover change and should therefore indicate 'no or very little change'. The cluster pattern and the semivariances methods performed satisfactory and were therefore included in the second phase. This leads to the conclusion that methods that beside reflectance values also include the spatial arrangement of those values are more promising than methods that only consider the values.

The cluster pattern and semivariance methods were applied to images from August 1989 and 1997 for validation with real land cover changes. Unfortunately, changes in the study area appeared to be very small over these eight years prohibiting a true validation.

In the third phase simulated images were created to test the methods under ideal circumstances. One image reflected an existing land cover pattern, which was subsequently changed to create fifteen other patterns and associated images. Five of those contained 5% changes, five 10% and in the last five 20% of the area was changed from agriculture into forest or built-up area. Only the outcomes of the 20% change images exceeded the threshold derived from the 7 and 8 September comparison. The conclusion must therefore be that radiometric effects largely overshadow the spectral changes resulting from land cover conversions.

If it would be possible to reduce the radiometric effects, the cluster pattern method seems better suited for change detection than the semivariance method. On a scale between 0 and 1, the semivariance method shows a deviation of just 0.07 from the 'no change' score when 20% of the area in fact changed. For the same situation the cluster pattern method shows a 0.39 deviation, which makes it more likely that reliable detection of smaller changes is possible. Although at the end, the accuracy of the methods will determine whether they perform satisfactory or not.

The current study does not allow drawing pertinent conclusions on the performance of regionwise change detection as opposed to the conventional pixelwise approach. Both approaches are as yet not capable of detecting changes with the required accuracy and at the required spatial scale in the heterogeneous landscape of central Europe.

Changes of land cover occurred in patches with a mean size of 20ha. The 1.2km^2 pixels of NOAA-AVHRR are too large to detect such changes, particularly since the spectral contrasts between the land cover types are not very large.

Conversions between land cover types with contrasting signatures will be better detectable with NOAA-AVHRR images. For this area, representative for the central part of the European Union, sensors having smaller spectral bandwidths might show significant contrast and allow for detection of relevant changes.

Radiometric effects and misregistration of NOAA-AVHRR severely hampers change detection. New sensors might be better suited, but it will take several years before relevant time series will have been recorded. Till then NOAA-AVHRR might not be the optimal remote-sensing data source for continental change detection, but it certainly is the only available source.

101

THE VALUE OF MERIS' 300M PIXEL COMPARED TO THE 1100M PIXEL OF NOAA-AVHRR

7

The previous chapters showed that NOAA-AVHRR is not the ideal sensor to register changes in agriculture. NOAA's suitability for monitoring agriculture is marginal at pixel as well as regional level. Changes should comprise a minimum of 20% of a region in order to be detected, because of radiometric effects and misregistration. Within the European Union changes are generally much smaller, but even so, there is a demand for information on the location and type of those changes. This chapter will discuss the improvement that can be anticipated from the 300m pixel of MERIS compared to the 1100m pixel of AVHRR. For this purpose a new method is proposed and developed: the so-called Stained Glass Procedure. This method aims at determining the relative improvement in object recognition when the spatial resolution of sensors improves.

7.1   Introduction

Until recently, no sensors other than NOAA-AVHRR were available to operate at the European scale. At the moment, two new promising sensors are or will soon be in orbit and acquiring data. MODIS is mounted on the TERRA satellite, launched in December 1999, and has three different pixel sizes, 250m for two bands, 500m for five bands, and 1000m for the remaining 29 bands (NASA, 2000). The ENVISAT satellite is scheduled for launch in November 2001. ENVISAT carries several sensors, one of which is the MEdium Resolution Imaging Spectrometer: MERIS (ESA, 2000). This sensor is characterised by a high spectral resolution: 15 bands in the visible and near-infrared with bandwidths of 1.8 to 30nm (table 7.1). The pixel size will be 300m at nadir. The sensor is developed for marine applications, but its characteristics are such that it is expected to have a large potential for land applications. For this study data of either satellite were not available yet. In this chapter attention is focussed on MERIS.

Table 7.1 Spatial and spectral characteristics of MERIS

Pixel size at nadir: 300m		
Band Nr.	Band centre (nm)	Bandwidth (nm)
1	412.5	10
2	442.5	10
3	490	10
4	510	10
5	560	10
6	620	10
7	665	10
8	681.25	7.5
9	705	10
10	753.75	7.5
11	760	2.5
12	775	15
13	865	20
14	890	10
15	900	10

The sensors that are commonly used for land applications are SPOT-HRV, Landsat TM and NOAA-AVHRR (table 7.2) with pixel sizes of 20, 30 and 1100m, respectively. No sensors designed for land applications with a pixel size between 30 and 1100m exist, so far causing an information gap at the intermediate spatial resolutions. For marine applications, the LISS, WiFS and MOS sensors (table 7.2) mounted on the IRS1c are available, having pixel sizes of 25, 180 and 500m, respectively. The WiFS and MOS pixels seem to fit nicely in the pixel size gap of the land application sensors. A drawback to the usage of images from the MOS sensor is that it does not have global coverage and that its spectral quality is rather poor (Clevers *et al.*, 2000). The applicability of WiFS images is limited because they consist of just two bands. MERIS will have global coverage and has 15 high-resolution spectral bands, and will thus form a well-suited alternative to the currently available medium-resolution images.

Since MERIS data are not available yet, its performance can only be estimated using planned specifications, while its actual characteristics remain to be seen. Besides, in order to make estimations based on real data images from other, existing sensors are to be used.

A common way to compare the value of different images for land applications is by performing a classification and comparing the accuracies (e.g. Clevers *et al.*, 1999). In order to obtain reliable results ground truth is required. A second drawback is that classification results depend heavily on object definition and the ground truth used for training (Lillesand and Kiefer, 2000). These factors severely hamper classification accuracy assessment. This task becomes even more complex when images with different spatial resolution are to be compared.

Table 7.2 Spatial and spectral characteristics of six sensors. Pixel sizes are in meters. Spectral coverage and band centre are in nanometers. All IRS1c-MOS bands are 10nm wide.

	NOAA-AVHRR	IRS1c-MOS	IRS1c-WiFS	Landsat-TM	IRS1c-LISS	SPOT-HRV
Pixel size at nadir	1100	500	180	30	25	20
Band number	Spectral coverage	Band centre	Spectral coverage	Spectral coverage	Spectral coverage	Spectral coverage
1	580-680	409.2	620-680	450-520	520-590	500-590
2	725-1100	444.2	770-860	520-600	620-680	610-680
3	630-690	486.6		630-690	770-860	790-890
4	10300-11300	521.6		760-900	1550-1700	
5	11500-12500	571.5		1550-1750		
6		616.6		10400-12500		
7		650.5		2080-2350		
8		685.4				
9		749.9				
10		869.1				
11		1012.7				
12		814.9				
13		943.9				

An alternative to classification was found in object recognition. Objects form a part of the Earth's surface and can be reflected by several adjacent pixels, e.g. individual agricultural fields, a set of agricultural fields or patches of forest. Object recognition or image segmentation is used to improve classification results by assigning all pixels that form an object to the same class (Gorte, 1998). Janssen (1990) proposed a field based classification for an agricultural area, while McCormick (1997) described a method for image segmentation in order to improve forest stand classification.

Instead of classifying the objects, here the so-called Stained Glass Procedure for comparing the images acquired with different spatial resolutions is proposed. Objects representing areas with similar reflectance are retrieved from the images by filtering and subsequently converted into polygons. The more variance the polygons (segments) will explain in high-resolution images, the more detail will be available after classification of these images. Consequently, the spectral variation in the image is here used as a surrogate for land cover information. If a relation can be established between pixel size and explained variance, the value of the MERIS pixel can be estimated.

The aim of this chapter is to estimate the added value of the 300m MERIS pixel for land applications in relation to existing sensors based on object recognition and hence its suitability for change detection. In particular, the added value in comparison to the AVHRR pixel size is of interest. Effects of different spectral characteristics of the considered sensors are beyond the objective of this study and will be eliminated.

7.2   Data and Methods

A set of satellite images recorded in the same period and showing the same area was used in this chapter (table 7.3). All images were georeferenced to the same reference image with root mean square error (rmse) values varying between 0.25 and 0.8 pixel. Based on visual interpretation, images were selected for which disturbing atmospheric influences were minimal. Clouds observed were excluded from the analysis as much as possible. Moreover, the atmospheric influence is assumed constant over the area and hence, atmospheric distortion is supposed not to affect the segmentation result.

Each image has its own spectral characteristics (table 7.2).To reduce the influence of different spectral coverage only the bands in the red and near-infrared part of the spectrum were considered here. The analysis was performed on bands 1 and 2 for NOAA-AVHRR, bands 5, 6, 7, 8, 9, 10, 12 for MOS, bands 1 and 2 for WiFS, bands 3 and 4 for Landsat TM, and bands 2 and 3 for LISS.

In contrast to the other chapters of this thesis, the study area of this chapter is not located in southern Germany, but due to image availability a study site in the central part of the Netherlands was chosen. It covers part of the nature reserve the 'Veluwe' and the 'river area' with agricultural fields (arable and grassland) and built-up areas. Typical field sizes range from 2 to 3 ha.

The method referred to as the so-called Stained Glass Procedure is developed to estimate the explained variance in a high-resolution image for a given pixel size. It first calculates the explained variances for images with a range of pixel sizes and through these values a function is fitted, which describes the relation between pixel size and explained variance. The procedure consists of the following steps:

Table 7.3 Acquisition dates of the analysed images

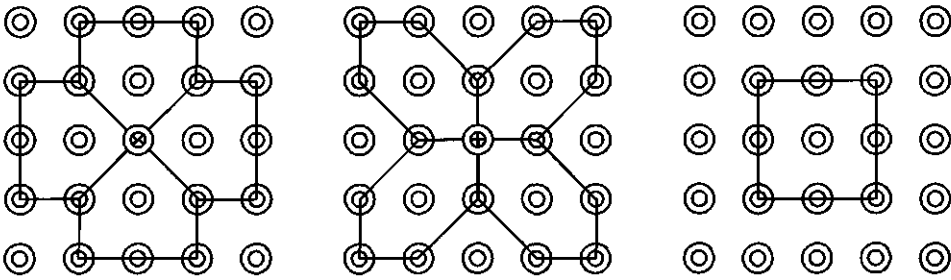| Sensor	Acquisition date
NOAA-AVHRR	11 August 1997
IRS1c-MOS	22 September 1997
IRS1c-WiFS	7 August 1997
Landsat TM	10 August 1997
IRS1c-LISS	7 August 1997

Figure 7.1 Edge-preserving smoothing filter. Black lines delineate the nine areas for which variance is calculated for each individual band. Per area the variances are summed and the one area showing lowest total variance is selected. For this area the mean values of the bands are calculated and assigned to the central pixel.

1. Bands of all sensors are standardised to a mean of 128 and a standard deviation of 20, so all bands show equal variance and will have equal weight during the procedure.

2. An edge-preserving smoothing filter (figure 7.1) is applied to the images. This filter stresses transitions in an image, while rather homogenous areas will get assigned even more similar values. So local variance is filtered out, while edges remain and become even better visible. Steps 3 and 4 describe the actual filtering process.

3. For each of the nine areas in figure 7.1 variance is calculated for all bands and they are summed per band.

4. The area showing lowest total variance is selected and the mean value of the pixels in this area is assigned to the central pixel for the respective bands. For each band the new value is thus based on the same combination of surrounding pixels.

Steps 3 and 4 are repeated nine times. This number is empirically derived and selected such that no changes are observed anymore.

5. The segments emerging in the image are nearly homogenous and are converted into polygons.

6. The Landsat-TM image is overlaid with these polygons and the variance of the pixels within each polygon is calculated for bands 3 (red) and 4 (near-infrared) separately.

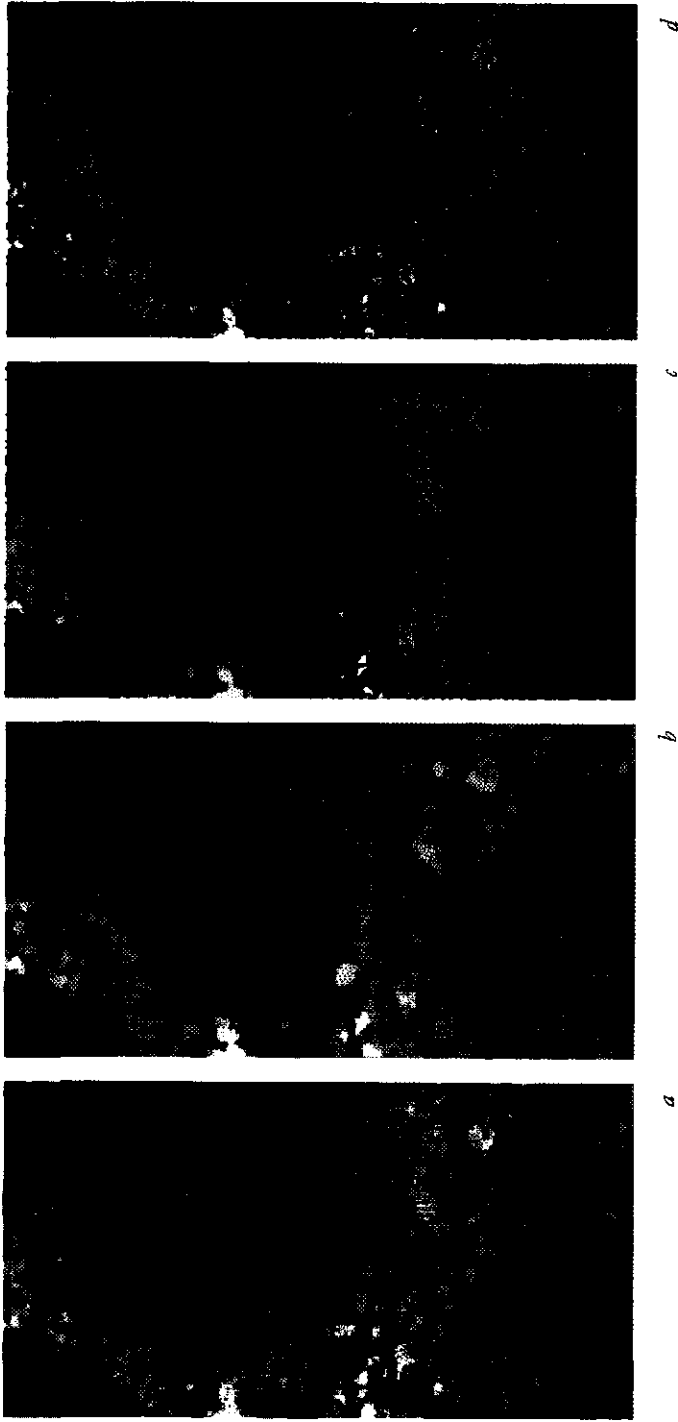7. The explained variance Var_{ex}, again for bands 3 and 4, is calculated by

107

Figure 7.2 Illustration of the Stained Glass Procedure. Four stages of the MOS image (b12, 9, 5 on RGB) are shown. In a) the original image is displayed, b) shows the image after being filtered nine times (see text), in c) the filtered image is overlaid with the polygons obtained from b), and in d) the original image is overlaid with those polygons.

$$Var_{ex} = 1 - \frac{\sum_{i=1}^{n} Var_i * area_i}{Var_{total} * \sum_{i=1}^{n} area_i} \qquad (7.1)$$

where Var_i indicates the variance of the i-th polygon, n equals the total number of polygons, Var_{total} is the variance in the entire Landsat TM image and $area_i$ is the area of the i-th polygon.

8.   The values of Var_{ex} are plotted against the respective pixel sizes and through these points a function is fitted for the two Landsat TM bands, where an optimal fit was the prime criterion for the function.

9.   The MERIS pixel size of 300m is given as input to the functions for band 3 and 4 to calculate the associated values of explained variance, assuming that it will follow the trends found for the included images.

7.3   Results

By applying the Stained Glass Procedure, images go through different stages: the original image is first standardised, next it is subject to the edge preserving smoothing filter, after which the emerging segments are transformed into polygons. Figure 7.2 shows these stages for the MOS image and illustrates the name of the procedure. It is interesting to see that the original image looks rather blurred, but when it is overlaid with the polygons emerging from the filtering procedure spatial patterns become more apparent.

The polygons resulting from the filtering are overlaid over the Landsat TM image of the study area to calculate the explained variation. All images included in the procedure were recorded around the same date in the same year. Figure 7.3 shows the polygons from NOAA-AVHRR, IRS-MOS and IRS-WiFS, and the boundaries of a smaller area that is enlarged in figure 7.4. The polygons from IRS-LISS are too small to appear recognisable when displayed at the scale of figure 7.3. In figure 7.4 they can be distinguished and for comparison the polygons from the other images are displayed as well.

In figure 7.4a all individual fields visible in the TM image are outlined by the LISS polygons. The polygons in figures 7.4b, 7.4c and 7.4d show less correspondence to the spatial patterns in the TM image. However, in figures 7.3a, 7.3b and 7.3c, showing less detail, there clearly is a match between the polygons and the image patterns. For land cover studies at the local scale the LISS image appears to provide the right amount of detail, while this is not feasible for continental studies. For that purpose one of the lower-resolution images seems more promising.
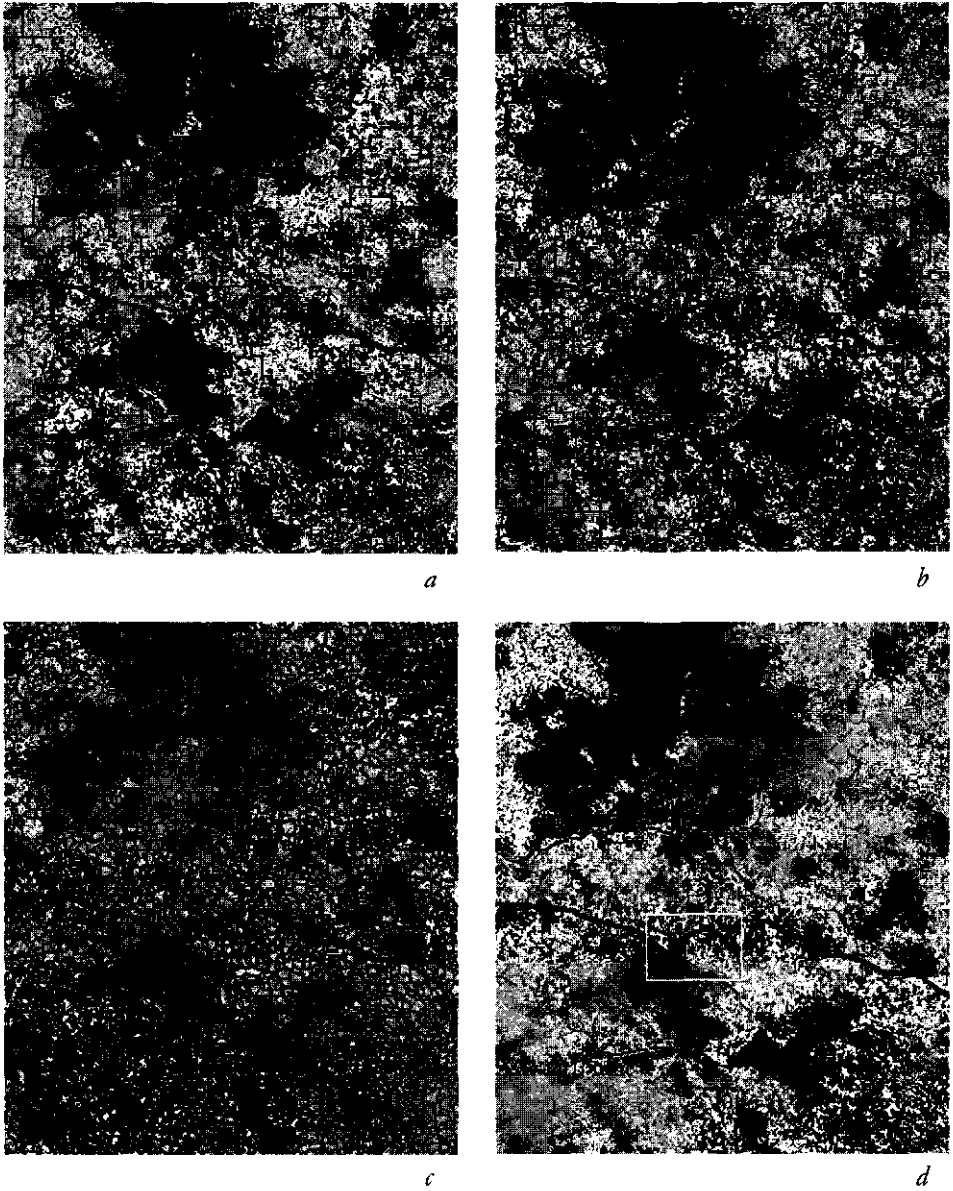
109

Figure 7.3 Polygons resulting from the different images overlaid over a Landsat TM image. In *a*, *b*, and *c* polygons from respectively NOAA-AVHRR, IRS-MOS and IRS-WiFS are shown. In *d* the area displayed in figure 7.4 is indicated.

The explained variance increases, as expected, with decreasing pixel size (figure 7.5). NOAA-AVHRR generated the lowest values, 15 and 18% for bands 3 and 4, respectively. For MOS the values increased somewhat, yielding 22 and 25%. The WiFS-values showed a strong increase compared to the former two images, particularly for band 3, where the explained variance was almost doubled, from 22 to 42%. Band 4, with 37%, showed a 50% improvement for WiFS. Polygons from the LISS image, having a pixel size smaller than Landsat TM, explained 71 and 78% of the variance in the TM image. The Landsat image itself, not included in the figure, yielded 68 and 81% explained variation.

The values of explained variance were plotted against pixel size in an X-Y plot and a function is fitted through these data points: a logarithmic function for band 3 and a power function for band 4, both with a correlation of 0.99. The one criterion for the selection of the function type was an optimal fit, as it would be used to predict the explained variance for a pixel size of 300m. According to the functions the explained variance for a (300m) MERIS pixel is 33% for band 3 and 30% for band 4. The relative improvement of MERIS compared to NOAA-AVHRR is 120% ((33-15)/15) for band 3 and 70% ((30-18)/18) for band 4.

7.4   Discussion

In this chapter the Stained Glass Procedure was presented and used as an alternative method to compare the value of different sensors for classification. The procedure was here applied to estimate the significance of the 300m MERIS pixel for land applications compared to other sensors with varying pixel sizes. Instead of classifying the individual images and ranking the respective classification accuracies, the variance in a high-resolution image explained by objects retrieved from images with different pixel sizes was determined. By fitting a function through the results, it was possible to assess how much variance would be explained by the polygons from a MERIS image.

An advantage of the Stained Glass Procedure over conventional classification processes is that it is more objective. For a supervised classification homogenous areas are required for the training set which should have statistically sound reflectance values, i.e. a true representation of the respective classes (Gorte, 1998; Lillesand and Kiefer, 2000). Particularly for the lower resolution images it is not feasible to obtain homogenous training sets, even when just the general classes like forest, agriculture, built-up area and water are considered. The requirement of a normal distribution is even more difficult to fulfil. As a consequence classification strongly depends on the training set, which makes it susceptible to subjectivity. The Stained Glass Procedure does not include any subjective decision and is as such better suited for objective comparison.

Figure 7.4 (on next two pages) Detail of the study showing polygons from IRS-LISS (*a*), IRS-WiFS (*b*), IRS-MOS (*c*) and NOAA-AVHRR (*d*).
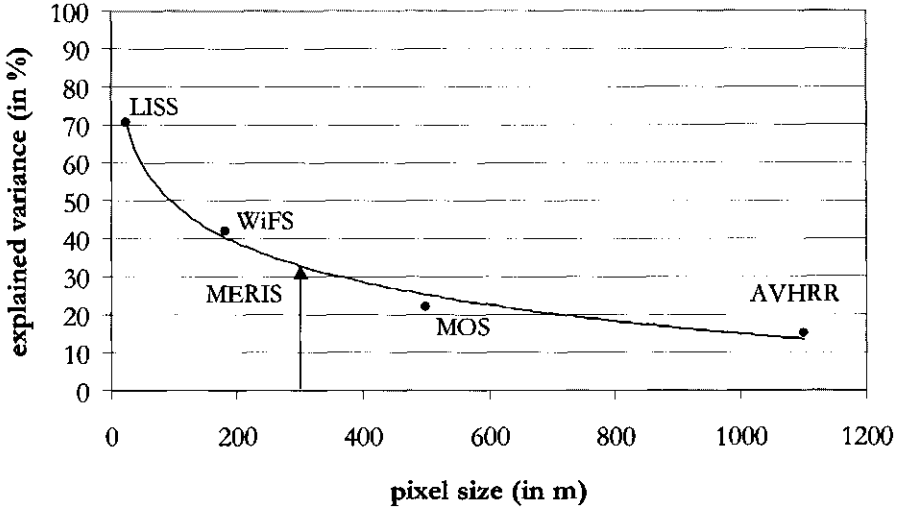
a

b

c

d
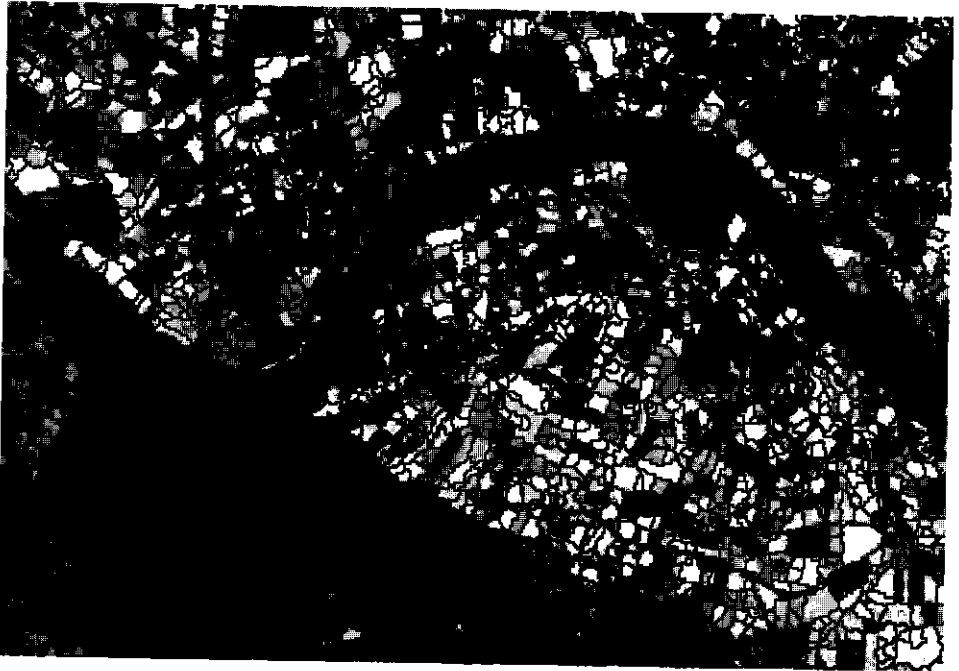
Explained variances of Landsat TM band 3
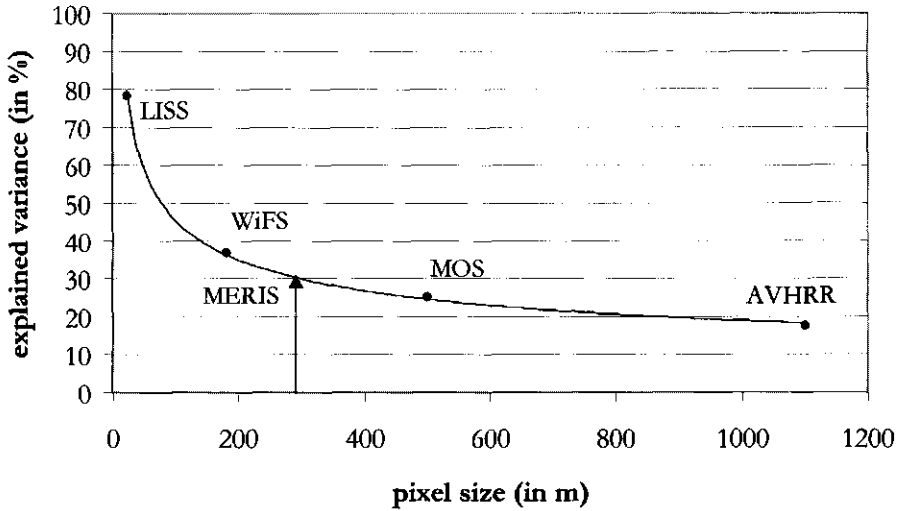

Explained variances of Landsat TM band 4

Figure 7.5 Explained variances of the sensors for Landsat TM band 3 and 4. For band 3 a logarithmic function is fitted through the points, for band 4 a power function. Both functions show over 99% fit.

114

Four different images were included in this study: NOAA-AVHRR, IRS-MOS, IRS-WiFS and IRS-LISS, with pixel sizes of 1100, 500, 180 and 25m, respectively. A Landsat TM image served as reference image. Just those bands covering the red and near-infrared part of the spectrum were included in the analysis, so the different spectral characteristics of the sensors would not affect the results. For both red and near-infrared bands, the explained variance increased with decreasing pixel size.

Because the values for explained variance are based on just one image for each pixel size, the actual values may differ somewhat from those found here. The general pattern found here, however, is expected to be representative for the actual situation.

The explained variance, as calculated in this study, will increase as spatial resolution will increase. The highest value for the explained variance will be obtained for the TM resolution, i.e. the image used as a reference, with the individual pixels as polygons. Then a value of 100% is achieved, but each object consists of only one pixel. Larger objects will always explain less than 100% of total variation, because of local variation within images. Moreover, apart from other disadvantages the spatial resolution of e.g. Landsat TM is too detailed for application of land cover monitoring at the continental scale. So, there is a trade-off between number of polygons and explained variance.

Figure 7.3 shows that the polygons derived from AVHRR roughly follow, but clearly not perfectly, the contours of the patches of the major land cover classes in the TM image. The MOS derived polygons seem to provide a better match, whereas the WiFS derived polygons seem to give an oversegmentation of the main cover types. The LISS polygons seem to reflect most of the individual objects at the surface (figure 7.4). Depending on the application, the desired classification level is to be determined.

The estimated values for MERIS showed improvements of 120 and 70% for the red and near-infrared bands relative to the NOAA-AVHRR image. AVHRR has 5 broad spectral bands, while MERIS has 15 narrow bands. The 300m pixel combined with the (still theoretically) high-quality spectral data is expected to improve the results even further, although the contribution of reliable spectral information is difficult to predict. For change detection, MERIS is expected to produce images less sensible to misregistration due to the push-broom principle of the sensor. This principle reduces distortions towards the edge of images, whereas the whisk-broom principle applied in AVHRR is notorious for its edge-distortions especially at large scan angles.

7.5   Conclusions

A new method, the Stained Glass Procedure, was used to assess the suitability of MERIS for object recognition. It was developed as an objective alternative to classification to compare images with different resolution independent of training sets.

This chapter showed that MERIS images are expected to show significantly more detail in terms of object recognition than AVHRR images, when pixel sizes are compared. Given the spectral detail that will be provided by MERIS, relative improvements are assumed to be even larger. And due to the push-broom sensor misregistration will be a lesser problem to MERIS than to AVHRR.

CONCLUSIONS AND RECOMMENDATIONS

8

The overall objective of this study was to develop a change detection method at the European scale to provide policymakers with a quick overview of locations where changes in environmental impact of agriculture occurred within the European Union. NOAA-AVHRR was the only suitable satellite sensor system at the start of this study with regard to orbit, spatial resolution and spectral bands. The central issue was to define characteristics of the method such that they would match agriculture as well as NOAA-AVHRR. Further requirements are that the information on changes should be readily available shortly after image acquisition and at a scale suitable to the European Union.

Different aspects of change detection have been studied: -spatial observation units, -measures to characterise environmental impact, and -actual change detection. An excursion outside change detection was made by a study to solve the problem of small clouds reducing the usability of NOAA-AVHRR images. Finally, the potential of MERIS' 300m pixels for land applications was estimated.

8.1 Conclusions

Change in agricultural area is a suitable indicator for change in environmental impact of agriculture. There is still a need for variables indicating change in environmental impact due to in- or extensification.

Environmental impact of agriculture is currently expressed in terms of units input (labour, chemicals) or units output (yield). These variables are derived

from statistics, which hampers international comparison and up-to-date information supply. In order to be detectable with NOAA-AVHRR images, measures to characterise environmental impact should be expressed in terms of land cover. Environmental impact of agriculture can be divided into two components: the area used for agriculture and agricultural intensity. The larger the area, the larger the impact will be; the higher the intensity, the larger the impact will be. The area used for agriculture is directly related to land cover and changes in area are therefore very suitable to locate changes in environmental impact. Higher intensities will result in higher yields, which will show as more biomass per unit land. Annual fluctuations prohibit the use of yield as direct measure, so ratios correcting for those fluctuations were introduced. Those ratios showed contradictory behaviour for different crops and consequently no measure to characterise intensity was available here to validate change detection methods for this aspect of environmental impact.

NOAA-AVHRR seems not suited for change detection of environmental impact of agriculture at the European scale.

NOAA-AVHRR has a pixel size of 1.2km², which exceeds the average European field size many times. Furthermore, the European landscape is very fragmented and heterogeneous, resulting in many mixed pixels, even when general classes are used. Consequently the NOAA-AVHRR pixel does not match with the short range spatial variability of the European landscape.

Two factors further reduce the suitability of NOAA-AVHRR for change detection: radiometric effects, due to atmospheric disturbances and sensor instability, and spatial misregistration. In AVHRR rotating mirrors are used to register radiation (the whiskbroom principle) and these introduce more spatial inaccuracies than the push-broom scanners, which use a linear array of radiance detectors.

Spatial observation units applied to NOAA-AVHRR show more internal coherence when based on biophysical than on socio-economic factors.

Part of this study investigated the optimal spatial mapping unit to assess environmental impact of agriculture. Administrative units (NUTS) or cells from a regular grid are currently the most encountered spatial observation units for monitoring. Statistics are provided per NUTS-region which make them an attractive base for monitoring. Grid cells are easy to use when data from different sources are to be combined. In NOAA-AVHRR images, however, the spatial units show no correspondence to NUTS regions or grid cells, whereas they reflect polygons obtained from the European soil map quite well. These polygons were aggregated based on their parent material characteristics into units of the desirable size. It is demonstrated that biophysical factors show better correspondence to the land cover units visible in NOAA-AVHRR images than socio-economic factors. The better correspondence of biophysical factors can be explained by the fact that

they determine the agricultural potential of land, while socio-economic factors are controlled and mapped on the base of administrative boundaries.

The planned MERIS sensor is anticipated to offer significant improvements for continental land cover applications, although the effects will be limited for change detection until relevant time series have been recorded.

MERIS is expected to reveal about twice as much detail as NOAA-AVHRR, when just comparing pixel sizes. This is judged as a relevant improvement for change detection. Besides, MERIS has 15 narrow spectral bands in the visible and near-infrared part of the spectrum, where NOAA-AVHRR has two broad bands. In addition, MERIS uses a push-broom scanner, which is less sensitive to geometric distortions than the whiskbroom scanner with rotating mirrors, which is mounted in AVHRR. So the concept of MERIS looks very promising, although time series of at least 5 to 10 years are required to detect relevant changes at the European scale.

Small clouds limiting the use of NOAA-AVHRR images can best be replaced by estimated land cover radiation data obtained with geostatistical methods.

Cloud contamination of images severely hampers the usefulness of remote sensing for land applications. The useful area in NOAA-AVHRR images can be considerably extended when small clouds are replaced by estimated land cover radiation data. Conventional methods to replace clouds are entirely based on time series, but methods including spatial information result in significantly better estimates. Methods including both spatial and temporal information performed even slightly better, while a stratified approach produced less reliable estimates.

It was necessary to develop several new methods to perform the analyses of this study, because so far they were not available in literature or software packages.

The **Geometric Similarity Index** (chapter 3) was developed to determine the geometric correspondence between two partitions of one area. It is entirely based on the geometry of the polygons, so no thematic information is needed or included. The basic assumption is that intersections between polygons strongly vary in size, when the polygons match quite well, while they will have comparable sizes, when the polygons show little correspondence. Consequently the ratio between the largest and next largest intersection of one polygon will lie close to 1 if the two partitions are dissimilar, while it will deviate from 1 if the partitions are similar.

The **Stained Glass Procedure** (chapter 7) was used to assess the level of detail that can be achieved with a certain pixel size compared to other pixel sizes. Spectral variation in a high-resolution image serves here as surrogate to land cover ground truth data. Images are segmented into polygons, and subsequently the variance in the high-resolution images explained by these polygons is determined.

119

REFERENCES

Atkinson, P.M., Webster, R. and Curran, P.J., 1994. Cokriging with airborne MSS imagery. Remote Sensing of Environment, 50: 335-345.

Avery, D.T., 1999. The importance of high farm yields to wildlife conservation. In: D.L. Michalk and J.E. Pratley (Editors), Agronomy - Growing a Greener Future. Proceedings of the 9th Australian Agronomy Conference 20-23 July 1998. Australian Society of Agronomy, Wagga Wagga, Australia.

Bakker, T.W.M., Klijn, J.A. and Van Zadelhoff, F.J., 1981. Nederlandse kustduinen. Pudoc, Wageningen.

Belward, A.S., Estes, J.E. and Kline, K.D., 1999. The IGBP-DIS global 1-km land-cover data set DISCover: a project overview. Photogrammetic Engineering & Remote Sensing, 65(9): 1013-1020.

Bennett, A.J., 2000. Environmental consequences of increasing production: some current perspectives. Agriculture, Ecosystems and Environment, 82: 89-95.

BLSD, 1990a. Ernte der Hauptfrüchte 1989. Statistische Berichte. Bayerisches Landesamt für Statistik und Datenverarbeitung.

BLSD, 1990b. Flächenerhebung 1989 -tatsächliche Nutzung-. Statistische Berichte. Bayerisches Landesamt für Statistik und Datenverarbeitung.

BLSD, 1994a. Ernte der Hauptfrüchte 1993. Statistische Berichte. Bayerisches Landesamt für Statistik und Datenverarbeitung.

BLSD, 1994b. Flächenerhebung 1993 -tatsächliche Nutzung-. Statistische Berichte. Bayerisches Landesamt für Statistik und Datenverarbeitung.

Borak, J.S., Lambin, E.F. and Strahler, A.H., 2000. The use of temporal metrics for land cover change detection at coarse spatial scales. International Journal of Remote Sensing, 21(6&7): 1415-1432.

Bouma, J. and Droogers, P., 1998. A procedure to derive land quality indicators for sustainable agricultural production. Geoderma, 85: 103-110.

Bouma, J., Varallyay, G. and Batjes, N.H., 1998. Principal land use changes anticipated in Europe. Agriculture, Ecosystems and Environment, 67: 103-119.

Brouwer, F.M., 1995. Indicators to monitor agri-environmental policy in The Netherlands. Mededeling 528, Agricultural Economics Research Institute (LEI-DLO), The Hague, The Netherlands.

Brouwer, F.M. and Berkum, S.V., 1996. CAP and environment in the European Union. Analysis of the effects of CAP on the environment and an assessment of existing environmental conditions in policy. Wageningen Pers, Wageningen, 171 pp.

Burrough, P.A., 1986. Principles of geographical information systems for land resources assessment. Monographs on soil and resources survey. Clarendon Press, Oxford, 194 pp.

CEC, 1985. Soil map of the European Communities 1:1,000,000. Commission of the European Communities, Directorate-General VI (Agriculture), Luxembourg.

CEC, 1993. CORINE Land Cover technical guide, European Union. Directorate Generale Environment, Nuclear Safety and Civil Protection, Luxembourg.

Christakos, G., 1992. Random field models in earth sciences. Academic Press, San Diego.

Clevers, J.G.P.W., Vandysheva, N.M., Mücher, C.A., Vassilenko, G.I., Filonov, S.V., Zhoukova, G.A., Izotova, V.P., Gurov, A.F., Nieuwenhuis, G.J.A., Addink, E.A., 1999. Agricultural land use monitoring with improved remote sensing techniques. Final report. LUW-GIRS-199902, Agricultural University, Wageningen.

Clevers, J.G.P.W., Vonder, O.W., Schok, H.A. and Addink, E.A., 2000. Multisensor RS Capabilities Land. Report 3: Applications of multisensor remote sensing satellite sensors. USP-2 Report 00-20, BCRS, Delft.

Coppin, P.R. and Bauer, M.E., 1996. Digital change detection in forest ecosystems with remote sensing imagery. Remote sensing reviews, 13: 207-234.

Cressie, N., 1991. Statistics for spatial data. John Wiley and Sons, New York.

Curran, P.J., 1988. The semivariogram in remote sensing: an introduction. Remote Sensing of Environment, 24: 493-507.

De Jong, S.M. and Burrough, P.A., 1995. A fractal approach to the classification of mediterranean vegetation types in remotely sensed images. Photogrammetic Engineering & Remote Sensing, 61(8): 1041-1053.

De Wit, M.J.M., 1999. Nutrient fluxes in the Rhine and Elbe basins. PhD Thesis, University Utrecht, Utrecht, 163 pp.

Defries, R.S. and Townshend, J.R.G., 1994. NDVI-derived land cover classifications at a global scale. International Journal of Remote Sensing, 15(17): 3567-3586.

EEA, 1995a. Environment in the European Union - 1995; Report for the review of the fifth environmental action programme, Office for Official Publications of the European Community, Luxembourg.

EEA, 1995b. Europe's Environment: The Dobris assessment, Office for Official Publications of the European Communities, Luxembourg.

EEA, 1998. Europe's Environment: The Second Assessment. European Environmental Agency, http://www.eea.eu.int/frdocu.htm.

ESA, 2000. ENVISAT, Internet: http://envisat.esa.int/, downloaded 28/11/2000.

EU, 1999a. Agriculture and environment. In: D. VI (Editor), Internet: http://europa.eu.int/comm/dgo6/envir/en/index.htm, downloaded 21/01/1999.

EU, 1999b. Evaluation of agri-environmental programmes. In: D. VI (Editor), State of application of regulation (EEC) no.2078/92, Internet: http://europa.eu.int/comm/dgo6/envir, downloaded 21/01/1999, pp. 150.

Eurostat, 2000. Eurostat, Internet: http://europa.eu.int/comm/eurostat/, downloaded 06/11/2000.

FAO, 1993. FESLM: An international framework for evaluating sustainable land management. World Resources Report 73, FAO, Rome.

FAO, 2000. FAO Statistics, Internet: http://apps.fao.org.

Gahegan, M. and Ehlers, M., 2000. A framework for the modelling of uncertainty between remote sensing and geographic information systems. ISPRS Journal of Photogrammetry & Remote Sensing, 55: 176-188.

GIC, 2000. Tatsachen ueber Deutschland. German Information Centre, Internet: http://194.94.238.74/tatsachen_ueber_deutschland/englisch/buch/07/04.html, downloaded 15/08/00.

Goovaerts, P., 1997. Geostatistics for natural resources evaluation. Applied geostatistics series. Oxford University Press, New York, 483 pp.

Gorte, B., 1998. Probabilistic segmentation of remotely sensed images. Ph.D. Thesis, Wageningen University, Wageningen, 143 pp.

Gorte, B., 1999. Supervised image classification. In: A. Stein, F. Van der Meer and B. Gorte (Editors), Spatial statistics for remote sensing. Remote sensing and digital image processing. Kluwer Academic Publishers, Dordrecht, pp. 153-162.

Grigg, D., 1995. An introduction to agricultural geography. Routledge, London, 217 pp.

Gutman, G. and Ignatov, A., 1995. Global land monitoring from AVHRR: potential and limitations. International Journal of Remote Sensing, 16: 2301-2309.

Hijmans, R.J., Guiking-Lens, I.M. and Van Diepen, C.A., 1994. WOFOST 6.0. User's guide for the WOFOST 6.0 crop growth simulation model. Technical document 12, DLO-Winand Staring Centre, Wageningen.

Holben, B.N., 1986. Characteristics of maximum-value composite images from temporal AVHRR data. International Journal of Remote Sensing, 7: 1417-1434.

Hooijer, A.A. and Van der Wal, T., 1994. CGMS version 3.1; User manual. 15.1, SC-DLO and Joint Research Centre, Wageningen, The Netherlands.

HSL, 1990a. Ernteberichterstattung der landwirtschaftlichen Feldfrüchte und des Grünlandes 1989. Statistische Berichte. Hessisches Statistisches Landesamt.

HSL, 1990b. Flächenerhebung 1989 -tatsächliche Nutzung-. Statistische Berichte. Hessisches Statistisches Landesamt.

HSL, 1994a. Ernteberichterstattung der landwirtschaftlichen Feldfrüchte und des Grünlandes 1993. Statistische Berichte. Hessisches Statistisches Landesamt.

HSL, 1994b. Flächenerhebung in Hessen im Jahr 1993, tatsächliche Nutzung. Statistische Berichte. Hessisches Statistisches Landesamt.

Hutchinson, G.E., 1957. Concluding Remarks, Population studies: animal ecology and demography Cold Spring Harbor symposia on quantitative biology. The Biological Laboratory, New York, pp. 415-427.

Isaaks, E.H. and Srivastava, R.M., 1989. Applied geostatistics. Oxford University Press, New York, 561 pp.

ISCU, UNEP, FAO and WMO, 1995. Global Terrestrial Observing System - GTOS: Turning a sound concept into a practical reality, Nairobi.

Janssen, L.L.F., Jaarsma, M.N. and Van der Linden, E.T.M., 1990. Integrating topographic data with remote sensing for land-cover classification. Photogrammetric Engineering & Remote Sensing, 56(11): 1503-1506.

Jongman, R.H.G., Braak, C.J.F.T. and Tongeren, O.F.R.V., 1987. Data analysis in community and landscape ecology. Pudoc, Wageningen, The Netherlands, 299 pp.

Journel, A.G. and Huijbregts, C.J., 1978. Mining geostatistics. Academic Press, 600 pp.

Kerdiles, H., 1998. Software processing AVHRR data for the communities of Europe (SPACE): algorithms used in SPACE version 2. Part 1: calibration, atmospheric correction and cloud detection, Space Applications Institute, Joint Research Centre of the European Union, Ispra.

Klijn, J.A., 1995. Hierarchical concepts in landscape ecology and its underlying disciplines. Report/DLO-Staring Centre 100, Wageningen, The Netherlands.

Lambin, E.F. and Ehrlich, D., 1996. The surface temperature-vegetation index space for land cover and land-cover change analysis. International Journal of Remote Sensing, 17(3): 463-487.

Lambin, E.F., Rounsevell, M.D.A. and Geist, H.J., 2000. Are agricultural land-use models able to predict changes in land-use intensity. Agriculture, Ecosystems and Environment, 82: 321-331.

Lambin, E.F. and Strahler, A.H., 1994a. Change-vector analysis in multitemporal space: A tool to detect and categorize land-cover change processes using high temporal resolution satellite data. Remote Sensing of Environment, 48: 231-244.

Lambin, E.F. and Strahler, A.H., 1994b. Indicators of land-cover change for change-vector analysis in multitemporal space at coarse spatial scales. International Journal of Remote Sensing, 15(10): 2099-2119.

LDSN-W, 1990a. Ernteberichterstattung über Feldfrüchte und Grünland in Nordrhein-westfalen 1989. Statistische Berichte. Landesamt für Datenverarbeitung und Statistik Nordrhein-Westfalen.

LDSN-W, 1990b. Flächenerhebung 1989 -tatsächliche Nutzung-. Statistische Berichte. Landesamt für Datenverarbeitung und Statistik Nordrhein-Westfalen.

LDSN-W, 1994a. Ernteberichterstattung über Feldfrüchte und Grünland in Nordrhein-westfalen 1993. Statistische Berichte. Landesamt für Datenverarbeitung und Statistik Nordrhein-Westfalen.

LDSN-W, 1994b. Flächenerhebung 1993 -tatsächliche Nutzung-. Statistische Berichte. Landesamt für Datenverarbeitung und Statistik Nordrhein-Westfalen.

Leemans, R. and Cramer, W., 1991. The IIASA database for mean monthly values of temperature, precipitation and cloudiness of a global terrestrial grid. RR-91-18, International Institute for Applied Systems Analysis (IIASA).

Leemans, R. and Van den Born, G.J., 1994. Determining the potential distribution of vegetation, crops and agricultural productivity. In: J. Alcamo (Editor), Image 2.0: integrated modeling of global climate change. Kluwer Academic Publishers, Dordrecht.

Lillesand, T.M. and Kiefer, R.W., 2000. Remote sensing and image interpretation. John Wiley & Sons, New York, 724 pp.

LNV, 1996. Gemeenschappelijk Landbouwbeleid op langere termijn. Discussienota. 24 596, The Hague, The Netherlands.

Loedeman, J.H. (Editor), 2000. 'Three-Line Linear' versus 'Multi-Head Array'. GIM International, 14(5): 1-6.

Lövenstein, H., Lantinga, E.A., Rabbinge, R. and Van Keulen, H., 1992. Principles of theoretical production ecology. Wageningen Agricultural University, 117 pp.

Mannion, A.M., 1995. Agriculture and environmental change Temporal and spatial dimensions. John Wiley & Sons, Chichester, UK, 405 pp.

Mas, J.-F., 1999. Monitoring land-cover changes: a comparison of change detection techniques. International Journal of Remote Sensing, 20(1): 139-152.

Matheron, G., 1965. La Theorie des Variables Regionalisees et ses Applications. Masson, Paris.

McBratney, A.B. and Webster, R., 1983. Optimal interpolation and isarithmic mapping of soil properties, V.Coregionalization and multiple sampling strategy. Journal of Soil Science, 34: 137-162.

McCormick, N., 1997. Automated forest stand mapping by spatial analysis of satellite imagery. In: P.J. Kennedy (Editor), Application of remote sensing in European forest monitoring, pp. 411-419.

Middelkoop, H., 1990. Uncertainty in a GIS: a test for quantifying interpretation output. ITC Journal, 3: 225-232.

Millot, M. and Loopuyt, P., 1997. Data, software, hardware and operations requirements, Crop yield forecasting methods. FAO, CEC-DG VI, CEC-JRC, CEC-Eurostat, Villefranche sur Mer, France, pp. 367-376.

Molenaar, M. and Cheng, T., 2000. Fuzzy spatial objects and their dynamics. ISPRS Journal of Photogrammetry & Remote Sensing, 55: 164-175.

Moody, A. and Strahler, A.H., 1994. Characteristics of composited AVHRR data and problems in their classification. International Journal of Remote Sensing, 15(17): 3473-3491.

Mücher, C.A., Steinnocher, K.T., Kressler, F.P. and Heunks, C., 2000. Land cover characterization and change detection for environmental monitoring of pan-Europe. International Journal of Remote Sensing, 21(6&7): 1159-1181.

NASA, 2000. MODIS Technical Specifications, Internet: http://modarch.gsfc.nasa.gov/MODIS/INSTRUMENT/MODIS_specs.html, downloaded 4/1/2000.

OECD, 1997a. Agri-environmental indicators: stocktaking report. COM/AGR/CA/ENV/EPOC(96)149/REV1, Organisation for Economic Co-operation and Development, Paris.

OECD, 1997b. Environmental indicators for agriculture. 51 98 07 1 P, Organisation for economic co-operation and development, Paris.

OECD, 1998. The environmental effects of reforming agricultural policies. 51 98 07 1 P, Organisation for economic co-operation and development, Paris.

Penning de Vries, F.W.T. and Van Laar, H.H. (Editors), 1982. Simulation of plant growth and crop production. Simulation Monographs. Pudoc, Wageningen, The Netherlands, 308 pp.

Pianka, E.R., 1976. Competition and niche theory. In: R.M. May (Editor), Theoretical ecology Principles and applications. Blackwell Scientific Publications, Oxford, pp. 114-141.

Prince, S.D. and Goward, S.N., 1996. Evaluation of the NOAA/NASA Pathfinder AVHRR Land Data Set for global primary production modelling. International Journal of Remote Sensing, 17(1): 217-221.

Rabbinge, R., Van Diepen, C.A., Dijsselbloem, L., De Koning, G.H.J., Van de Latesteijn, H.C., Woltjer, E., Van Zijl, J., 1994. Ground for choices: a scenario study on perspectives for rural areas in the European Community. In: L.O. Fresco, L. Stroosnijder, J. Bouma and H. Van Keulen (Editors), The future of the land: mobilising and integrating knowledge for land use options. Wiley, New York, pp. 95-121.

Rabbinge, R. and Van Diepen, C.A., 2000. Changes in agriculture and land use in Europe. European Journal of Agronomy, 13: 85-100.

RIVM, 1992. The environment in Europe: a global perspective. Report 481505001, National Institute for Public Health and Environment, Bilthoven, The Netherlands.

Scepan, J., Menz, G. and Hansen, M.C., 1999. The DISCover validation image interpretation process. Photogrammetric Engineering & Remote Sensing, 65(9): 1075-1081.

Schowengerdt, R.A., 1997. Remote sensing - models and methods for image processing. Academic Press, Boston, 522 pp.

Shriar, A.J., 2000. Agricultural intensity and its measurement in frontier regions. Agroforestry Systems, 49(3): 301-318.

Singh, A., 1989. Digital change detection techniques using remotely-sensed data. International Journal of Remote Sensing, 10(6): 989-1003.

Skole, D., 1996. Land Use and Land Cover Change (LUCC). Global Change Newsletter, No.25: 5.

SLB-W, 1990a. Ernte der Hauptfrüchte 1989. Statistische Berichte Agrarwirtschaft. Statistisches Landesamt Baden-Württemberg.

SLB-W, 1990b. Gemeindestatistik 1989. Ergebnisse der Flächenerhebung 1989 nach Gemeinden und Gemarkungen. Bodenflächen nach Art der tatsächlichen Nutzung. Statistik von Baden-Württemberg, Statistisches Landesamt Baden-Württemberg.

SLB-W, 1994a. Ernte der Hauptfrüchte 1993. Statistische Berichte Agrarwirtschaft. Statistisches Landesamt Baden-Württemberg.

SLB-W, 1994b. Gemeindestatistik 1993. Ergebnisse der Flächenerhebung 1993 nach Gemeinden und Gemarkungen. Bodenflächen nach Art der tatsächlichen Nutzung. Statistik von Baden-Württemberg, Statistisches Landesamt Baden-Württemberg

SLR-P, 1990a. Ernteberichterstattung über Feldfrüchte und Grünland in Rheinland-Pfalz 1989. Statistische Berichte. Statistisches Landesamt Rheinland-Pfalz.

SLR-P, 1990b. Nutzung der Bodenfläche 1989 (Ergebnisse der Flächenerhebung). Statistische Berichte. Statistisches Landesamt Rheinland-Pfalz.

SLR-P, 1994a. Ernteberichterstattung über Feldfrüchte und Grünland in Rheinland-Pfalz 1993. Statistische Berichte. Statistisches Landesamt Rheinland-Pfalz.

SLR-P, 1994b. Nutzung der Bodenfläche 1989 (Ergebnisse der Flächenerhebung - tatsächliche Nutzung). Statistische Berichte. Statistisches Landesamt Rheinland-Pfalz.

SLS, 1990a. Ernte der Hauptfrüchte 1989. Statistische Berichte Agrarwirtschaft. Statistisches Landesamt Saarland.

SLS, 1990b. Flächenerhebung 1989 -tatsächliche Nutzung-. Statistische Berichte. Statistisches Landesamt Saarland

SLS, 1994a. Ernte der Hauptfrüchte 1993. Statistische Berichte Agrarwirtschaft. Statistisches Landesamt Saarland.

SLS, 1994b. Flächenerhebung 1993 -tatsächliche Nutzung-. Statistische Berichte. Statistisches Landesamt Saarland

Stein, A., M., H. and Bouma, J., 1988a. Use of soil-map delineations to improve (co-) kriging of point data on moisture deficits. Geoderma, 43: 163-177.

Stein, A., Van Dooremolen, W., Bouma, J. and Bregt, A.K., 1988b. Cokriging point data on moisture deficit. Soil Science Society of America Journal, 52: 1418-1423.

Stow, D.A., 1999. Reducing the effects of misregistration on pixel-level change detection. International Journal of Remote Sensing, 20(12): 2477-2483.

Supit, I., Hooijer, A.A. and Van Diepen, C.A. (Editors), 1994. System description of the WOFOST 6.0 crop growth simulation model, Joint Research Centre, Commission of the European Communities, Brussels.

Tanré, D., Deroo, C., Duhaut, P., Herman, M., Morcrette, J.J., Perbos, J., Deschamps, P.Y., 1990. Description of a computer code to simulate the satellite signal in the solar spectrum: the 5S code. Technical note. International Journal of Remote Sensing, 11(4): 659-668.

Townshend, J.R.G., Justice, C.O., Gurney, C. and McManus, J., 1992. The impact of misregistration on change detection. IEEE Transactions on geoscience and remote sensing, 30(5): 1054-1060.

Tracy, M., 1997. Agricultural policy in the European Union and other market economies. APS-Agricultural Policy Studies in association with AGRA FOCUS, Brussels, 104 pp.

Turner, B.L., II and Doolittle, W.E., 1978. The concept and measure of agricultural intensity. Professional Geographer, 30(3): 297-301.

Turner, B.L., II, Moss, R.H. and Skole, D.L., 1993. Relating land use and global land-cover change: a proposal for an IGBP-HDP core project. IGBP-24, HDP-5, IGBP, Stockholm.

Uitermark, H.T., van Oosterom, P.J.M., Mars, N.J.J. and Molenaar, M., 1998. Propagating updates: finding corresponding objects in a multi-source environment, Proceedings of the International Symposium for Spatial Data Handling SDH '98, Vancouver, Canada.

UN, 1992. Rio declaration on environment and development, Internet http://www.igc.apc.org/habitat/agenda21/rio-dec.html, downloaded 25/07/00.

UN, 1999. The day of 6 billion, Internet http://www.unfpa.org/modules/6billion, downloaded 28 February 2001.

USGS, 2000. Advanced Very High Resolution Radiometer, Internet: http://edcwww.cr.usgs.gov/glis/hyper/guide/avhrr, downloaded 19 September 2000.

Van de Velde, R.J., Faber, W.S., Van Katwijk, V.F., Kuylenstierna, J.C.I., Scholten, H.J., Thewessen, T.J.M., Verspuij, M., Zevenbergen. M., 1994. The preparation of a European land use database. 712401001, National Institute of Public Health and Environmental Protection, Bilthoven.

Van der Bijl, G., 1997. Europees landbouwbeleid en milieu; de stand van zaken. CLM 297-1997, Centrum voor landbouw en milieu, Utrecht, The Netherlands.

Van der Meer, F.D., Bakker, W.H., Scholte, K., Skidmore, A.K., De Jong, S.M., Dorresteijn, M., Clevers, J.G.P.W., Epema, G.F., 2000. Scaling to the MERIS resolution: mapping accuracy and spatial variability. Geocarto International, 15(1): 37-47.

Van Diepen, C.A., 1991. An agrometeorological model to monitor the crop state on a regional scale in the European Community: concept, implementation and first operational outputs. In: Toselli and Meyer-Roux (Editors), Proceedings of the conference on the application of remote sensing to agricultural statistics. Commission of the European Community, Luxembourg, pp. 269-279.

VEGETATION, 1994. Vegetation Newsletter #1, Internet: http://vegetation.cnes.fr:8080/vgtnews/vgtnws01.html, downloaded 17/01/2001.

Veldkamp, A. and Fresco, L.O., 1997. Reconstructing land use drivers and their spatial scale dependence for Costa Rica (1973 and 1984). Agricultural Systems, 55(1): 19-43.

Whittaker, R.H., Levin, S.A. and Root, R.D., 1973. Niche, habitat, and ecotope. The American Naturalist, 107(955): 321-338.

Winter, S., 2000. Location similarity of regions. Photogrammetry & Remote Sensing, 55: 189-200.

Witte, J.P.M., 1998. National water management and the value of nature. Ph.D. Thesis, Wageningen Agricultural University, 223 pp.

Woodcock, C.E., Strahler, A.H. and Jupp, D.L.B., 1988a. The use of variograms in remote sensing: I. Scene models and simulated images. Remote Sensing of Environment, 25: 323-348.

Woodcock, C.E., Strahler, A.H. and Jupp, D.L.B., 1988b. The use of variograms in remote sensing: II. Real digital images. Remote Sensing of Environment, 25: 349-379.

Zobler, L., 1986. A world soil file for global climate modeling, NASA, New York.

ABSTRACT

Agricultural production in the European Union sharply rose during the second half of the 20th century. As a side-effect environmental impact increased as well, and resulted in widespread environmental problems, which policymakers now seek to reduce. Therefore, up-to-date, standardised information on environmental impact of agriculture is required covering the entire area of the Union. NOAA-AVHRR images seem well suited to provide part of this information, because 1) one image covers a large area, 2) so significant time series are available, and 3) they contain two relevant spectral bands for vegetation and crop studies. The objective of this study is to develop a change detection method to locate changes in environmental impact using NOAA-AVHRR images.

The required spatial observation units were defined such that they match both agriculture and NOAA-AVHRR. For this purpose a method was developed to determine the correspondence in geometry between two polygon sets. It was shown that polygons formed by bio-physical variables match patterns in AVHRR images better than those formed by socio-economic variables. The selected units were obtained from the soil map.

Once the spatial units were defined, measures could be sought that characterise environmental impact in terms of land cover, so they might be observable in the AVHRR images. A suitable measure was found in change in agricultural area, which will result in changed environmental impact if other factors remain unchanged. For changes in agricultural intensity, which will lead to changed environmental impact as well, no suitable measures exist.

Finally, three different change detection methods were proposed to detect changes in agricultural area using NOAA-AVHRR images. The methods aim at enhancing the information regarding agricultural change while minimising classification inaccuracy, spatial misregistration and radiometric effects. None of these methods proved successful in locating regions with changes in agricultural areas. The conclusion is that NOAA-AVHRR images seem not suited to detect changes in European agriculture.

Besides these aspects related to a change detection method, methods to solve cloud contamination of NOAA-AVHRR images were studied. Clouds often reduce the useful area in AVHRR images. Seven procedures, including conventional and geostatistical methods, to replace small clouds by estimated land radiation values were compared. The estimates from the geostatistical methods led to the best estimates of reflection values from the landscape underlying the clouds.

Next, the suitability of near-future remote-sensing systems was assessed for detecting changes in environmental impact of agriculture. MERIS is a sensor mounted on ENVISAT, a European satellite that will be launched in November 2001. Its announced specifications make it seem a promising information source for land applications at the continental scale. To estimate the value of its 300m pixel a new method is proposed, which is referred to as the Stained Glass Procedure. This

method relates pixel size to discernible detail, and predicts the level of detail detectable in another (here non-existing yet) image. According to the Stained-Glass Procedure, MERIS images will show twice as much detail as NOAA-AVHRR images, which is a significant improvement. Unfortunately, it will take quite some years before time series useful for change detection have been collected.

SAMENVATTING

Sterke intensivering van de landbouw in de tweede helft van de 20e eeuw heeft geleid tot een sterke toename van milieuproblemen binnen de Europese Unie. Momenteel richt de politiek zich op het beperken en oplossen van die problemen, waarvoor actuele en gestandaardiseerde informatie nodig is voor het hele gebied. NOAA-AVHRR satellietbeelden lijken zeer geschikt om deze informatie te leveren, omdat 1) één beeld een groot gebied bedekt, 2) er al ruim 20 jaar opnames van zijn, zodat er lange tijdseries bestaan, en 3) ze twee spectrale banden hebben die relevant zijn voor vegetatie en gewassen. Het doel van de studie beschreven in dit proefschrift is het ontwikkelen van een methode, die plaatsen kan opsporen waar veranderingen zijn opgetreden in het milieu-effect van de landbouw.

Hiertoe zijn allereerst de ruimtelijke waarnemingseenheden zo gedefinieerd dat ze bruikbaar zijn voor het bestuderen van milieu-effecten van de landbouw en voor het interpreteren van NOAA-AVHRR satellietbeelden. Om dit vast te stellen is er een methode ontwikkeld die de overeenkomst in geometrie tussen twee polygonensets bepaalt. Deze methode laat zien dat patronen van bio-fysische variabelen veel beter overeenkomen met patronen in NOAA-AVHRR beelden dan patronen van socio-economische variabelen. De waarnemingseenheden die uiteindelijk in dit onderzoek zijn gebruikt komen uit de bodemkaart.

Vervolgens is er naar een maat gezocht om het milieu-effect van de landbouw in uit te drukken. Om veranderingen in milieu-effecten op te sporen met satellietbeelden, moet deze maat kunnen worden gerelateerd aan veranderingen van de landbedekking. Een bruikbare maat is verandering van het landbouwoppervlak. Meer of minder landbouw zal zonder andere veranderingen leiden tot meer of minder milieu-effect in een regio. Als de landbouwintensiteit verandert zal het milieu-effect ook veranderen, maar helaas luidt de conclusie van dit onderzoek, dat er (nog) geen geschikte maat bestaat om deze intensiteitsveranderingen in uit te drukken.

Tenslotte zijn drie verschillende methoden voorgesteld om veranderingen in landbouwareaal op te sporen met NOAA-AVHRR beelden. De methoden richten zich op het versterken van de informatie over veranderingen en het beperken van verstorende factoren als classificatiefouten, ruimtelijke onnauwkeurigheid en radiometrische effecten. Met geen van deze methoden was het mogelijk om veranderingen in landbouwareaal te vinden. De conclusie is dat de (groffe) NOAA-AVHRR beelden ongeschikt lijken voor het opsporen van de veranderingen in de Europese landbouw.

Naast de verschillende aspecten van een opsporingsmethode, zijn verschillende methoden vergeleken om kleine wolken, die het onderliggende landschap aan het zicht onttrekken, uit NOAA-AVHRR beelden te verwijderen. Zeven methoden, zowel traditionele als geostatistische, zijn vergeleken om kleine wolken te vervangen door reflectiewaarden van het aardoppervlak. De geostatistische methoden leveren veel betere schattingen op.

Tenslotte is de geschiktheid van toekomstige remote sensing systemen geschat voor het opsporen van veranderingen in landbouw-milieueffecten. MERIS is een sensor aan boord van de ENVISAT, een Europese satelliet waarvan de lancering gepland staat voor november 2001. De aangekondigde eigenschappen van deze sensor zijn veelbelovend voor landtoepassingen op de continentale schaal. Om de waarde van 300m MERIS pixel te schatten is een nieuwe methode ontwikkeld, de Glas-in-Lood Methode. Deze methode kijkt naar het detail dat satellietbeelden met verschillende pixelgroottes laten zien, en voorspelt dan hoeveel detail een (hier een nog niet bestaand) beeld met een andere pixelgrootte zal laten zien. Volgens de Glas-in-Lood Methode bevatten MERIS-beelden twee keer zo veel detail als NOAA-AVHRR-beelden, wat een flinke verbetering is. Helaas duurt het nog een aantal jaren voordat MERIS lang genoeg om de aarde heeft gecirkeld om een tijdserie op te bouwen die bruikbaar is voor het opsporen van veranderingen.

CURRICULUM VITAE

Elisabeth Agnes Addink werd geboren op 26 december 1967 in Utrecht. In 1986 deed ze eindexamen aan het Stedelijk Gymnasium te Leiden, waarna ze voor een jaar naar Zweden ging als uitwisselingsstudent. Weer teruggekeerd begon ze in 1987 aan de studie Fysische Geografie aan de Universiteit Utrecht. Haar afstudeerrichting was Landschapskunde met een sterke nadruk op remote sensing. In maart 1993, direct na haar afstuderen, begaf ze zich opnieuw naar Scandinavië. Ditmaal naar Tromsø, Noorwegen, waar ze met behulp van satellietbeelden het milieu van de noord-Russische zeeën bestudeerde bij het milieu-adviesbureau Akvaplan-niva. Na een prachtige poolzomer trok ze zich voor de winter weer terug in Nederland, waar ze in februari 1994 bij de Universiteit van Amsterdam aan de slag kon met een literatuurstudie naar de mogelijkheden van remote sensing voor landdegradatie. In september van hetzelfde jaar begon ze in Wageningen aan haar promotieonderzoek. Vijf jaar later, in september 1999, werd haar aanstelling omgezet van AIO naar toegevoegd onderzoeker. In eerste instantie werkte ze nog volledig aan haar proefschrift, vanaf januari 2000 werkte ze voltijds aan een BCRS-project, MERIS for land Applications. In maart 2001 rondde ze haar proefschrift af.

Sinds april 2001 woont ze met haar man en dochter in Ann Arbor, Michigan, VS. Ze werkt bij de School of Natural Resources and Environment, aan de University of Michigan. Het project waar ze zich momenteel mee bezighoudt, richt zich op de effecten van verstedelijking op het milieu in zuidoost Michigan, de omgeving rond Detroit. Naast het inhoudelijke deel, heeft dit project ook als doel om het gebruik van GIS binnen en de samenwerking tussen verschillende onderzoeksscholen te stimuleren.